Identification of Novel Signatures of Murine Definitive Hematopoiesis

A DISSERTATION
SUBMITTED TO THE FACULTY OF
UNIVERSITY OF MINNESOTA
BY

Beau Webber

IN PARTIAL FULFILLMENT OF THE REQUIREMENTS
FOR THE DEGREE OF
DOCTOR OF PHILOSOPHY

Bruce Blazar, Advisor

January 2014

Acknowledgments

Advancing human knowledge was the fundamental objective in my pursuit of a doctoral degree in science and has been one of the most rewarding, yet deeply challenging pursuits I have undertaken. I would not have made it through such an endeavor had it not been for the exceptional people in my life.

The path from wide-eyed undergrad to seasoned PhD is fraught with obstacles that test ones will and often appear insurmountable. I would not have overcome such adversity had it not been for supportive mentorship and an amazing group of colleagues and friends. I would like to thank my mentor, Dr. Bruce Blazar, for his patience, guidance, and support throughout. I would also like to thank my committee, specifically Drs. Jakub Tolar and Michael Kyba for their advice and collaboration over the years.

The majority of chapter 2 was previously published with the assistance of co-authors Michelina Iacovino, Si Ho Choi, Jakub Tolar, Michael Kyba, and Bruce Blazar: DNA methylation of Runx1 regulatory regions correlates with transition from primitive to definitive hematopoietic potential in vitro and in vivo. Blood. 2013 Oct 24;122(17):2978-86.

Last, and most importantly, I would not be who I am today without the love and support of my family. Ever-present to cheer my successes, provide guidance in my failures; and most importantly, to challenge me to be a better person. For this I am ever grateful.

Abstract

Pluripotent stem cells (PSC) are a tantalizing prospect for a renewable source of patient-specific hematopoietic stem cells (HSC), however efforts to obtain PSC derived HSC capable of long-term engraftment have largely failed. We set out with the primary aim of identifying novel molecular signatures of definitive hematopoiesis, so that these signatures could be applied to improve generation and isolation of HSC *in vitro.* Toward this end we pursued both discovery and application based strategies centered on *Runx1*; a transcription factor that is critical for the development of definitive HSC.

The discovery arm identified epigenetic modifications at *Runx1* cis-regulatory elements that temporally associate with the transition from primitive to definitive hematopoiesis *in vivo*. We replicated these signatures *in vitro* by overexpressing HOXB4 in hematopoietic progenitors derived from murine embryonic stem cells (ESC), and found that HOXB4 directly interacts with the definitive-specific distal *Runx1* promoter and mediates increased transcription, loss of DNA methylation, and acquisition of active histone modifications at this locus.

We next applied our understanding of *Runx1* regulation to generate a panel of clonal mESC lines harboring targeted, single-copy fluorescent reporters under the transcriptional control of *Runx1* cis-regulatory elements. These lines were used to interrogate the hematopoietic activity of each element independent of copy number and chromosomal position, allowing us to identify combinations that provided optimal activity and fidelity. Building upon this, we established mESC lines harboring synthetic fluorescent and bioluminescent mini genes replicating

the structure of the endogenous *Runx1* locus and demonstrated that these lines reflect the dynamic promoter switching that occurs at *Runx1* during hematogenesis. Sub-fractionation of embryoid body cells based on promoter activity revealed that nearly all colony forming cells (CFC) reside in the distal promoter expressing fraction. With this information we identified specific conditions that could further mature and expand distal positive cells. Collectively, this work identified a previously undescribed molecular signature of definitive hematopoiesis and the mechanism by which it is established. In addition, we applied this knowledge to generate tools with which to interrogate hematopoietic development *in vitro*, and have demonstrated their utility in optimizing strategies for obtaining definitive hematopoietic progenitors from PSC.

Table of contents

List of Tables

Chapter 2

List of Figures

Chapter 2

Chapter 3

Chapter 1:

Introduction

HSC Transplant, Limitations, and the Promise of PSC

Stem cell based therapies offer new and exciting possibilities for regenerative medicine. While often considered cutting edge or futuristic, stem cells have been used clinically to treat human disease for nearly a half-century in the form of bone-marrow transplant. The end of World War II ushered in a new era of medical research and prompted efforts which ultimately lead to seminal discoveries into the biology of marrow transplantation; namely that transplanted marrow is capable of rescuing recipients from lethality associated with acute exposure to ionizing radiation[1]. Shortly thereafter, the radioprotective effect of marrow was found to come from its ability to establish life-long donor-derived hematopoiesis in the recipient[2,3]; a phenomenon later found to manifest via the presence of rare hematopoietic stem cells (HSC) within the transplanted marrow; each capable of generating all mature lineages of the hematopoietic system, while simultaneously retaining the ability to self-renew over the life-span of the organism[4-6]. The reconstituting ability of HSCs is now exploited clinically to treat a multitude of human diseases including hematopoietic malignancies such as leukemia, lymphoma, and myeloma; as well as inborn errors of metabolism, and more recently in the correction of genetic skin disorders and even HIV[7-9].

Significant advancements have been made in the practice of HSC transplant, yet the procedure remains challenging, with morbidity and mortality occurring in a significant portion of recipients, predominantly due to complications associated with immunological mismatch, stemming from a lack of suitable HLA matched donors [7]. Additionally, insufficient HSC content within the graft can

result in graft failure; a problem that stems largely from the extreme rarity of HSC and a lack of effective methods for their expansion *ex vivo*[10]. Umbilical cord-blood has emerged as a promising new source of HSC, but is not without many of the complications associated with transplant of marrow derived HSC[11]. Substantial efforts to expand/and or maintain HSC e*x vivo* have been met with limited success, though recent high-throughput screens have identified small molecules capable of expanding and/or maintaining HSC *ex vivo* [12,13]. Though the long-term effects of these molecules remain under investigation, they have nonetheless shown enough promise to warrant clinical investigation in humans. In light of these limitations, there remains a pressing need for novel sources of HSC for transplantation.

Pluripotent stem cells (PSC) such as embryonic stem cells (ESC) and the more recently derived induced pluripotent stem cells (iPSC) offer exciting prospects for renewable and patient-specific sources of *in vitro* derived HSC[14-19]. PSC are characterized by their ability to self-renew in culture while maintaining pluripotency, and in the case of iPSC, can be derived from a specific individual; thus circumventing complications associated with immunological mismatch. Shortly after their isolation, human PSC were shown to possess the capacity to undergo hematopoietic differentiation *in vitro*[20]. In spite of the successful derivation of many mature hematopoietic lineages from PSC, efforts to generate HSC capable of long-term engraftment have largely stagnated.

A significant obstacle to the derivation of engraftable HSC from PSC is the fact that PSC hematopoietic specification is biased toward a transient, early

embryonic phase of blood generation that is referred to as primitive hematopoiesis[21,22]. Primitive hematopoiesis predominantly generates cell types that serve the purpose of oxygen supply and tissue remodeling within the embryo, but do not contribute to the HSC pool that sustains life-long hematopoiesis after birth. The so called definitive phase of hematopoiesis occurs later in development and is the predominant source of HSC that are responsible for life-long reconstitution of adult hematopoiesis. It is definitive HSC that possess the unique capacity to provide long-term hematopoietic reconstitution posttransplant. Thus, the major hurdle to the realization of PSC derived HSCs is our present inability to specify and efficiently isolate definitive HSC during *in vitro* differentiation of PSC.

Hematopoietic ontogeny

The mammalian hematopoietic system is tasked with replenishing millions of mature blood cells in a tightly controlled manner on a daily basis. Maintaining this output over the course of a lifetime is accomplished by a small population of HSC residing in the bone marrow. Substantial progress has been made in defining the adult hematopoietic hierarchy and the intrinsic and extrinsic signals that direct the formation of each committed lineage from HSC, however the developmental processes that lead up to the emergence of HSC in the embryo are less clear.

Early studies of vertebrate development in chick embryos identified the extra-embryonic yolk sac (YS) as the first site of blood formation [23]. The observation that YS blood formation occurs in a spatiotemporally similar manner

as the YS vasculature prompted speculation that primitive blood and endothelial cells arise from a bipotential mesodermal precursor, termed a 'hemangioblast' [24]. It was not until much later that direct evidence for the presence of a mammalian hemangioblast (HB) was suggested during *in vitro* differentiation of mouse embryonic stem cells (mESC) [25,26]. Confirmation of an *in vivo* hemangioblast came via the use transgenic mice expressing green fluorescent protein (GFP) from the murine *brachyury* locus[27]. Here, it was observed that at day 7.0-7.5 a subset of mesodermal cells located within the posterior region of the primitive streak begin to express *brachyury* and the vascular endothelial growth factor receptor *Flk1* (VEGFR-2), and when placed in supportive culture conditions are able to give rise to both adherent endothelial and non-adherent hematopoietic progeny at a clonal level. These cells were dubbed blast-colony forming cells (BL-CFC) [28]. In the embryo, a subset of the *brachyury* expressing mesodermal cells eventually migrate to the YS, where they produce the endothelial and primitive hematopoietic cells that make up characteristic blood islands[29,30]. At this time, the prevailing wisdom held that mesoderm derived HB located in the YS produced the HSC of the adult hematopoietic system[29,31-33].

The theory of a YS origin for adult vertebrate HSC was questioned early on by results from quail-chick grafting experiments, whereby the cells (and thus cellular progeny) of each species can be distinguished by the appearance of the nuclei. In these experiments, two-day old (pre-vascularization) quail embryos were grafted onto chick YS and allowed to progress through hematopoietic development [34]. Upon examination of peripheral hematopoietic organs, all mature

blood types were derived from quail; suggesting that the origin of adult definitive HSC resides within the embryo proper, and not the YS. Analogous experiments using amphibian embryos reached a similar conclusion[35]. The theory of an embryonic origin of HSC would remain controversial until the findings were corroborated by rigorous transplantation experiments in mice. In these studies, systemic transplantation of embryonic tissues from E8-12 identified that the first HSC capable of long-term, multilineage reconstitution of adult hematopoiesis arise not in the yolk sac, but autonomously within the aorta-gonad-mesonephros (AGM), vitelline, and umbilical arteries of E10.5 embryos [36-38]. Around E12 HSC activity can be detected within other anatomical regions, including the YS and fetal liver, but because this follows the onset of circulation, it cannot be ruled out that these regions are seeded by HSC or pre-HSC emanating from the AGM. As the HSC numbers present in the E12 fetal liver exceed that which can be produced in the AGM alone, an additive contribution of HSC from YS, placenta, or other anatomical regions cannot be completely dismissed; whether through *de novo* generation or via the maturation of HSC precursors generated elsewhere [39]. Nonetheless, the AGM is widely considered the primary site of HSC generation within the embryo. Once formed, nascent HSC enter the circulation and colonize the fetal liver where they undergo significant expansion prior to a final transition to bone marrow[39].

One of the important observations made in early studies was the close proximity of nascent hematopoietic cells and vasculature; specifically vascular endothelium lining the floor of the dorsal aorta and umbilical and vitelline

arteries[40,41]. Lineage tracing experiments in transgenic mice expressing Cre recombinase under the control of the vascular endothelium restricted *VE-cadherin* regulatory elements supported the endothelial origin of AGM derived HSC[42]. This process would later be directly observed in a series of elegant time-lapse microscopy experiments. Eilken *et al* utilized *in vitro* differentiation of mESC engineered to express fluorescent reporters under control of *VE-cadherin* regulatory elements. In these experiments mesodermal precursors isolated based on *Flk1* expression were placed in culture and observed as they underwent hematogenesis. Time-lapse videos clearly demonstrated the formation of VE-Cadherin+ endothelial clusters that began to bud non-adherent CD41 and CD45+ hematopoietic cells[43]. Similar time-lapse observations of this process in zebrafish and in aortic explants from mouse embryos would set forth the model in which HSC form via a novel endothelial-to-hematopoietic transition (EHT)[44,45]. Further dissection of this process brought forth a model where a bipotential HB is not the *direct* precursor of embryonic hematopoietic cells but rather that an intermediate, hemogenic endothelium (HE) is formed which then directly produces non-adherent, definitive hematopoietic cells within the embryo [43,46]. Utilizing a novel *ex vivo* stromal co-aggregation strategy and systematic transplantation analyses of fluorescence activated cell sorting (FACS) purified cell populations, Rybostov *et al.* refined the phenotypic hierarchy of hematogenesis within the AGM region. In these studies, VE-cadherin+CD45-CD41+ type I pre-HSC residing within the wall of the aorta transition to VE-cadherin+CD45+CD41+ type II pre-HSC before ultimately becoming mature

HSC as defined by their ability to engraft without the need for an *ex vivo* maturation step[47].

Germ layer interactions between mesoderm and endoderm are necessary for embryonic hematogenesis [48-51]. Specifically, the activity of VEGF, bFGF, and TGF-β1 have been identified as endodermal signals important for specifying hematopoiesis from mesodermal progenitors[52]. Hedgehog signaling is important for the formation of definitive hematopoiesis in zebrafish, and for the formation of hematopoietic cells during *in vitro* differentiation of ESC, possibly due to its role in the formation of aortic vasculature[53-55]. Indeed, Hedgehog signaling lies upstream of the VEGF and Notch signaling pathways; both of which are crucial to the formation of HSC from aortic endothelium[54,56]. In addition, both Wnt and BMP4 signaling are important to the formation of blood within the embryo, in part due to their effects on mesodermal patterning[57-59].

The activities of these signaling pathways are integrated into a complex network of interacting transcription factors [60,61]. Apical blood regulators including *Cdx4* and Hox members initiate transcriptional programs required for the specification of blood[62,63]. Notable downstream transcription factors include: *Gata2* [64], *Scl* [65,66], *Lmo2,* [67,68], *Fli1*[69], and the runt-related transcription factor-1 (*Runx1*) [70,71]; all of which are required for definitive hematopoiesis [69,72]. *In vivo* studies using knockout mESC lines by Lancrin *et al.* placed the temporal requirement for SCL at the transition from hemangioblast to hemogenic endothelium, and confirmed the observations of others that *Runx1* is required for the transition from hemogenic endothelium to definitive hematopoiesis[73]. As the

phenotypic characterization of hemogenic endothelium has been refined, regulators of its formation have been identified. Iacovino *et al.* identified *HoxA3* as an apical regulator of hemogenic endothelium; essentially functioning as a molecular gatekeeper to the initiation of hematopoiesis by activating a large cohort of endothelial specific genes while simultaneously repressing hematopoietic specific genes including *Runx1*[74]. The transcription factor *Sox17* has recently been found to play a role in the generation and expansion of hemogenic endothelium via modulation of the Notch pathway[75]. Complex regulatory circuits have been identified between many of these transcription factors, underscoring that hematogenesis is a dynamic, multifaceted interplay that must be intricately regulated [76].

The information gleaned from these studies has provided valuable insight into the basic biology of blood development, and continues to pave the way for applied efforts to obtain transplantable HSC from PSC.

Hematopoietic Differentiation of PSC

PSC have demonstrated their utility as a tool for the interrogation of developmental processes leading to the formation of blood; allowing both easy access and observation of intermediate stages of development and, particularly in the case of mESC, their amenability to genetic modification .

Spontaneous differentiation of mESC *in vitro* provided the first evidence of their capacity to undergo hematopoietic differentiation[77]. When removed from conditions promoting pluripotency, mESC generate complex three dimensional embryoid bodies (EB) containing cell types derived from multiple germ layers.

Characteristic blood islands with similar appearance and cellular composition to that of YS can be observed within these structures. Methylcellulose based colony-forming unit (CFU) assays over the time-course of EB formation demonstrated that hematogenesis occurs in a sequence similar to that *in vivo,* with primitive erythroid cells (EryP) appearing first at day 6, followed by more definitive cell types of the erythroid lineage (EryD) and macrophages at later time-points[78]. Although the embryonic to adult globin switch occurs within EBs, the inability to produce other adult definitive lineages, namely lymphoid cells and CFU-Spleen, suggests that *in vitro* ESC differentiation is biased toward the primitive type hematopoiesis observed in the yolk-sac[79,80]. As expected based on these observations, EB derived hematopoietic progenitors have not been demonstrated to have the capacity to significantly repopulate adult hematopoiesis after transplantation, although a few studies have observed trace levels of chimerism in immune deficient mouse strains when transplanting cells from late stage EBs[81,82].

These limitations prompted the development of new differentiation strategies aimed at promoting definitive hematopoiesis and, ultimately, engraftable HSC. One of the first broad modifications was the co-culture of ESC with hematopoietic-supportive stromal cells. The OP9 stromal line derived from the calvaria of M-CSF deficient mouse embryos was one of the first to demonstrate reproducible induction of multi-lineage hematopoiesis from ESC, including low levels of lymphoid cells, albeit restricted to B and NK cell lineages[83]. Considering the fact that lymphoid capacity is a trait thought to be

relegated to adult-type definitive hematopoietic progenitors, the fact that progenitors obtained from OP9 co-cultures fail to engraft suggests that the current definitions of primitive and definitive hematopoiesis may require refinement, or that additional maturation steps may be required to obtain HSCs capable of homing to, and/or thriving within the adult marrow microenvironment. The latter explanation is particularly interesting in light of the fact that YS derived progenitors from E 9.0 embryos are able to generate long-term reconstitution when transferred directly into the liver of newborn recipients[84].

Attempts to overcome this hurdle via the enforced expression of cell intrinsic regulators have shown mixed success. Retroviral transduction of day 5 EB cells with the *Bcr/Abl* oncogene followed by *in vitro* expansion and transplantation produced multi-lineage hematopoietic chimerism, but perhaps not surprisingly, ultimately resulted in leukemia[85]. A recent report documented the ability of a short isoform of *Runx1,* Runx1a, to promote both the formation and short-term engraftment capacity of hESC derived hematopoietic progenitors, however questions have been raised as to whether this was the result of oncogenic transformation[86]. Perhaps the most successful example of cell intrinsic modulation of HSC development from PSC has come via the overexpression of the definitive HSC specific homeotic regulator, *HoxB4.* By merging HoxB4 overexpression and OP9 co-culture, Kyba *et al.* were able to demonstrate the generation of hematopoietic cells capable of leukemia-free, long-term multi-lineage engraftment from both ESC and YS[87]. This latter discovery strengthens the argument that cell intrinsic regulatory pathways can be effectively modulated

in such a way as to confer “definitiveness” unto formerly primitive hematopoietic cells. In addition to its utility for interrogating the molecular profile of definitive hematopoiesis, HoxB4 has allowed proof of concept experiments for gene correction of PSC followed by hematopoietic differentiation, transplant, and subsequent therapeutic correction of disease[88,89].

Unfortunately, one of the most consistent themes across the many systems for hematopoietic differentiation is a lack of reproducibility. This has less to do with the merit of the individual studies as it does the inherent variability introduced by undefined culture conditions; whether via the supplementation of culture media with fetal calf serum or through the use of stromal cell lines for co-culture or the generation of conditioned media. To avoid this problem, many groups have opted to explore fully defined culture systems based off the insights gleaned from basic research into the development of HSC *in vivo*. The first step along the path from pluripotency to blood is the transition to an epiblast stage; a process can be accomplished simply by removing PSC from the conditions that maintain pluripotency [90]. The second step of specifying mesoderm from the epiblast stage is promoted by the addition of BMP4 [91,92]. Additional factors are required for the formation of hemangioblast from mesoderm, as evidenced by the lack of BL-CFC in cultures supplemented with BMP4 alone. The addition of appropriate levels of VEGF is sufficient for low levels of BL-CFC activity; however the combination of VEGF, bFGF, and Activin A dramatically enhances the formation of HB [91]. Final specification to the hematopoietic lineage is promoted by a wide array of hematopoietic cytokines, including stem-cell factor (SCF),

thrombopoietin (TPO), FMS-like tyrosine kinase ligand (Flt3), interleukin-3 (IL-3), and interleukin-6 (IL-6) [87,93].

Collectively, these findings have provided a platform from which to build in the ongoing effort to identify conditions that promote the final transition to definitive HSC. Undoubtedly, these efforts will be fostered by the identification of new phenotypic and molecular signatures of definitive HSC.

The Role of *Runx1* in Definitive Hematopoiesis

The Runt-related transcription factor, *Runx1* (also known as AML1 and Pebp2α), and its shared binding partner CBFβ are part of the evolutionarily conserved core-binding factor (CBF) family of transcriptional regulators. Members of this family are distinguished by a 128 amino acid region of homology to the *Drosophila* pair-rule gene *runt.* This evolutionarily conserved 'runt domain' functions to specify Runx1 binding to its target DNA sequence, YGYGGT, and to mediate the interaction with its β-subunit, CBFβ.

In mouse and (man), three *Runx* genes have been identified; *Runx1 (AML1), Runx2 (AML3),* and *Runx3 (AML2);* with each performing different tasks during embryonic development. In humans, RUNX1 and CBFβ are frequently sites of oncogenic translocations in acute myeloid leukemia (AML) and acute lymphoid lymphoma (ALL), underscoring an important hematopoietic role for *Runx1*[94]. In the embryo, *Runx1* is notable for its important role in the formation of definitive HSC during development as evidenced by the fact that *Runx1* knockout embryos die by E12.5, exhibiting a complete lack of definitive hematopoiesis [95]. Interestingly, the loss of Runx1 appears to preferentially

impact intra-embryonic definitive, but not the earlier primitive waves of hematopoietic development. Subsequent studies have specified its requirement to the transition from HE to definitive HSC[96]. The precise role of Runx1 in the transition from HE is currently under investigation. Genome-wide analysis of changes to the epigenetic landscape mediated by Runx1 during this transition identified global rearrangements in the binding profiles of master hematopoietic regulators SCL, Fli1, and C/EBPβ[97]. These rearrangements were associated with the modulation of pathways associated with hematopoiesis and cell morphology. Thus Runx1 expression in HE is responsible for global induction of hematopoietic cell fate, underscoring its role as a master regulator of the hematopoietic program.

Organization and Transcriptional Regulation of *Runx1*

The murine *Runx1* locus covers roughly 220kb on chromosome 16, and contains 7 alternately spliced exons; allowing for the generation of an assortment of alternately spliced isoforms. Transcription initiates from two spatially distant, alternative promoters; the Proximal (P2) promoter is located just upstream of the second exon, while the Distal (P1) promoter is located ~100kb upstream from P2. The two promoters are separated by the first exon and an unusually large (~100kb) intron. Located ~23kb downstream form the P1 promoter, and within the first intron, is an enhancer element that confers hematopoietic specificity to the two *Runx1* promoters via its interaction with Gata2, Ets factors, and the SCL/Lmo2/Ldb1 complex[98,99]. When isolated in plasmid-based reporter assays

and transgenic mice, neither promoter appears to direct hematopoietic specific transcription [100].

The *Runx1* locus is particularly interesting in that the P1 and P2 promoters are differentially active during hematopoietic development [101]. Specifically, P1 activity dominates only in definitive hematopoietic stem and progenitor cells of the FL and adult[102,103]. Structural differences have been noted between the two promoters, with the proximal promoter being described as resembling that of "housekeeping" gene promoters in that it contains binding sites for more generic transcriptional regulators and few sites associated with lineage-specific transcription factors [100]. On the other hand, the P1 promoter is more complex in terms of transcription factor binding sites, with experimentally validated binding sites for lineage-specific transcription factors, including Gata and Runx1, pointing to its potential autoregulation[101,104]. The mechanism of translation also differs between the two promoters, with P1 translation occurring via a cap-dependent mechanism, while P2 translation occurs via a cap-independent IRES-mediated process [105]. The P1-*Runx1* isoform (Runx1c) differs from the P2-*Runx1* isoform (Runx1b) in its 5' UTR, and by the inclusion of unique amino acids at its N terminus. The biological roles of these isoforms are currently under investigation, though several studies have noted differences in DNA-binding affinity, and the ability of each isoform to promote cellular proliferation and differentiation[106,107].

The striking temporal association of the *Runx1* promoter switch with the formation of definitive HSC provides a unique signature with which to further dissect the molecular and phenotypic profiles of primitive and definitive

hematopoiesis. In doing so, it will become possible to more readily identify conditions that bias PSC differentiation toward definitive hematopoiesis, and ultimately HSC.

Chapter 2.

DNA methylation of *Runx1* regulatory regions correlates with transition from primitive to definitive hematopoiesis *in vitro* and *in vivo*.

Foreward

The transcription factor Runx1 (AML1) is a central regulator of hematopoiesis and is required for the formation of definitive hematopoietic stem cells (HSC). Runx1 is alternatively expressed from two promoters: the proximal (P2) prevails during primitive hematopoiesis, while the distal (P1) dominates in definitive HSC. While some transcription factor binding sites and cis-regulatory elements have been identified, a mechanistic explanation for the alternative promoter usage remains elusive. We investigated DNA methylation of known Runx1 cis-elements at stages of hematopoietic development in vivo, and during differentiation of murine embryonic stem cells (ESC) in vitro. We find at the P1 promoter, loss of methylation correlated with the primitive to definitive transition in vivo. In vitro, hypomethylation, acquisition of active chromatin modifications, and increased transcriptional activity at P1 are promoted by direct interaction with HoxB4, a transcription factor that confers definitive repopulation status on primitive hematopoietic progenitors. These data demonstrate a novel role for DNA methylation in the alternative promoter usage at the Runx1 locus, and identify HoxB4 as a direct activator of the P1 promoter. This epigenetic signature should serve as a novel biomarker of HSC potential in vivo, and during ESC differentiation in vitro.

Introduction

Understanding the molecular pathways governing the development of mammalian hematopoietic stem cells is crucial to identifying methods for their derivation from pluripotent cell sources. Of the key players involved in the formation of HSC, the runt-related transcription factor, *Runx1,* plays an essential role. Without *Runx1,* hemogenic endothelium of the aorta-gonad-mesonephros (AGM) does not undergo hematopoietic transition and *Runx1* knockout embryos fail to survive past 12.5 days gestation with a complete loss of definitive hematopoiesis[95,96,108,109]. This defect is mirrored during hematopoietic differentiation of embryonic stem (ES) cells *in vitro,* underscoring the role of *Runx1* as a fundamental regulator of the hematopoietic program during development[73,110].

Runx1 serves as the α-subunit of the core binding factor complex and is the most common translocation in acute myeloid leukemia in humans[94,111]. Defining regulation of the *Runx1* locus is necessary to understand the complex functional roles and tightly regulated activity of *Runx1* during HSC development and hematopoietic malignancy. *Runx1* transcription is controlled by two developmentally regulated alternative promoters and an intronic enhancer (+23) element[98-101]. Intriguingly, promoter usage follows a pattern whereby the proximal (P2) promoter initiates early in primitive hematopoiesis, while distal (P1) promoter driven transcription appears later in definitive hematopoietic cells[103,112]. Strikingly, distal promoter predominance is temporally associated with peak HSC expansion in the fetal liver and continues into adult marrow where purified HSC utilize the

distal promoter almost exclusively[101,103,106,113]. While *Runx1* core promoter elements fail to restrict reporter expression to the hematopoietic lineage, the intronic +23 enhancer is sufficient to drive hematopoietic specificity via interaction with Gata2, Ets factors, and the SCL/Lmo2/Ldb1 complex[99,100]. While much has been learned about *Runx1* promoter and enhancer usage, the precise mechanisms responsible for the observed promoter switch are not understood.

DNA methylation is an epigenetic regulatory mechanism that contributes prominently to embryonic development and lineage commitment in the hematopoietic system[114-116]. Recent advances in genome-wide analysis of methylation have identified tissue specific differentially methylated regions (TDMR) as dynamic regulators of gene expression during development and disease[117]. Further evidence suggests that intronic enhancers are frequently TDMR involved in lineage commitment and can influence the usage of alternative promoters[117,118]. In spite of these observations, methylation of the *Runx1* regulatory elements has not yet been assessed in the context of hematopoietic development, and relatively little is known about the mechanisms underlying the *Runx1* promoter switch.

Here, we examine the DNA methylation status of *Runx1* regulatory elements at stages of hematopoietic development *in vivo* and during hematopoietic differentiation of ESC *in vitro.* We find the proximal (P2) promoter is unmethylated in all cell types examined including pluripotent murine embryonic stem cells (mESC). In accordance with its role as a hematopoietic specific enhancer, a striking loss of methylation is observed at the +23 enhancer element

upon commitment to the hematopoietic lineage *in vivo* and *in vitro.* We show that hypomethylation of the distal promoter region is correlated with definitive HSC potential *in vivo,* and can be promoted during *in vitro* hematopoietic differentiation by HOXB4. Concordantly, HOXB4 overexpression promotes P1 transcription and an increased P1/P2 mRNA ratio. Chromatin immunoprecipitation (chIP) analyses in mESC derived hematopoietic cells overexpressing HOXB4 show that P1 is preferentially bound by HOXB4, acquires histone modifications permissive to transcription, and undergoes a decrease in occupancy by the maintenance methyltransferase DNMT1. Thus, decreased methylation, acquisition of active chromatin modifications, and increased transcriptional activity at the P1 promoter is promoted *in vitro* via physical interaction with HOXB4.

Materials and Methods

ESC culture and differentiation

mESC were cultured on irradiated murine embryonic fibroblasts (MEFs) in KO DMEM (Gibco) supplemented with 15% FBS, 0.1 mM nonessential amino acids (GIBCO), 2 mM glutamax, (Invitrogen), penicillin/streptomycin (Gibco), 0.1 mM β-mercaptoethanol, and 1000 U/mL LIF(Millipore), at 37°C in 5% CO_2. ES cells were differentiated as embryoid bodies (EB) as previously described[119]. Briefly, mESC were aggregated in hanging drops EB media consisting of IMDM supplemented with 15% FBS, 6 μM monothioglycerol (Sigma), 200 μg/ml human iron-saturated holo-transferrin (Sigma), 50 μg/ml ascorbic acid (Sigma), and penicillin-streptomycin (Gibco) in 5% CO_2 at 37°C for 48 hrs. Hanging drop EBs

were transferred to 10 cm ultra-low adherence dish (Corning) in EB media and incubated on an orbital shaker at 70 rpm in 5% CO_2 at 37°C. After an additional 24 hours an 80% media change was performed and EBs were returned to shaking incubation for three days.

OP9 co-culture and HOXB4 overexpression

At day-6, EBs were dissociated and transduced with either MSCV-IRES-GFP control or MSCV-HoxB4-IRES-GFP via spin infection at 2500 rpm for 1.5 hrs followed by 4 hrs additional contact with viral supernatant. Cells were washed with PBS, and plated onto sub-confluent OP9 (Kindly provided by Dr. Mervin Yoder, Indiana University) in hematopoietic expansion (HE) media consisting of Iscove's Modified Dulbecco's Medium (IMDM) supplemented with 10% FBS, 5 ng/mL VEGF (Peprotech), 40 ng/mL TPO (Peprotech) , 40 ng/mL Flt-3L (Peprotech), penicillin/streptomycin (Gibco), 2 mM glutamax (Invitrogen) in 5% O2. Semi-adherent cells were passaged by trypsinization every 4-5 days. For histone and Dnmt1 chromatin immunoprecipitation experiments, a doxycyclin inducible HOXB4 mESC line was utilized[87,119]. CD41+ cells from day 6 embryoid bodies were collected for chIP analysis and the remainder were plated onto OP9 with or without 500ng/ml doxycyclin and cultured as described above.

Embryo dissection and cell isolation

C57BL/6 mice were paired in the evening and the following morning (E0.5) females were checked for presence of vaginal plugs. Mice were housed in a specific pathogen-free facility and used with the approval of the University of Minnesota's institutional animal care committee. Yolk sac dissection and cell

preparation was performed as described[120]. Single cell suspensions from fetal liver were prepared as described previously[121].

Cell fractionation

Fluorescence-activated cell sorting was performed using FACSAria. All antibodies were from eBioscience unless otherwise noted. Embryoid body and OP9 co-cultures were stained with c-Kit-APC (2B8), CD41-PE (Mwreg-30), and CD45-APC (30-F11). Fetal liver (FL) cells were stained with the following biotinylated monoclonal antibodies: Ter119 (TER-119), Gr-1 (RB6-8C5), CD3 (500A2), and B220 (RA3-6B2), followed by incubation with anti-biotin microbeads (Miltenyi) according to manufacturer's recommendations and depleted using an AutoMACS (Miltenyi). Lineage negative fraction was stained with CD48-FITC (TC15-12F12.2), CD150-PE (mShad), and Sca1-APC (D7). Yolk sac cells were enriched for CD41 by first labeling with CD41-PE antibody, followed by incubation with anti-PE microbeads and magnetic separation according to manufacturer recommendations (Miltenyi). Adult marrow KLS+SLAM cells were isolated by lineage depletion via MACS Lin Cell Depletion Kit (Miltenyi), per manufacturer protocol. Lineage negative fraction was then stained with c-Kit-APC (2B8), Sca-1-PE-Cy7 (D7), CD48-FITC (TC15-12F12.2), and CD150-PE (mShad) for 20 min @ 4 degrees per manufacturer protocol. Propidium iodide was used to exclude dead cells in all FACS purifications.

Bisulfite sequencing and methylation analysis

Genomic DNA was isolated using the DNeasy Blood and Tissue kit (Qiagen) according to manufacturer's recommendations for isolation from

mammalian cells. Bisulfite conversion was performed using the Epitect Bisulfite kit (Qiagen) according to manufacturer's protocol for low amounts of DNA. Primers were designed to specifically amplify converted DNA using the publicly available MethPrimer program (http://www.urogene.org/methprimer/index1.html). Single-step PCR amplification was conducted using Accuprime Supermix I or II (Invitrogen) for +23, and P1/P2 respectively. Amplification products were visualized by gel electrophoresis and bands were excised and purified using the QIAquick Gel Extraction kit (Qiagen). Purified PCR products were inserted into the PCR4-TOPO vector (Invitrogen) and individual clones were sequenced. Alignment and methylation analysis were performed using the online QUMA program (http://quma.cdb.riken.jp/). Sequenced clones with at least 90% non-CpG cytosine conversion and at least 90% sequence homology were retained for analysis.

Quantitative RT-PCR

OP9 co-cultures were collected and OP9 stromal cells were depleted via differential plastic attachment. RNA was isolated using the RNeasy Plus Micro kit (Qiagen). First-strand cDNA synthesis was performed using the Superscript VILO cDNA Synthesis kit (Invitrogen). Quantitative PCR was performed using Platinum SYBR Green qPCR Supermix (Invitrogen), and normalized to GAPDH. Primers used were described previously[113].

Chromatin immunoprecipitation

ChIP assays were performed according to previously described protocol with slight modifications[122]. OP9 co-cultures were collected via trypsinization and

OP9 cells were depleted via plastic attachment. Roughly 10^7 total cells were crosslinked for 10 min in 1% formeldahyde. Chromatin was sheared via sonication to generate fragments between 200-500 bp. The sonicated chromatin was incubated with the indicated antibodies overnight at 4°C and followed by incubation with 30 µl of Magna ChIP Protein A+G magnetic beads (Millipore) for 2 hours. Beads were washed with RIPA buffer and TE buffer containing 50 mM NaCl. The immunoprecipitated complexes were eluted from the beads by heating at 65°C and reverse crosslinked by overnight incubation at 65°C. Immunoprecipitated DNA was treated with RNaseA and proteinase K, and purified using Qiagen PCR purification kit. Immunoprecipitations were performed using a rabbit anti-*HoxB4* monoclonal (EP1919Y, Epitomics), rabbit anti-histone H3 Acetyl (K9) monoclonal (Y28, Epitomics), anti-H3K4me3 (ab8580, Abcam), anti-H3K27me3 (ab6002, Abcam), and anti-Dnmt1 (ab13537, Abcam). Immunoprecipitations were performed twice independently for each sample. Primers used for chIP-qPCR are available upon request.

Statistics

Statistical analysis of methylation between individual populations was performed using the online QUMA program (http://quma.cdb.riken.jp/). Differences between grouped methylation data were determined by unpaired 2-tailed *t* test, with *P* values less than 0.05 considered significant. All other analysis was performed using a Student *t* test, with P value less than 0.05 considered significant.

Results

Proximal Runx1 (P2) promoter is unmethylated regardless of lineage or developmental status

The exceptionally large size of the *Runx1* locus (224kb) limited our ability to perform locus-wide exploratory bisulfite sequencing. We thus focused on *Runx1* regulatory elements previously confirmed to exhibit hematopoietic activity[99] (Figure 1 A, Supplemental Table 1). The proximal *Runx1* (P2) promoter is the most CpG dense (63% GC, 1.03 CpG observed/global expected) of the three *Runx1* elements analyzed and the only one to contain a classic CpG island (GC > 50%, Obs/Exp > 0.6). To determine if the proximal *Runx1* promoter is differentially methylated during hematopoietic development *in vivo* we analyzed bisulfite-treated genomic DNA from E14.5 mouse embryonic fibroblast cells (MEFs), E8.5 yolk sac (YS) CD41+ , E14.5 fetal liver (FL) Lin-Sca-1+CD48-CD150+, and adult marrow Lin-c-Kit+Sca-1+CD150+CD48- (KLS+SLAM) cells; representing non-hematopoietic, primitive hematopoietic, and two stages of definitive HSC respectively (Figure 1 B, Supplemental Figure 1A-B). To parallel this analysis *in vitro* using mESC, we utilized an established two-stage differentiation process (Figure 1 B). mESC were first differentiated as embryoid bodies (EB) for six days to obtain primitive c-Kit+CD41+ progenitors (Supplemental Figure 2 A). Since HOXB4 overexpression is an efficient method to obtain ES-derived hematopoietic progenitors capable of robust long-term reconstitution post-transplant[87], we utilized overexpression of HOXB4 and co-culture on hematopoietic supportive OP9 stromal cells to obtain mESC-derived

definitive HSC. Day 6 EB cells were infected with MSCV-HOXB4-IRES-GFP or MSCV-IRES-GFP control virus and co-cultured on OP9 cells. The GFP+c-Kit+CD45+ fraction was isolated from HOXB4 and control co-cultures after six days (6 + 6 days); and from HOXB4 co-cultures at eleven days (6 + 11 days) at which point no hematopoietic cells were observed in the control co-cultures (Supplemental Figure 2 B).

Figure 1.

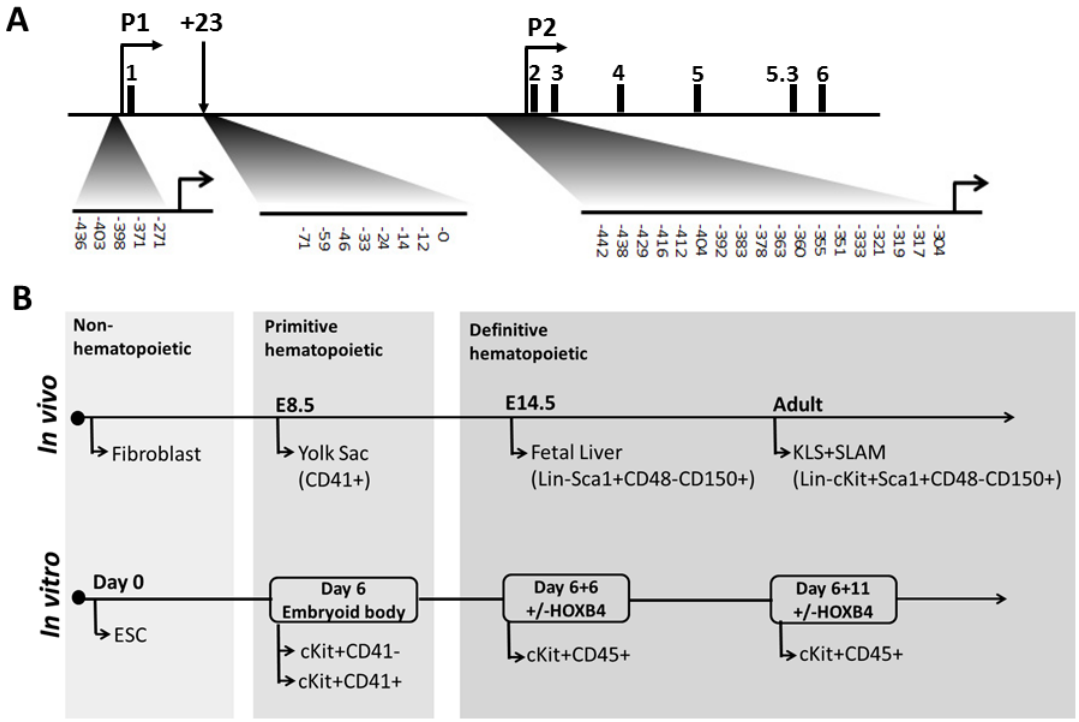

Figure 1. Runx1 genomic locus and cell populations for bisulfite analysis

(A) Murine Runx1 locus and CpGs analyzed by bisulfite sequencing. For P1 and P2 CpG# represents distance from transcription start site (TSS). For +23 CpG# represents distance from 3' end of PCR amplicon. (B) Cell populations isolated in vivo, and from ES cell differentiation strategy for bisulfite analysis.

In vivo, we find the proximal (P2) promoter to be unmethylated in MEFs, a non-hematopoietic control (0.8% ± 0.79%) (Figure 2 A). No change in P2 promoter methylation was associated with primitive hematopoiesis as P2 was also unmethylated in E8.5 YS CD41+ cells (1.7% ± 0.85%) (Figure 2 A). This absence of P2 promoter methylation continues in E14.5 FL Lin-Sca-1+CD48-CD150+ cells (3.1% ± 1.63%), and in adult marrow KLS+SLAM (0% ± 0%) (Figure 2 A), indicating that the *Runx1* proximal (P2) promoter does not exhibit differential methylation between lineages, or during hematopoietic development *in vivo.* While previous reports indicate a P1 bias in FL and adult HSC[101,106,113], our data indicate that the methylation status of the P2 promoter does not establish this bias.

The absence of P2 promoter methylation was mirrored *in vitro* in undifferentiated mESC (1.4% ± 0.91) and did not change in day 6 EB c-Kit+CD41+ cells (2.1% ± 1.02) (Figure 2 B). P2 remained unmethylated in day 6 + 6 OP9 co-cultures in both control c-Kit+CD45+ cells (2.2% ± 1.79), as well as HOXB4 overexpressing cells at day 6+6 (0.6% ± 0.56) and day 6 + 11 (1.2% ± 0.82) (Figure 2 B). These observations are consistent with previous reports that CpG dense core promoter regions are predominantly unmethylated[123,124], and that P2 expression exhibits a lower degree of lineage restricted expression than P1 during development[125]. Indeed, global DNA methylation data released by the ENCODE Consortium confirms a foci of hypomethylation at the P2 promoter in multiple cell lineages[126].

Figure 2.

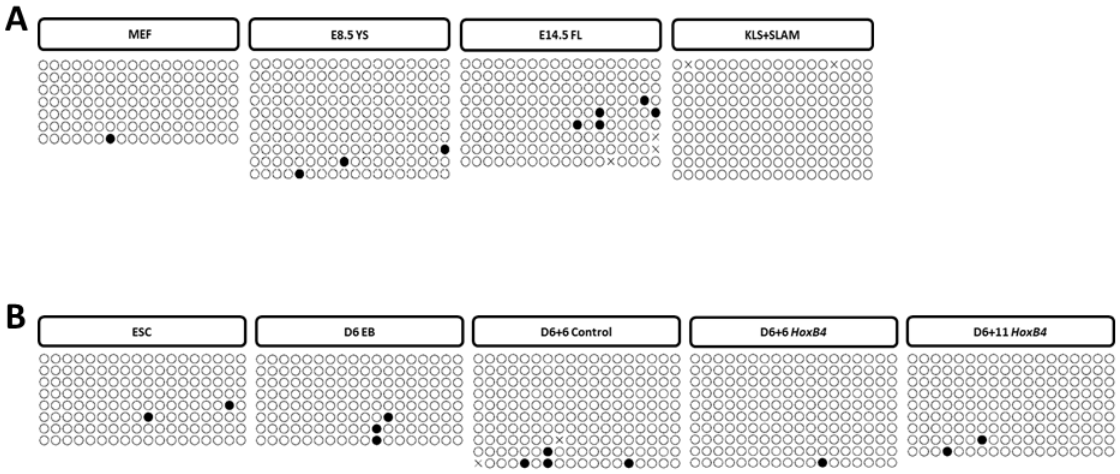

Figure 2. Bisulfite analysis of proximal Runx1 promoter

(A) Methylation patterns of the Runx1 proximal (P2) promoter in cells derived from E14.5 murine embryonic fibroblast cells (MEFs), E8.5 yolk sac (YS) CD41+ (E8.5 YS), E14.5 FL Lin-Sca-1+CD48-CD150+ (E14.5 FL), and adult marrow Lin-c-Kit+Sca-1+CD150+CD48- (KLS+SLAM). Sequencing reactions of individual amplicons are represented by each row of circles. Open circles denote unmethylated CpGs, and filled circles represent methylated CpGs. (B) Methylation patterns in murine ES cells (mESC), day 6 embryoid body c-Kit+CD41+ (D6 EB) and from OP9 co-cultures: GFP+c-Kit+CD45+ cells isolated from IRES-GFP control group at day 6 (D6+6 Control); and HOXB4-IRES-GFP group at day 6 (D6+6 HoxB4) and day 11 (D6+11 HoxB4).

Hypomethylation of the +23 enhancer correlates with the hematopoietic lineage

The recently described intronic +23 enhancer element has been shown to drive hematopoietic specific transcription[99]. Sequence analysis of this region shows low CpG density and does not specify a classic CpG island (58% GC, 0.31 Obs/Exp). *In vivo,* we find the +23 enhancer is highly methylated in MEFs (79.4% ± 4.66), but methylation is significantly decreased in E8.5 YS CD41+ cells (1.7% ± 1.22), E14.5 FL Lin-Sca-1+CD48-CD150+ (18.8% ± 8.29), and adult KLS+SLAM (4.2% ± 2.54) (Figure 3 A-B). These results demonstrate that +23 enhancer hypomethylation occurs during embryonic hematopoiesis and continues into fetal and adult hematopoiesis.

Figure 3.

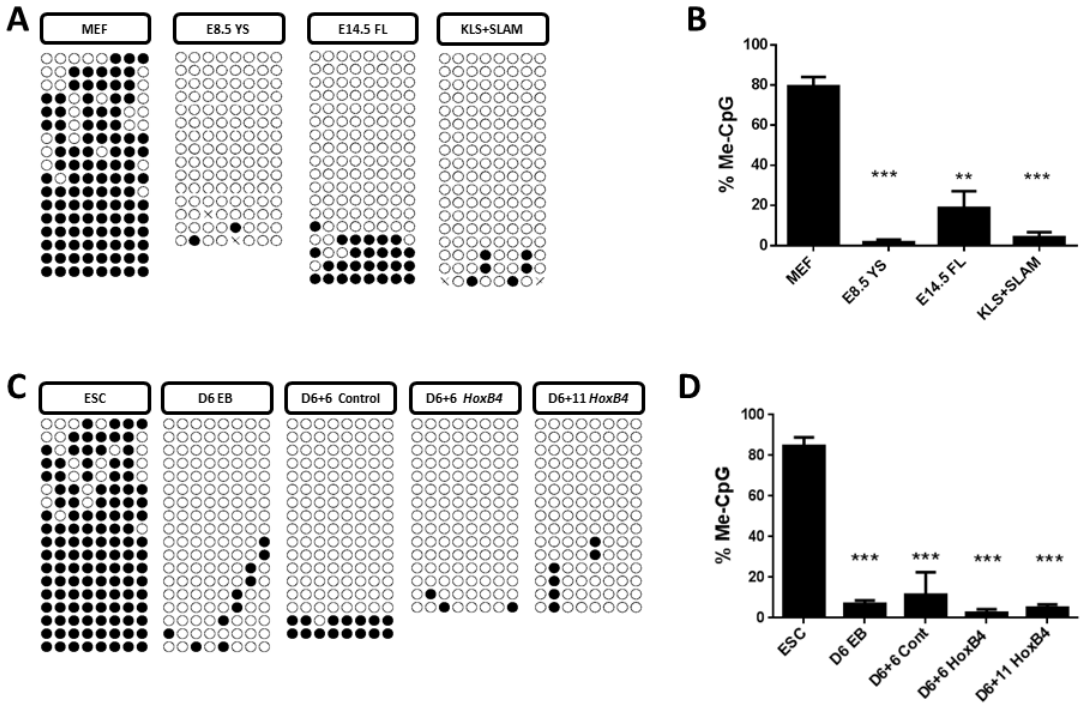

Figure 3. Bisulfite analysis of +23 enhancer methylation

(A) Methylation patterns of the Runx1 +23 enhancer in cells from in vivo-derived E14.5 murine MEFs, E8.5 YS CD41+ (E8.5 YS), E14.5 FL Lin-Sca-1+CD48-CD150+ (E14.5 FL), and adult marrow Lin-c-Kit+Sca-1+CD150+CD48- (KLS+SLAM). Sequencing reactions of individual amplicons are represented by each row of circles. Open circles denote unmethylated CpGs, and filled circles represent methylated CpGs. (B) Quantification of %CpG methylation at +23 in hematopoietic populations derived in vivo, ***P < .001, **.001 < P < .01, *.01 < P < .05. (C) Methylation patterns in mESC day 6 embryoid body c-Kit+CD41+ (D6 EB) and from OP9 co-cultures: GFP+c-Kit+CD45+ cells isolated from IRES-GFP control group at day 6 (D6+6 Control); and HOXB4-IRES-GFP group at day 6 (D6+6 HoxB4) and day 11 (D6+11 HoxB4). (D) Quantification of %CpG methylation at +23 in cell populations isolated during hematopoietic differentiation of mESC, ***P < .001, **.001 < P < .01, *.01 < P < .05.

This correlation of +23 hypomethylation and the hematopoietic lineage also occurs during hematopoietic differentiation of mESC. The +23 enhancer is methylated to a high degree in undifferentiated mESCs (84.7% ± 4.23), followed by a significant decrease in day 6 EB c-Kit+CD41+ hematopoietic cells (6.9% ± 1.81) that is maintained in OP9 co-cultured control c-Kit+CD41+ cells at day 6 + 6 (11.4% ± 11.1) and in HOXB4 overexpressing cells at both day 6 + 6 (2.5% ± 1.81) and day 6 +11 (5% ± 1.64) (Figure 3 C-D). To further define the hematopoietic specificity of +23 hypomethylation, we compared the +23 methylation profile of day 6 EB c-Kit+CD41- cells to that of day c-Kit+CD41+ cells since CD41 is the earliest known marker of hematopoiesis[47,127]. We found that +23 hypomethylation strongly correlated with the acquisition of hematopoietic fate as defined by CD41 (70.9% ± 6.1 vs. 6.9% ± 1.81, P = 0.0002) (Figure 4 A). In contrast, there is no statistically significant difference in the methylation of the distal promoter between these populations (Figure 4 B).

Enhancer methylation has been shown to influence gene expression[128]. We examined the expression of the P1 and P2 mRNA in day 6 EB c-Kit+CD41- and c-Kit+CD41+ cells, and found that both P1 and P2 transcriptional activities are increased in c-Kit+CD41+ cells (Figure 4 C). Thus, +23 methylation influences the activity of both *Runx1* promoters in a manner that correlates with CD41 acquisition.

Figure 4.

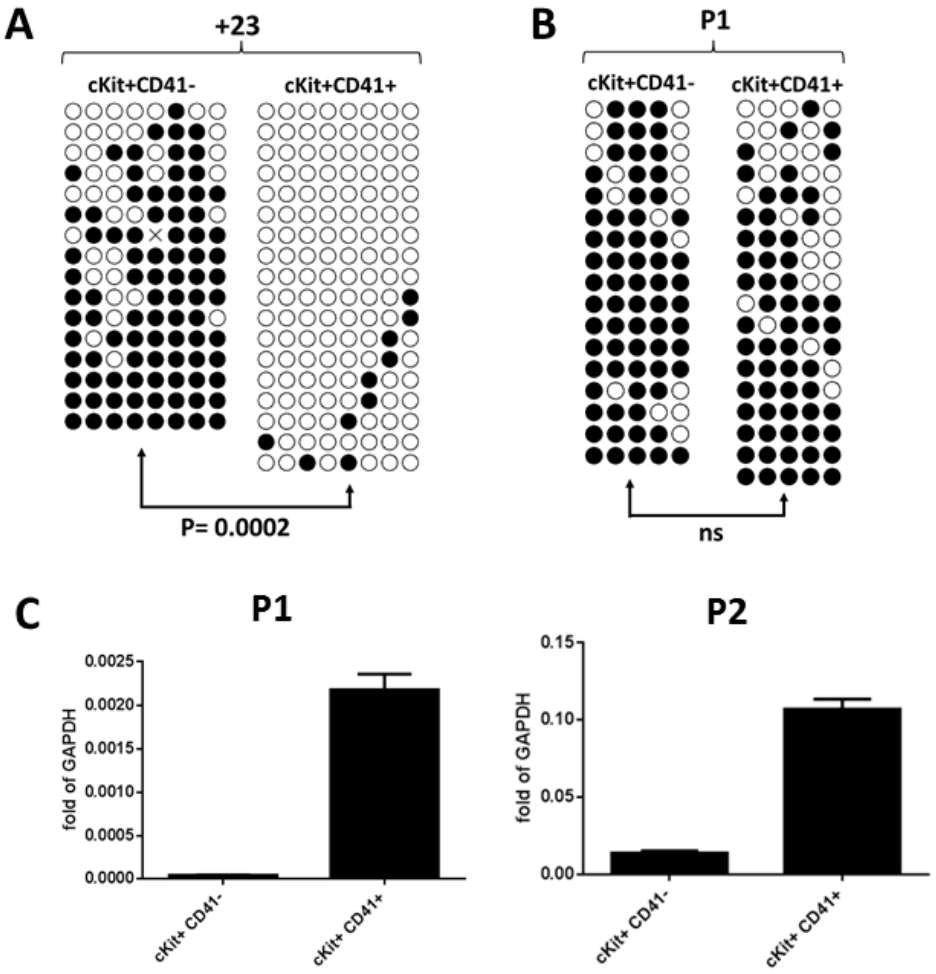

Figure 4. Bisulfite analysis and Runx1 expression in day 6 EB subpopulations

(A) Methylation patterns of the Runx1 +23 enhancer in c-Kit+CD41- and c-Kit+CD41+ cells from day 6 EBs. (B) Methylation patterns of the Runx1 distal (P1) promoter in c-Kit+CD41- and c-Kit+CD41+ cells from day 6 EBs. (C) RT-qPCR analysis of Runx1 P1 and P2 mRNA isoforms in c-Kit+CD41- and c-Kit+CD41+ cells from day 6 EBs.

Distal Runx1 (P1) promoter hypomethylated in HSC in vivo

Several studies have observed that expression of the P1 *Runx1* mRNA isoform is specifically upregulated in definitive hematopoietic cells during development, and comprises the majority of *Runx1* transcript in HSC[101,106,113]. While the proximal P2 promoter is CpG dense and structurally similar to housekeeping promoter elements[100], the distal P1 promoter is more complex in terms of transcription factor binding sites and comparatively CpG poor (46% GC, 0.25 Obs/Exp). Consistent with the definitive hematopoiesis-specific activity of the P1 promoter, a high degree of methylation is observed in MEFs (86.3% ± 3.76) (Figure 5 A-B). Compared to MEFs, there is a modest yet statistically significant decrease in P1 promoter methylation in E8.5 YS CD41+ (48.6% ± 5.45) (Figure 5 A-B). However, an even greater degree of P1 hypomethylation is observed in definitive HSC, where E14.5 FL Lin-Sca-1+CD48-CD150+ (8.1% ± 3.89) and KLS+SLAM (9% ± 5.65) cells exhibit a significantly lower level of P1 methylation compared to E8.5 YS CD41+ cells (Figure 5 A-B).

Figure 5.

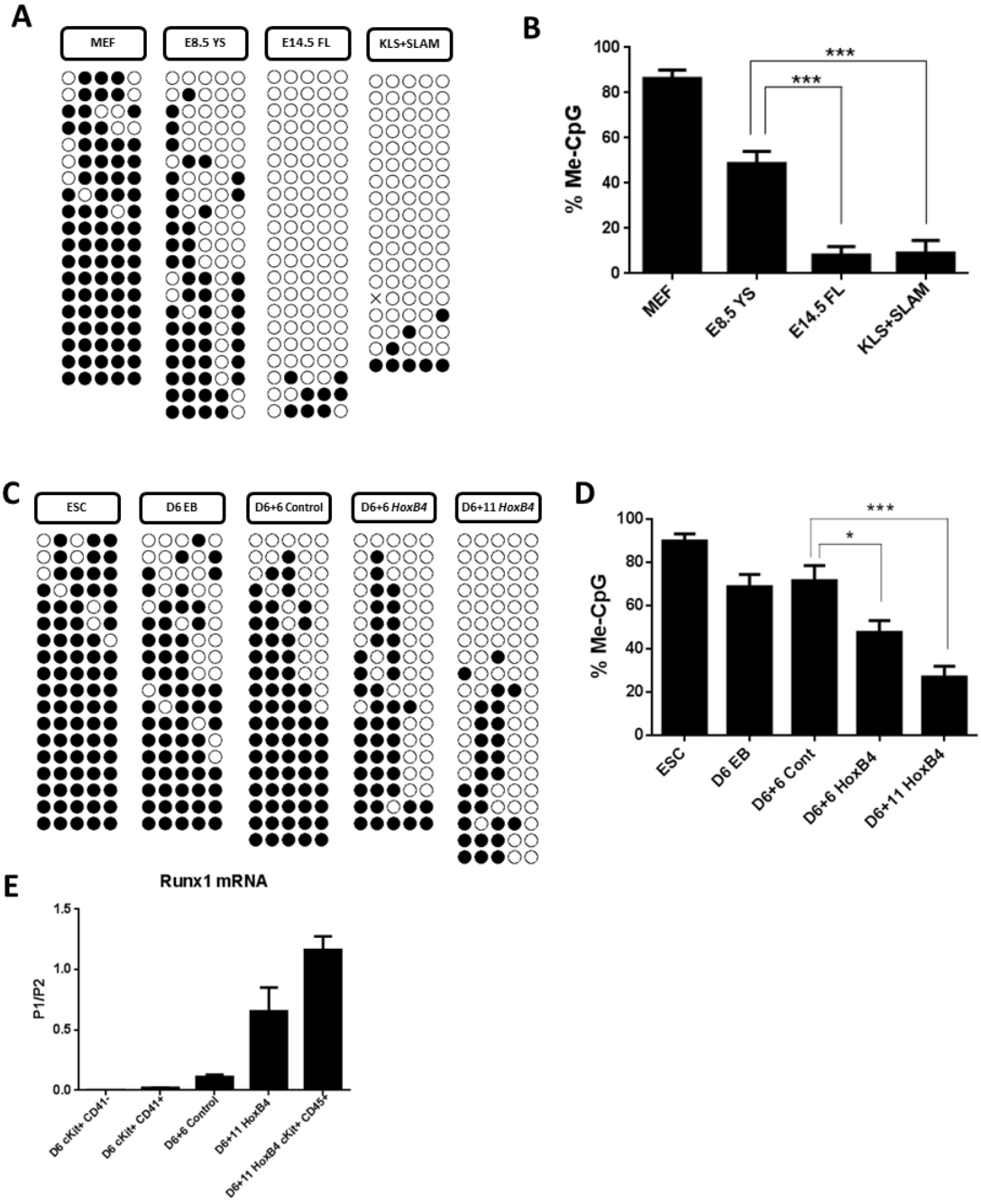
A
MEF
E8.5 YS
E14.5 FL
KLS+SLAM
B
% Me-CpG
***
***
MEF
E8.5 YS
E14.5 FL
KLS+SLAM
C
ESC
D6 EB
D6+6 Control
D6+6 HoxB4
D6+11 HoxB4
D
% Me-CpG
***
*
ESC
D6 EB
D6+6 Cont
D6+6 HoxB4
D6+11 HoxB4
E
Runx1 mRNA
P1/P2
D6 cKit+ CD41-
D6 cKit+ CD41+
D6+6 Control
D6+11 HoxB4
D6+11 HoxB4 cKit+ CD45+

Figure 5. Bisulfite analysis and mRNA expression from distal Runx1 promoter

(A) Methylation patterns of the Runx1 distal (P1) promoter in cells from in vivo-derived E14.5 MEF, E8.5 YS CD41+ (E8.5 YS), E14.5 FL Lin-Sca-1+CD48-CD150+ (E14.5 FL), and adult marrow Lin-c-Kit+Sca-1+CD150+CD48- (KLS+SLAM). Sequencing reactions of individual amplicons are represented by each row of circles. Open circles denote unmethylated CpGs, and filled circles represent methylated CpGs. (B) Quantification of %CpG methylation at P1 in hematopoietic populations derived in vivo, ***P < .001, **.001 < P < .01, *.01 < P < .05. (C) Methylation patterns in mESC, day 6 embryoid body c-Kit+CD41+ (D6 EB) and from OP9 co-cultures: GFP+c-Kit+CD45+ cells isolated from IRES-GFP control group at day 6 (D6+6 Control); and HOXB4-IRES-GFP group at day 6 (D6+6 HoxB4) and day 11 (D6+11 HoxB4). (D) Quantification of %CpG methylation at P1 in cell populations isolated during hematopoietic differentiation of mES cells, ***P < .001, **.001 < P < .01, *.01 < P < .05. (E) P1 mRNA/P2 mRNA levels after normalization to Gapdh over the course of hematopoietic differentiation in vitro.

HoxB4 alters P1 promoter methylation and transcriptional activity in vitro

We next determined whether this *in vivo* epigenetic signature of definitive HSC is replicated during mESC differentiation. Like the +23 enhancer, P1 is highly methylated in undifferentiated mESC (90% ± 3.3) (Figure 5 C-D). Paralleling our results *in vivo*, a modest decrease is observed in day 6 EB c-Kit+CD41+ cells (68.9% ± 5.65) and in OP9 co-cultured control c-Kit+CD45+ cells at day 6 + 6 (71.6% ± 7.06) (Figure 5 C-D). However, in OP9 co-cultured c-Kit+CD45+ cells overexpressing HOXB4, we observe a significant decrease in P1 methylation compared to control cells at day 6 + 6 (47.8% ± 5.4), followed by a further decrease by day 6 + 11 (27% ± 5.08), corresponding to a population shown to possess more robust hematopoietic repopulating potential after adoptive transfer *in vivo* (Figure 5 C-D). These data demonstrate that the *Runx1* P1 promoter is methylated in pluripotent mESC and remains methylated in the first wave of c-Kit+CD41+ hematopoietic progenitors. Maturation to c-Kit+CD45+ progenitors on OP9 alone does not change this methylation profile, whereas overexpression of HOXB4 during this process results in decreased P1 methylation.

To determine whether P1 hypomethylation is linked to promoter switching during differentiation, we examined relative P1 vs. P2 mRNA levels using isoform specific quantitative RT-PCR. As expected, P2 dominates in primitive EB-derived cell populations and in OP9 control co-cultures (Figure 5 E). However, the P1/P2 ratio is higher in HoxB4 overexpressing OP9 co-cultures, and even higher in purified c-Kit+CD45+ hematopoietic cells overexpressing HoxB4 (Figure 5 E).

These data suggest that HoxB4 induced P1 hypomethylation is associated with a consequent increase in the P1/P2 mRNA ratio *in vitro.*

HoxB4 directly activates the Runx1 P1 promoter

It was unclear whether the mechanism underlying HOXB4-mediated activation of P1 was direct, or indirect. To examine this question, we performed chIP analysis in ESC derived hematopoietic cells during differentiation to examine the level of HOXB4 binding at *Runx1* regulatory regions. We find that HOXB4 preferentially binds the P1 promoter upon overexpression at D6+6 and D6+11, thus identifying a direct role for HOXB4 in the modulation of P1 transcriptional activity (Figure 6 A).

We next explored changes in chromatin organization over the time-course of hematopoietic differentiation. Bivalency of lineage-specific genes is a hallmark of pluripotency and involves the co-localization of active (H3K4me3) and repressive (H3K27me3) histone modifications which subsequently resolve to the presence of one or the other during lineage commitment[129]. We find that H3K27me3 is uniformly absent at P1, +23, and P2 as compared to a silenced control region (*Pitx1)* at all time-points, demonstrating that the *Runx1* locus is primed for activation early in the hematopoietic lineage and is not altered by HOXB4 overexpression (Figure 6 B). Consistent with our expression data, H3K4me3 is enriched at the P2 promoter and an active control locus (*Gapdh*) over the course of differentiation and is not altered by HOXB4 (Figure 6 B). Conversely, H3K4me3 presence at the P1 promoter is significantly increased upon overexpression of HOXB4 by D6+6 and is maintained through D6+11

(Figure 6 B). Finally, we find that H3K9Ac – a mark of actively transcribed promoters – is present throughout differentiation at P2, but is significantly increased at P1 only in D6+11 HoxB4 overexpressing cells (Figure 6 C); a finding that is consistent with both our methylation and expression data in that this time-point coincides with the highest degree of P1 hypomethylation and maximal level of P1 expression *in vitro*[130]. From these collective results, we conclude that HOXB4 preferentially binds to the *Runx1* P1 promoter, and stimulates transcription via decreased methylation and establishment of a permissive chromatin state in ESC derived hematopoietic cells.

Figure 6.

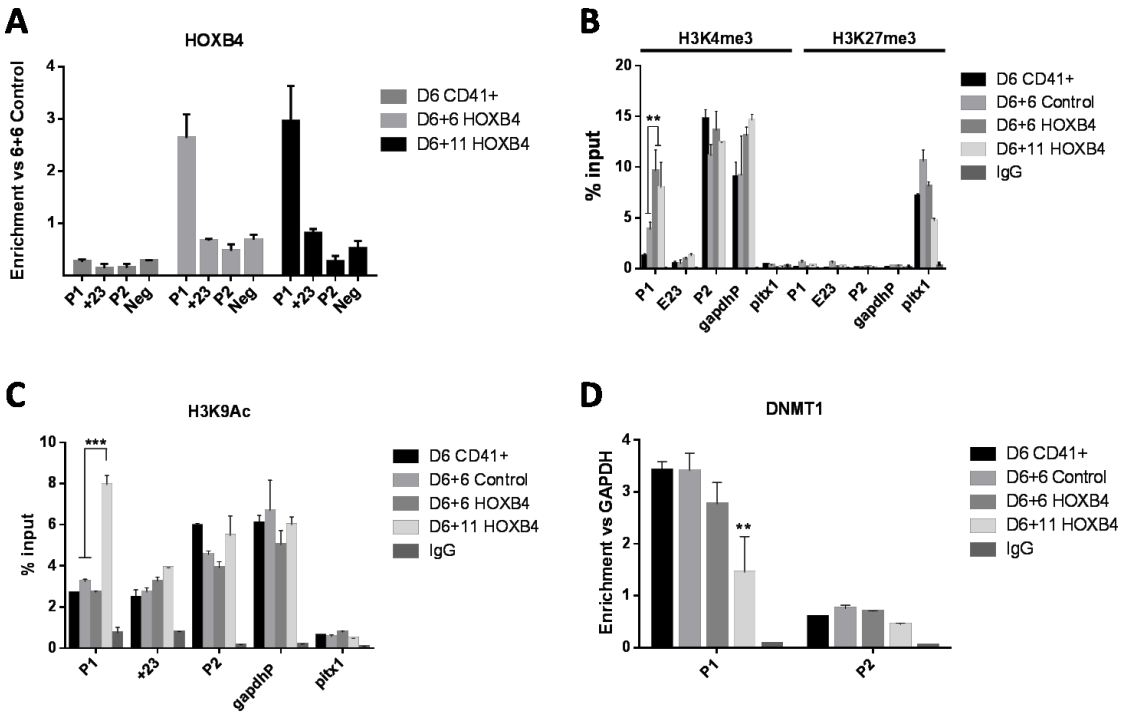
A
HOXB4
Enrichment vs 6+6 Control
D6 CD41+
D6+6 HOXB4
D6+11 HOXB4
P1
+23
P2
Neg
B
H3K4me3
H3K27me3
% input
D6 CD41+
D6+6 Control
D6+6 HOXB4
D6+11 HOXB4
IgG
P1
E23
P2
gapdhP
pitx1
C
H3K9Ac
% input
D6 CD41+
D6+6 Control
D6+6 HOXB4
D6+11 HOXB4
IgG
P1
+23
P2
gapdhP
pitx1
D
DNMT1
Enrichment vs GAPDH
D6 CD41+
D6+6 Control
D6+6 HOXB4
D6+11 HOXB4
IgG
P1
P2

Figure 6. Runx1 chIP analysis

(A) Quantitative PCR analysis of chromatin immunoprecipitation performed against HOXB4. Data were normalized to the percent of pre-immunoprecipitation input for each sample, and are expressed as the fold change versus the D6+6 control population. Data are representative of at least two independent immunoprecipitations. (B) Quantitative PCR analysis of chromatin immunoprecipitation performed against H3K4me3 and H3K27me3. Data are expressed as the percent of pre-immunoprecipitation input for each sample and are representative of at least two independent immunoprecipitations, ***P < .001, **.001 < P < .01, *.01 < P < .05. (C) Quantitative PCR analysis of chromatin immunoprecipitation performed against H3K9Ac. Data are expressed as the percent of pre-immunoprecipitation input for each sample and are representative of at least two independent immunoprecipitations, ***P < .001, **.001 < P < .01, *.01 < P < .05. (D) Quantitative PCR analysis of chromatin immunoprecipitation performed against Dnmt1. Data are expressed as the fold change versus Gapdh control locus for each sample and are representative of at least two independent immunoprecipitations, ***P < .001, **.001 < P < .01, *.01 < P < .05.

Dnmt1 occupancy at P1 is decreased in HOXB4 overexpressing cells

DNA methylation patterns are either maintained during replication via the activity of the maintenance methyltransferase DNMT1, or established *de novo* by DNMT3a and DNMT3b[131-133]. To determine whether the loss of methylation at P1 is accompanied by decreased interaction with members of the DNA methyltransferase family, we measured the level of DNMT1, DNMT3a, and DNMT3b occupancy at the *Runx1* promoters. We did not detect binding of DNMT3a or DNMT3b to P1 (data not shown), however we found that DNMT1 did interact with P1, and this interaction was significantly decreased at D6+11 in HOXB4 overexpressing cells (Figure 6 D). As expected, occupancy was universally low at the hypomethylated P2 promoter at all time-points (Figure 6 D). These data are consistent with a mechanism in which DNMT1 is occluded from accessing the P1 promoter in the presence of HOXB4, resulting in a gradual loss of established methylation patterns over subsequent cell divisions.

Runx1 P1 methylation as signature of definitive HSC

Finally, to compare our *in vivo* and *in vitro* observations that P1 methylation is correlated with definitive HSC during development we grouped all cell populations studied based on whether or not they are known to possess hematopoietic repopulating capacity and compared mean levels of P1 promoter methylation. This comparison indicated that P1 promoter hypomethylation correlated with repopulating capacity in a similar fashion *in vivo* and *in vitro* (Figure 7 A). To increase the resolution of P1 promoter demethylation we applied

the same grouped comparison to the individual CpG dinucleotides in the P1 promoter and found that overall methylation was significantly decreased for each CpG, with the exception of the CpG located at position -371 relative to the P1 transcription start site. In particular, the CpGs located at position -436 and -271 were the most significantly different between repopulating and non-repopulating cell types (Figure 7 B).

Figure 7.

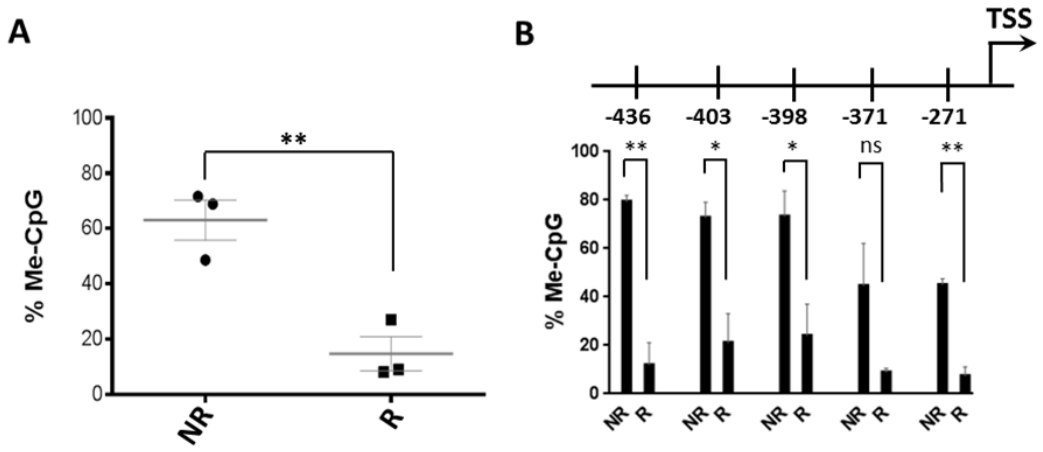

Figure 7. Comparison of P1 methylation in repopulating and non-repopulating cell types

(A) %CpG methylation at P1 promoter in repopulating (R) and non-repopulating (NR) cell populations. Bar indicates the mean, ***P < .001, **.001 < P < .01, *.01 < P < .05; unpaired t test. (B) Percent methylation at individual CpG within P1 promoter in repopulating (R) and non-repopulating (NR) cell populations. Bar indicates the mean, ***P < .001, **.001 < P < .01, *.01 < P < .05; unpaired t test.

Discussion

Here, we identify previously un-described changes in DNA methylation at *Runx1* regulatory regions during hematopoietic development. These changes are associated with commitment to the hematopoietic lineage, and distinguish definitive repopulating HSC populations from earlier, primitive non-repopulating cells. We find that the CpG dense proximal P2 promoter is unmethylated in mESC, and remains unmethylated regardless of lineage and stage of hematopoietic development. Conversely, the +23 intronic enhancer is methylated in mESC, non-hematopoietic fibroblasts, and c-Kit+CD41- cells from day 6 EBs, but is dramatically hypomethylated upon acquisition of CD41 and remains unmethylated throughout hematopoietic development. Importantly, we demonstrate that hypomethylation of the distal P1 *Runx1* promoter is specific to cell populations enriched in definitive repopulating capacity *in vivo*. Moreover, in mES-derived c-Kit+CD41+ hematopoietic progenitors, the distal P1 promoter remains methylated at similar levels to that observed in E8.5 YS. Overexpression of HOXB4 results in a significant decrease in P1 methylation consistent with its ability to generate mES-derived hematopoietic progenitors capable of long-term repopulation in transplant recipients[87]. Thus, our results identify hypomethylation of the distal *Runx1* promoter as a novel epigenetic signature of repopulating hematopoietic cells during development, and provide critical insight into the dynamic epigenetic changes influencing the *Runx1* locus.

The developmental processes leading to the formation of definitive HSC rely on the properly orchestrated activity of a complex network of critical

transcription factors to guide genetic programs associated with differentiation. *Runx1* is a critical transcription factor involved in the development of definitive HSC[95,96,110] and, not surprisingly, is frequently dis-regulated in hematopoietic malignancy[94,111]. A diverse array of *Runx1* mRNA isoforms have been identified[134], and arise through a combination of alternative splicing as well as alternate promoter usage[100,101,112,135]. As methods for genome-wide analysis of CpG methylation have improved, a growing number of TDMR associated with normal and abnormal development have been identified[136]. Previously, it was unknown whether the *Runx1* regulatory regions are TDMR. In the case of the *Runx1* proximal P2 promoter, our data now indicate it is not a TDMR as P2 is unmethylated in a wide array of cell types. This observation is consistent with previous reports at other CpG rich core promoters[123,124], and is supported by genome wide DNA methylation profiles released by the ENCODE Consortium[126]. That the P2 methylation pattern is established at the pluripotent stage, and does not change in differentiated cell types or during hematopoietic development suggests that methylation of the P2 does not influence lineage specific changes in P2 transcription during development. It seems unlikely that P2 methylation acts as an “on/off” switch since the P2 isoform is detected in a diverse array of cell types[125], including undifferentiated mESCs[137], and the P2 promoter remains unmethylated in FL and adult HSC even though P1 is the dominant promoter in these populations[101,106,113]. Therefore, our observations suggest that P2 methylation is not involved in the lineage restriction of P2 during development. Intriguingly, intragenic TDMR 3’ of P2 have been identified, raising the possibility

that methylation at these regions could have a role in the regulation of P2 activity[114].

In contrast to the proximal promoter, the +23 intronic enhancer is a TDMR, and while the hematopoietic specific activity of the *Runx1* +23 enhancer element is documented[99], our data are the first to identify changes in CpG methylation at the +23 enhancer element during hematopoietic development. Previous data indicating that methylation of intronic enhancer elements influences tissue-specific gene expression[128], further supports a role for +23 enhancer methylation in the transcriptional activity of *Runx1*. We confirm this hypothesis by clearly demonstrating that +23 hypomethylation strongly correlates with increased transcription at both *Runx1* promoters at the earliest stage of hematopoietic development, though P2 remains the dominant mRNA isoform in these populations. There is evidence that intragenic DNA methylation influences alternate promoter usage[118], however our observations indicate that +23 hypomethylation is not a significant factor in the observed P1/P2 switch, but rather acts as an epigenetic rheostat for the *Runx1* locus, mediating hematopoietic specific amplification of *Runx1* expression. We cannot rule out the possibility that +23 hypomethylation facilitates a more permissive state for P1 transcription by allowing improved mRNA elongation[138], though this does not fit our observation that +23 enhancer methylation is lost early in development when P2 still dominates compared to adult HSC[101,113]. Considering our data that P1 hypomethylation results in a shift to P1 biased expression, a more probable explanation is that +23 methylation is a non-biased regulator of transcription from

both promoters, and the usage bias is determined by the epigenetic status of P1. Studies utilizing clonal cell populations with well-defined mRNA isoform expression profiles, or episomal reporters in which methylation can be artificially manipulated might help to refine the role of methylation in regulating promoter usage, however the utility of these assays is limited by the lack of developmental and genomic context. Regardless, our data clearly demonstrate that +23 methylation influences its enhancer capacity, and provide a novel epigenetic signature of the hematopoietic lineage which can be applied to optimize methods for direct conversion of other lineages to a hematopoietic fate[139].

Derivation of robust numbers of *in vivo* long-term repopulating HSC from pluripotent cell sources such as ES and induced pluripotent stem cells is of therapeutic interest. Critical to the success of these efforts is the identification of signatures associated with the formation of definitive HSC during development. While their precise role in the regulation of gene transcription is not-fully understood, TDMR and differential DNA methylation has nonetheless proven useful for identifying differences in cell populations. This is highlighted by the utilization of DNA methylation patterns to determine whether somatic cells have been successfully reprogrammed to a pluripotent state[140,141]. We have identified the P1 distal *Runx1* promoter as a novel TDMR, and demonstrate that hypomethylation of this region differentiates primitive non-repopulating progenitors and definitive repopulating HSC during embryonic development *in vivo*. Our observation that unmodified hematopoietic progenitors derived from mESC do not undergo this decrease in P1 methylation suggests a failure in the

epigenetic transition to adult-type definitive hematopoiesis. By overexpressing HOXB4 in ESC derived hematopoietic cells we show it is possible to promote epigenetic remodeling of the Runx1 locus during differentiation of ESC to hematopoietic cells *in vitro*. The hypomethylation of P1 induced by HOXB4 results in an increased P1/P2 mRNA ratio, and thus links P1 hypomethylation to the P2 to P1 promoter switch observed during hematopoietic development. Mechanistically, we show that when overexpressed, HOXB4 preferentially binds P1, supporting a model in which the epigenetic remodeling and increased transcription of P1 is mediated via physical interaction of HOXB4 with this locus. Recent HOXB4 chIP-Seq data support our findings that HOXB4 interacts with the *Runx1* distal promoter, albeit using a slightly different ESC differentiation method, suggesting that this is a robust biological phenomenon[93]. Whether demethylation of P1 in the presence of HoxB4 is an active or passive process remains unclear. However our observation that P1 methylation is only slightly decreased at D6+6 and becomes more pronounced by D6+11 is congruent with a passive loss of methylation. This is supported by reports finding that active demethylation often occurs rapidly—within minutes or hours, and results in nearly complete de-methylation of the region in question[142,143]. As HOXB4 physically binds Runx1 P1, it is conceivable that HOXB4 or a HOXB4-associated complex could physically or functionally occlude the activity of factors involved in maintaining DNA methylation, such as Dnmt1. Indeed, our data demonstrating a decrease in Dnmt1 occupancy of P1 in HOXB4 overexpressing cells is consistent with this model. Over successive rounds of DNA replication this would result in a loss of

Runx1 P1 methylation. Previous reports that differentiation induced hypomethylation of lineage specific CpG-poor promoters correlate with transcription factor binding further supports this explanation[144].

The fact that epigenetic remodeling of P1 could be achieved by overexpressing HOXB4 demonstrates that this *in vivo* epigenetic signature is valid during ES cell differentiation and can potentially be replicated if the appropriate extracellular cues are applied during the differentiation process, whether *in vivo* or *in vitro*, via the induction of appropriate transcription factor circuits. Our single CpG group analysis identifies the CpGs located -436 and -271 from the P1 transcription start site as the most significantly hypomethylated in definitive repopulating cell populations, and presents an attractive target for high-throughput analysis of changes in P1 methylation during hematopoietic differentiation of ESC/iPS.

Acknowledgments

We wish to thank Troy Lund, Mark Osborn and Istvan Szatmari for valuable advice and technical assistance.

Supplemental Tables

Table S1. Bisulfite primers and amplicon properties

Locus	Forward Primer	Reverse Primer	Amplicon Size	#CpGs
P1	TGTTTTTATTAAGAATTTAGTTTTTT	CTTTTCTTACTCTCTCTATCCTATAC	219bp	5
+23	ACTACTACAAAAACAAACTACCCAC	TTTTTAAAGAGTTTGGGATGTTGATA	151bp	8
P2	TGATTTTTAGGTTTAGGGTTTTTT	AACCCAAATTCAAATCCCAC	184bp	18

Supplemental Figures

Figure S1.

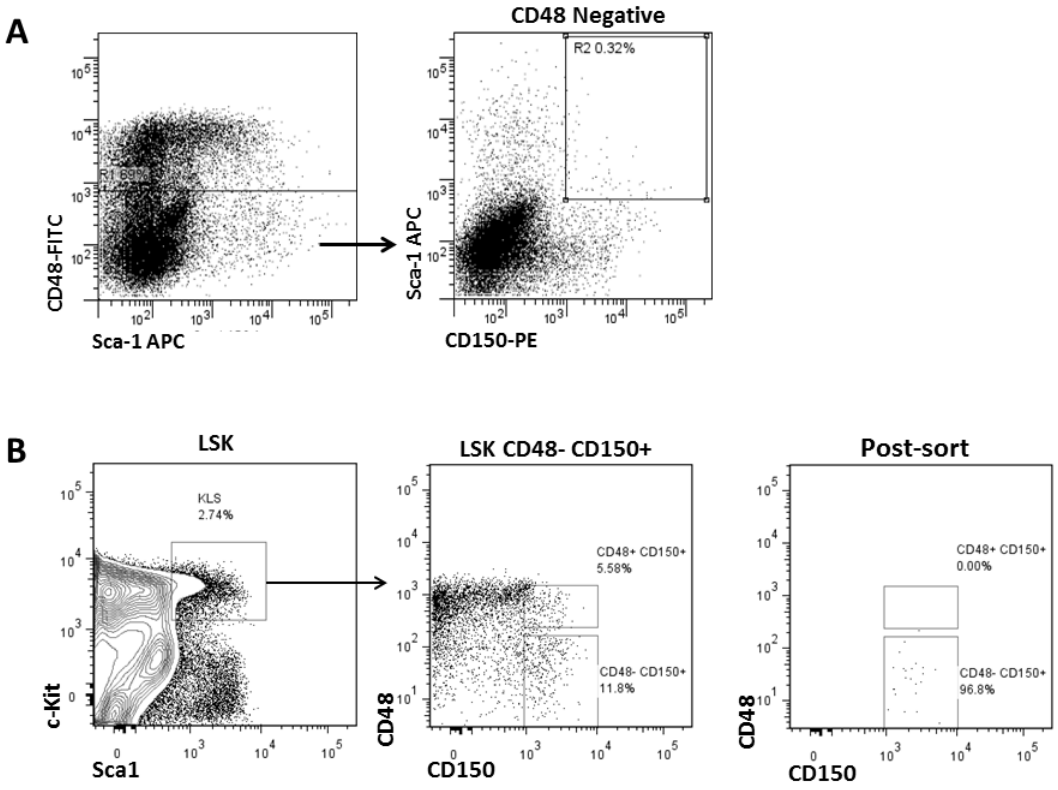

Figure S1. Surface antigen profiles and purification of E14.5FL and KLS+SLAM.

(A) Representative surface antigen profile and gating strategy used to enrich Sca-1+CD48-CD150+ from E14.5 FL after magnetic bead depletion of lineage positive fraction. (B) Isolation of linage negative c-Kit+Sca-1+CD48-CD150+ (KLS+SLAM) fraction from adult marrow after magnetic bead depletion of lineage positive fraction.

Figure S2

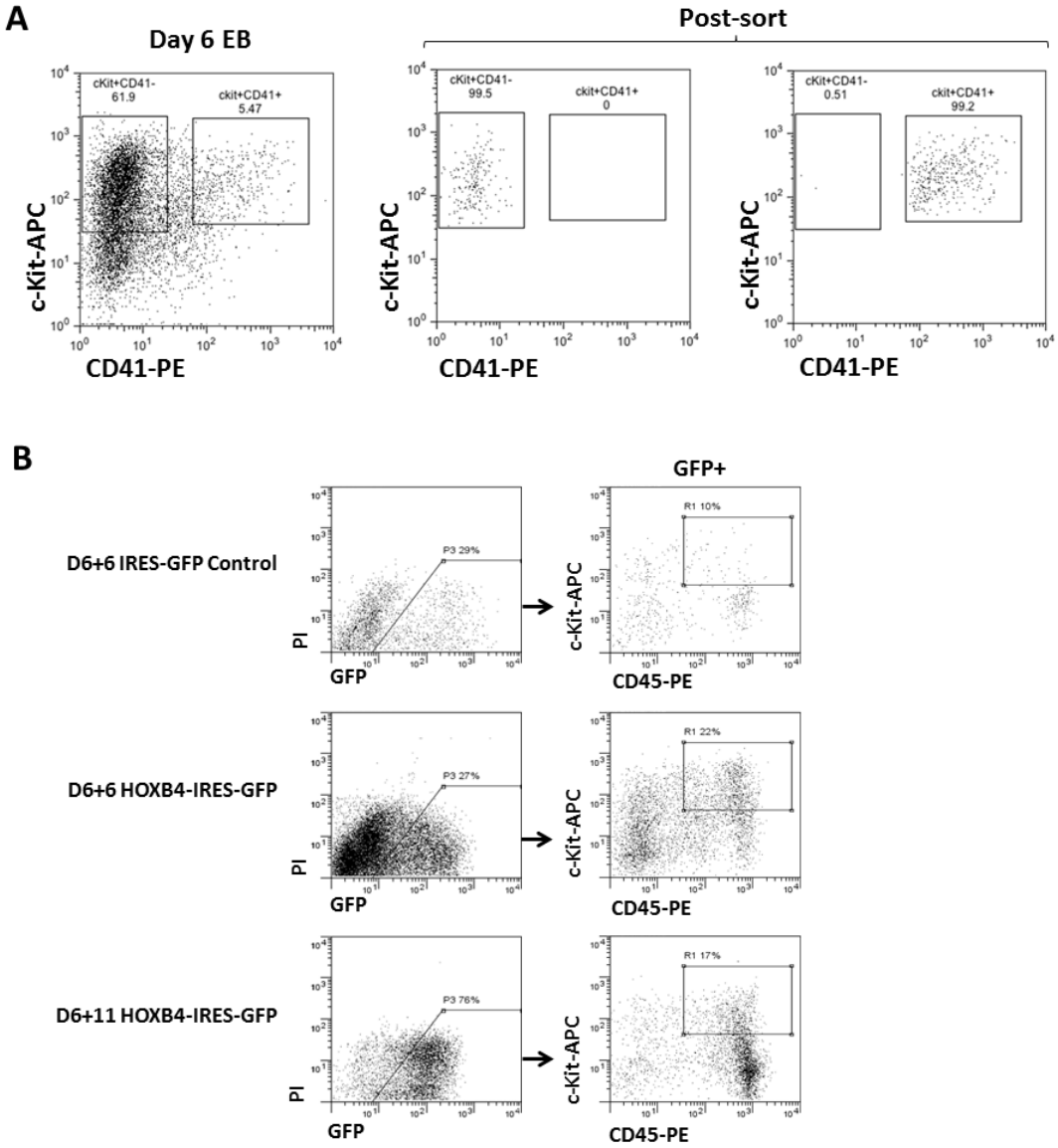

Figure S2. Surface antigen profiles and purification of hematopoietic populations from ES cell differentiations.

(A) Surface antigen profile and FACS purification of c-Kit+CD41- and c-Kit+CD41+ cell fractions from day 6 EBs. (B) Representative surface antigen profile and gating strategy used to isolate GFP+c-Kit+CD45+ population from OP9 co-cultures.

Chapter 3.

Targeted single copy Runx1 reporter mESC lines for interrogation and enhancement of definitive hematopoiesis from mESC

Foreward

The association of *Runx1* promoter switching with formation of definitive HSC provides a unique molecular signature with which to characterize definitive hematopoietic cells during *in vitro* differentiation of PSC. We generated clonal mESC lines harboring targeted, single copy fluorescent reporter constructs under transcriptional control of combinations of known *Runx1* regulatory elements. In this system, the P1 and P2 promoters are capable of directing subtly different, but hematopoietic specific transcription. The strength and specificity of each promoter is increased by the +23 enhancer, though this effect is biased toward the activity of the associated promoter. Dual-fluorescent and bio-luminescent reporter constructs containing all elements in their appropriate *cis* context accurately reflected endogenous *Runx1* promoter switching. Day 8 embryoid body subpopulations delineated by promoter activity exhibited unique surface antigen profiles and differ in their expression of key hematopoietic transcriptions factors. We find that virtually all multi-potential CFC in day 8 embryoid bodies are contained within the P1+ population, and identify specific stromal based co-culture conditions that allow the expansion of hematopoietic progenitors within this population. Our dual-bioluminescent reporter allows non-invasive and highly sensitive analysis of *Runx1* expression, making it ideal for high-throughput screening applications. Altogether, our novel dual-promoter reporter mESC lines provide a new platform for identifying conditions promoting definitive hematopoiesis, and the compact nature of our synthetic reporter constructs will

allow their rapid transfer into knockout mESC lines and disease model derived induced pluripotent stem cells (iPSC) for further investigation.

Introduction

Pluripotent stem cells (PSC) have the potential to serve as a renewable source of hematopoietic stem cells (HSC) for transplant, however current differentiation strategies are biased toward the generation of primitive hematopoietic cells that are incapable of long-term multilineage engraftment posttransplant. As many phenotypic and molecular pathways are shared by primitive and definitive hematopoiesis, identification of discrete signatures of each has been difficult. Long-term engraftment remains the gold standard benchmark for definitive HSC, but is inherently retrospective and logistically taxing; thus restricting its application to very low throughput screens. Efforts to enhance specification toward definitive hematopoiesis would be fostered by the development of new phenotypic and molecular signatures that distinguish definitive from primitive waves of hematopoiesis; particularly those that are amenable to high-throughput screens and/or prospective isolation of rare definitive progenitors during *in vitro* differentiation.

The runt-related transcription factor, *Runx1,* is specifically required in hemogenic endothelium for successful transition to HSC during embryonic development, and is thus a useful genetic indicator of the hematopoietic lineage during *in vitro* differentiation of PSC[71,145]. Its utility as a specific indicator of definitive hematopoiesis is precluded however, by the fact that it is also expressed in early yolk-sac, prior to the formation of intra-embryonic definitive HSC[101,103]. Transcription of the *Runx1* locus can be further subdivided based on the activities of alternative proximal (P2) and distal (P1) promoter elements

[104,134,135]. Interestingly, the transcriptional activity of these promoters is developmentally regulated, such that the activity of the proximal promoter predominates in primitive hematopoiesis and hemogenic endothelium, while the distal promoter becomes active only in definitive hematopoietic progenitors, and is the dominant promoter in fetal liver (FL) and adult HSC[101-103,112,146]. In light of this observation, P1 promoter activity and the presence of its associated mRNA isoform, Runx1c, would serve as a useful indicator of the onset of definitive hematopoiesis during PSC differentiation.

The exploitation of P1 driven *Runx1* expression as a novel molecular signature of definitive hematopoiesis is hampered by the fact that, as an intracellular transcription factor, it can only be detected by RT-PCR of Runx1c mRNA, or by intracellular staining of the associated protein isoform; neither of which is amenable to the prospective isolation of viable cells for subsequent characterization. To circumvent this issue, the regulatory elements of the P1 promoter could be co-opted to drive the expression of proteins that are more readily detectable without the need for cell disruption, i.e. fluorescent, bioluminescent, and membrane bound proteins. Indeed, minimal regulatory regions of both the P1 and P2 promoters have been identified, however in plasmid based reporter assays and in transgenic animals, neither promoter was capable of driving hematopoietic transcription [99,100]. Instead, hematopoietic specificity of each promoter relied on the presence of an enhancer element (+23) located within the first intron[99]. This element was capable of driving hematopoietic specific transcription from both P1, P2, and a heterologous

promoter element via its interaction with Gata2, Ets factors, and the SCL/Lmo2/Ldb1 complex[98]. Unfortunately, these studies did not identify a setting in which the specific activity of the P1 promoter element could be replicated. Alternatively, Sroczynska *et al.* took the approach of targeting reporter encoding cDNAs to the P1 and P2 loci in murine embryonic stem cells (mESC), which effectively allowed the dissection of their discrete activities during *in vitro* and *in vivo* hematopoietic development[103]. This elegant study confirmed the definitive specific activity of the P1 promoter and allowed the prospective isolation of P1+ cells by fluorescence activated cell sorting (FACS), however this approach requires two laborious gene targeting steps and is thus impractical for application in knockout mESC lines and disease model derived induced pluripotent stem cells (iPSC); applications which would be valuable to the investigation of novel regulatory pathways involved in the specification of definitive hematopoiesis and the effects that certain diseases have on this process. In addition, knock in strategies usually disrupt one allele of the gene in question, which may have unintended consequences. This is particularly true for *Runx1,* as its expression levels are tightly regulated and autoregulatory mechanisms have been identified[135,147]. Not surprisingly, *Runx1* haploinsufficiency has documented biological consequences[148,149] . The development of synthetic, readily transferrable reporter constructs that recapitulate the *Runx1* promoter switch would overcome many of these limitations.

In the present study, we used an mESC line that allows efficient targeting of DNA constructs to the transgene permissive hypoxanthine guanine

phoshoribosyl transferase 1 (*Hprt*) locus to generate a panel of clonal mESC lines harboring single copy fluorescent reporter constructs under the transcriptional control of different combinations of *Runx1* regulatory elements [119]. Using these lines, we find that endogenous *Runx1* promoter switching is accurately reported when the P1, +23, and P2 regulatory elements are in *cis,* and in their appropriate genomic orientation. Our dual fluorescent and bioluminescent reporter mESC lines allowed the non-invasive monitoring and prospective isolation of cell populations based on promoter activity. These subfractions were distinct in their surface antigen profiles and in the expression of key hematopoietic transcription factors. We found that the P1+ population contained nearly all multi-potential colony-forming cells (CFC) in day 8 EBs, and exhibited the most robust hematopoietic expansion in stromal based co-cultures. Finally, we demonstrate the utility of this system by identifying a specific set of culture conditions that are most effective in expanding hematopoietic progenitors from the P1+ population.

Materials and Methods

Generation of p2Lox reporter constructs

P1, P2, and +23 constructs were cloned from genomic DNA by PCR using primers that were previously described[99]. Creation of reporter constructs was performed using standard overlap based isothermal assembly[150], and inserted into PacI and Not1 linearized p2Lox. Primers used for cloning are available upon request.

ESC culture, differentiation, and genetic modification

mESC were cultured on irradiated murine embryonic fibroblasts (MEFs) in KO DMEM (Gibco) supplemented with 15% FBS, 0.1 mM nonessential amino acids (GIBCO), 2 mM glutamax, (Invitrogen), penicillin/streptomycin (Gibco), 0.1 mM β-mercaptoethanol, and 1000 U/mL LIF(Millipore), at 37°C in 5% CO_2. ES cells were differentiated as embryoid bodies (EB) as previously described[119]. Briefly, mESC were aggregated in hanging drops EB media consisting of IMDM supplemented with 15% FBS, 6 μM monothioglycerol (Sigma), 200 μg/ml human iron-saturated holo-transferrin (Sigma), 50 μg/ml ascorbic acid (Sigma), and penicillin-streptomycin (Gibco) in 5% CO_2 at 37°C for 48 hrs. Hanging drop EBs were transferred to 10 cm ultra-low adherence dish (Corning) in EB media and incubated on an orbital shaker at 70 rpm in 5% CO_2 at 37°C. After an additional 24 hours an 80% media change was performed and EBs were returned to shaking incubation for three days. For two-dimensional HE cultures, day 4 Flk1+ cells were plated onto gelatin coated plates in the indicated media and assessed

48hr later. Inducible cassette exchange mediated targeting of reporter constructs to *Hprt* was performed as previously described[119].

Stromal co-culture and HOXB4 overexpression

AGM stromal lines were maintained as previously described[151]. For co-culture experiments, day 8 EB derived mCherry+GFP+ cells were plated onto sub-confluent stroma in hematopoietic expansion (HE) media consisting of Iscove's Modified Dulbecco's Medium (IMDM) supplemented with 10% FBS, 5 ng/mL VEGF (Peprotech), 40 ng/mL TPO (Peprotech) , 40 ng/mL Flt-3L (Peprotech), and where indicated, 20 ng/ml Il-3 and IL-6; penicillin/streptomycin (Gibco), 2 mM glutamax (Invitrogen) in 5% O2. For HoxB4 overexpression experiments, day 6 EBs were dissociated and transduced with either MSCV-IRES-GFP control or MSCV-HoxB4-IRES-GFP via spin infection at 2500 rpm for 1.5 hrs followed by 4 hrs additional contact with viral supernatant. Cells were washed with PBS, and plated onto sub-confluent OP9 in HE media supplemented with 10% FBS, 5 ng/mL VEGF, 40 ng/mL TPO, and 40 ng/mL Flt-3L. Cells were passed every 4-5 days.

Colony forming unit assays

Individual colony assays were conducted with 50,000 input cells and plated in M3434 (StemCell Technologies) on 35mm dishes. Primitive erythroid colonies were counted after 6 days, all other colonies counted at day 10.

FACS analysis and cell purification

Flow analysis was performed on BD Fortessa. Fluorescence-activated cell sorting was performed using FACSAria. All antibodies were from eBioscience

unless otherwise noted. Embryoid body and stroma co-cultures were stained with c-Kit-APC (2B8), CD41-PacBlue (Mwreg-30), CD45-APC eFluor780 (30-F11), Tie2-PE (Tek4), Cd11b- APC eFluor780 (M1/70)and CD150-PE (mShad). Flk1+ cells were enriched using Flk1-APC (Avas12a1), and purified with Anti-APC microbeads (Miltenyi) according to manufacturer recommendations.

Quantitative RT-PCR

RNA was isolated using the RNeasy Plus Micro kit (Qiagen). First-strand cDNA synthesis was performed using the Superscript VILO cDNA Synthesis kit (Invitrogen). Runx1 isoform specific RT-qPCR was performed using Platinum SYBR Green qPCR Supermix (Invitrogen), and normalized to GAPDH. Primers used for isoform specific RT-PCR were described previously[113]. All other expression analyses were performed using Taqman gene expression assays, and the following probe sets: Runx1 Mm01213404_m1, Gata1 Mm01352636_m1, Gata2 Mm00492301_m1, Gata3 Mm00484683_m1, PU.1 Mm03048233_m1, SCL Mm01187033_m1.

Bioluminescence imaging

Bioluminescent imaging was conducted using the Xenogen IVIS imaging system (Caliper Life Sciences, Hopkinton, MA) according to manufacturer instructions. Data are presented as total flux.

Statistics

Statistical analysis was performed using a Student *t* test, with P value less than 0.05 considered significant.

Results

Inducible cassette exchange allows rapid generation of targeted, single copy *Runx1* reporter mESC lines

The activity of randomly integrated tissue-specific reporter constructs is influenced by both copy-number and the chromatin structure of their integration site, making the unbiased interrogation of regulatory element function difficult. As previous studies have shown that tissue-specific regulatory elements retain their fidelity when targeted to the ubiquitously expressed *Hprt* locus, we reasoned that this setting would allow unbiased examination of *Runx1* regulatory element activity during *in vitro* differentiation of mESC[152-154]. To test this hypothesis, we generated reporter constructs in which GFP is under the transcriptional control of the P1 or P2 promoters alone, or in combination with the +23 enhancer region[99] (Figure 1 A). To overcome the relatively low efficiency of homology based targeting, we used a previously described mESC line in which the *Hprt* locus can be targeted with high efficiency via cre/lox mediated inducible cassette exchange (ICE)[119]. Using the ICE system, we were able to rapidly generate a panel of clonal mESC lines harboring single copies of our reporter constructs at the *Hprt* locus (Figure 1 B).

Figure 1.

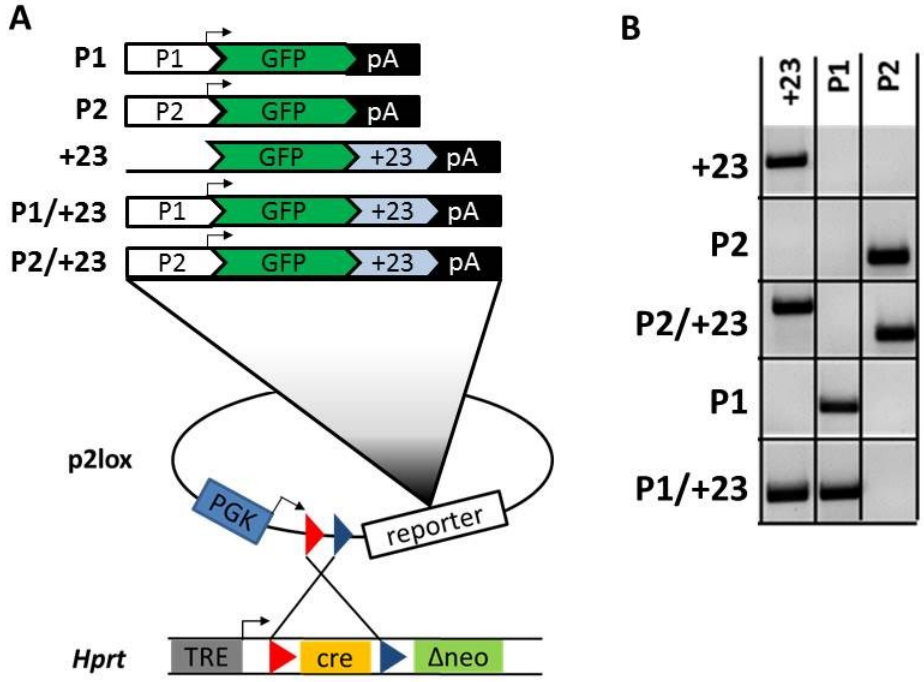

Figure 1. Construct design and *Hprt* targeting in mESC

(A) Construct design and cre/lox recombination mediated targeting to the *Hprt* locus. In the presence of cre, p2Lox cassette replaces cre ORF at *Hprt* and places a PGK promoter and ATG upstream of neomycin resistance gene. (B) PCR based genotyping analysis of clonal mESC lines after selection and expansion.

Hematopoietic specificity of *Runx1* reporter constructs during *in vitro* differentiation of mESC

To assess the hematopoietic specificity of *Runx1* regulatory elements in our mESC lines, we differentiated them as EB and performed flow cytometry based analysis of GFP expression at day 6, when hematopoietic progenitor activity becomes readily detectable[155] (Figure 2 A). As CD41 is the earliest marker of the hematopoietic lineage during mouse development, we examined the co-expression of GFP and CD41[127]. In contrast to previous reports, we find that both the P1 and P2 promoters alone are sufficient to enrich GFP expression in CD41+ hematopoietic cells (Figure 2 B). Consistent with previous studies, we show that the +23 element is sufficient to promote hematopoietic specific transcription, and increases both the intensity and specificity of hematopoietic transcription from the P1 and P2 promoters (Figure 2 C). Runx1 P2 expression is specifically required in Tie2+ hemogenic endothelial cells for their subsequent transition to P1+ definitive hematopoietic cells[103]. To determine whether our individual reporter constructs reflected this pattern, we examined the co-expression of GFP and Tie2 in day 6 EB. As expected, the P2 and P2/+23 EBs have the highest percentage of Tie2+GFP+ cells (Figure 2 D). When compared to P2 and P2/+23, we find that a higher proportion of Tie2+GFP+ cells in the +23, P1, and P1/+23 EBs co-express CD41, suggesting that the transcriptional activity of these constructs reflects either a subset of HE undergoing endothelial-hematopoietic transition (EHT), or post-EHT hematopoietic cells that have not yet lost Tie2.

To test these two scenarios, we placed day 4 P1/+23 EB derived Flk1+ cells in two-dimensional culture and examined HE clusters for the expression of GFP and CD41 by fluorescence microscopy. We find that GFP+ cells are present in morphologically distinct clusters of adherent and non-adherent cells and that these cells co-express CD41 (Figure 2 F). This pattern of labeling adherent and non-adherent cells is also observed when day 4 Flk1+ cells are co-cultured with hematopoietic supportive OP9 stromal cells (Supplementary Figure 1 A). Based on these observations, we conclude that the P1/+23 construct labels CD41+ HE prior to the completion of EHT, and that this labeling continues in post-EHT hematopoietic cells.

Altogether, these data demonstrate that ICE mediated *Hprt* targeting allows rapid, unbiased examination of *Runx1* regulatory element activity during *in vitro* differentiation of mESC. All elements drive hematopoietic specific labeling, though subtle differences are observed between constructs. In particular, the P2 promoter appears to restrain +23 enhancer activity to CD41- HE, while the P1 promoter reinforces +23 activity in CD41+ cells emerging from HE. That the P1/+23 construct specifically labels emerging hematopoietic cells with high specificity suggests it may be optimal to screen for conditions that promote the emergence of *Runx1*+ hematopoietic cells during *in vitro* differentiation of mESC. Indeed, this construct reflects endogenous *Runx1* expression with high fidelity (Supplemental Figure 1 B).

Figure 2

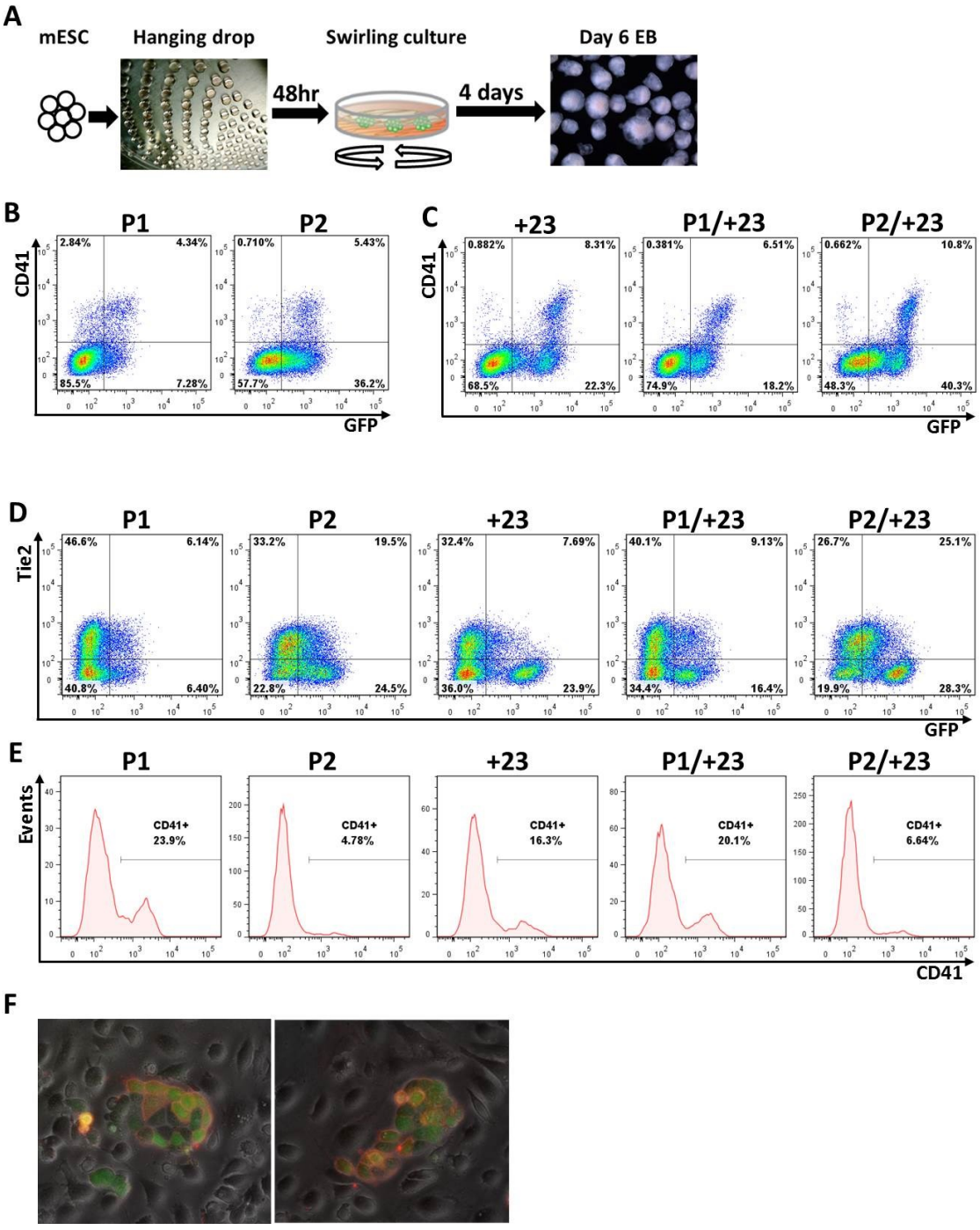
A
mESC
Hanging drop
48hr
Swirling culture
4 days
Day 6 EB
B
P1
P2
CD41
GFP
2.84%
4.34%
85.5%
7.28%
0.710%
5.43%
57.7%
36.2%
C
+23
P1/+23
P2/+23
CD41
GFP
0.882%
8.31%
68.5%
22.3%
0.381%
6.51%
74.9%
18.2%
0.662%
10.8%
48.3%
40.3%
D
P1
P2
+23
P1/+23
P2/+23
Tie2
GFP
46.6%
6.14%
40.8%
6.40%
33.2%
19.5%
22.8%
24.5%
32.4%
7.69%
36.0%
23.9%
40.1%
9.13%
34.4%
16.4%
26.7%
25.1%
19.9%
28.3%
E
P1
P2
+23
P1/+23
P2/+23
Events
CD41
CD41+
23.9%
CD41+
4.78%
CD41+
16.3%
CD41+
20.1%
CD41+
6.64%
F

Figure 2. Activity of *Runx1* reporter constructs in day 6 embryoid bodies.

(A) Embryoid body differentiation of reporter mESC. (B) FACS analysis of CD41 and GFP expression in P1 and P2 reporter EBs at day 6. (C) FACS analysis of CD41 and GFP expression in +23, P1/+23, and P2/+23 reporter EBs at day 6. (D) FACS analysis of Tie2 and GFP expression in reporter EBs at day 6. (E) FACS analysis of CD41 expression within the Tie2+GFP+ population of reporter EBs at day 6. (F) Fluorescence microscopy images of CD41 (red) and GFP (green) localization in adherent HE clusters formed during two-dimensional culture of day 4 EB Flk1+ cells.

Runx1 dual-promoter reporter constructs allow simultaneous monitoring of distinct hematopoietic populations during *in vitro* differentiation of mESC

The fact that the P1 and P2 promoters exhibit differential effects on the +23 enhancer suggested that these promoters may also exert contextual effects on each other. To assess this possibility, we generated dual-fluorescent and bioluminescent reporter constructs containing the P1, +23, and P2 regulatory elements in their appropriate genomic order and targeted them to the *Hprt* locus in mESC (Figure 3 A). To determine whether this context altered the activity of either promoter during differentiation, we performed FACS analysis of P1 driven GFP and P2 driven mCherry (Figure 3 A) expression over the course of EB differentiation. Consistent with previous reports of P2 derived Runx1b mRNA expression in mESC[137], day 1 EBs contain a residual mCherry+GFP- population that decreases rapidly and is virtually absent by day 3. At day 5 mCherry+GFP- cells reappear and increase in frequency by day 6, at which point their percentage plateaus until decreasing between days 7 and 8. Interestingly, a small population of mCherry+GFP+ cells emerges at day 6 and increase in frequency until day 8, when a distinct mCherry+GFP+ population is evident (Figure 3 B). In day 6 EB, the mCherry+GFP- and mCherry+GFP+ populations contain a higher frequency of CD41+ cells than the mCherry-GFP- population, however the highest level of CD41+ enrichment is observed in the mCherry+ GFP+ population. Consistent with our single-promoter findings, mCherry+GFP-Tie2+ cells are preferentially CD41-, whereas mCherry+GFP+Tie2+ cells are preferentially CD41+ (Figure 3 C). Additionally, we find that the mCherry+GFP+

subpopulation is highly enriched in cKit+CD41+ progenitors at day 6 compared to both the mCherry-GFP- and mCherry+GFP- fractions (Figure 3 D). Thus, while similarities exist between the activities of the P1 and P2 promoters in our single- and dual-promoter constructs, there are also notable differences; namely, P1-GFP+ cells are generally less frequent in the dual-promoter EBs at day 6, while their enrichment of CD41+ cells is higher. Taken together, these data demonstrate that the inclusion of all elements in *cis* results in the dynamic temporal labeling of phenotypically distinct cell populations during *in vitro* differentiation of mESC.

Figure 3

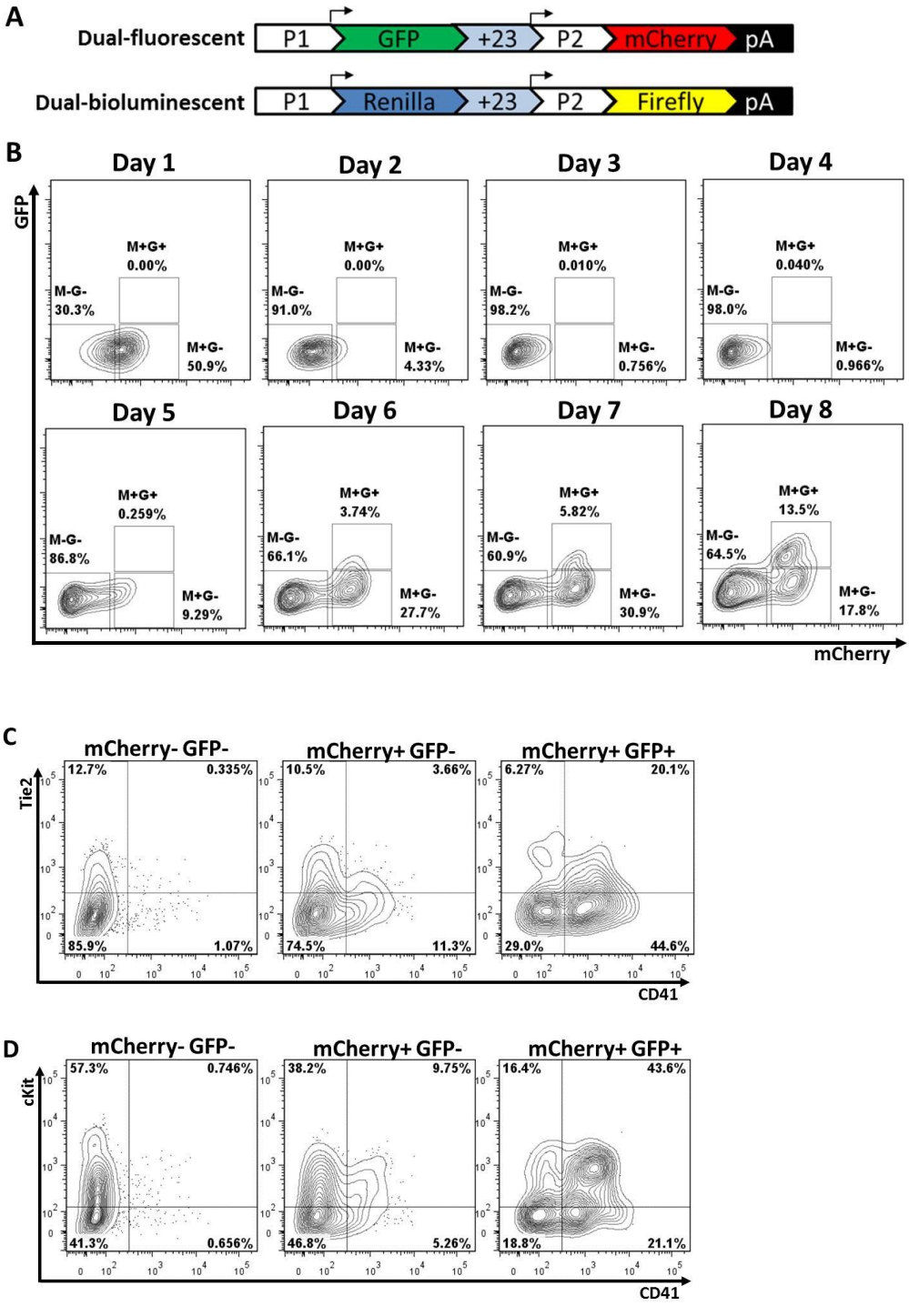
A
Dual-fluorescent
P1
GFP
+23
P2
mCherry
pA
Dual-bioluminescent
P1
Renilla
+23
P2
Firefly
pA
B
Day 1
M+G+ 0.00%
M-G- 30.3%
M+G- 50.9%
Day 2
M+G+ 0.00%
M-G- 91.0%
M+G- 4.33%
Day 3
M+G+ 0.010%
M-G- 98.2%
M+G- 0.756%
Day 4
M+G+ 0.040%
M-G- 98.0%
M+G- 0.966%
Day 5
M+G+ 0.259%
M-G- 86.8%
M+G- 9.29%
Day 6
M+G+ 3.74%
M-G- 66.1%
M+G- 27.7%
Day 7
M+G+ 5.82%
M-G- 60.9%
M+G- 30.9%
Day 8
M+G+ 13.5%
M-G- 64.5%
M+G- 17.8%
GFP
mCherry
C
mCherry- GFP-
12.7%
0.335%
85.9%
1.07%
mCherry+ GFP-
10.5%
3.66%
74.5%
11.3%
mCherry+ GFP+
6.27%
20.1%
29.0%
44.6%
Tie2
CD41
D
mCherry- GFP-
57.3%
0.746%
41.3%
0.656%
mCherry+ GFP-
38.2%
9.75%
46.8%
5.26%
mCherry+ GFP+
16.4%
43.6%
18.8%
21.1%
cKit
CD41

Figure 3. Dual-promoter reporter constructs and activity of dual-fluorescent construct during embryoid body differentiation

(A) Diagram of *Runx1* dual-reporter constructs targeted to *Hprt*. (B) FACS analysis of mCherry and GFP expressing populations over the time-course of EB differentiation. (C) Fluorescence activated cell sorting (FACS) analysis of Tie2 and CD41 expression within the mCherry/GFP sub-populations in day 6 EB. (D) FACS analysis of cKit and CD41 expression within mCherry/GFP sub-populations in day 6 EB.

Dual-promoter reporter constructs accurately reflect endogenous *Runx1* differential promoter usage

The distinct temporal and cell-type specific activities of the *Runx1* promoters in our dual-fluorescent construct resembled previous descriptions of endogenous *Runx1* promoter switching during development [101-103,113]. We thus wondered whether the dynamic reporter expression pattern observed during differentiation of our reporter mESC lines accurately reflected endogenous *Runx1* promoter usage. To address this question, we FACS purified the mCherry-GFP-, mCherry+GFP-, and mCherry+GFP+ sub-populations from day 8 EB (Figure 4 A), and examined the levels of endogenous P1 and P2 derived mRNA isoforms in each population by reverse-transcription quantitative polymerase chain reaction (RT-qPCR). Both the mCherry-GFP+ and mCherry+GFP+ populations express higher levels of the P1 and P2 isoforms than mCherry-GFP- cells, however P1 derived mRNA levels are ~4-fold higher in mCherry+GFP+ versus mCherry+GFP- cells (Figure 4 B). Because it is not possible to prospectively FACS enrich the equivalent populations from our dual-bioluminescent reporter line, we instead compared the levels of P1-*Renilla* and P2-Firelfy luciferases in day 5 EBs to that of day 6 EB, as this time-point represented the first appearance of P1+ cells in our dual-fluorescent reporter experiments. We find that the levels of both P2-*Firefly* and P1-*Renilla* are higher in day 6 versus day 5 EB, which reflects endogenous *Runx1* mRNA isoform levels in both temporal specificity and magnitude (Figure 4 C, D).

Figure 4

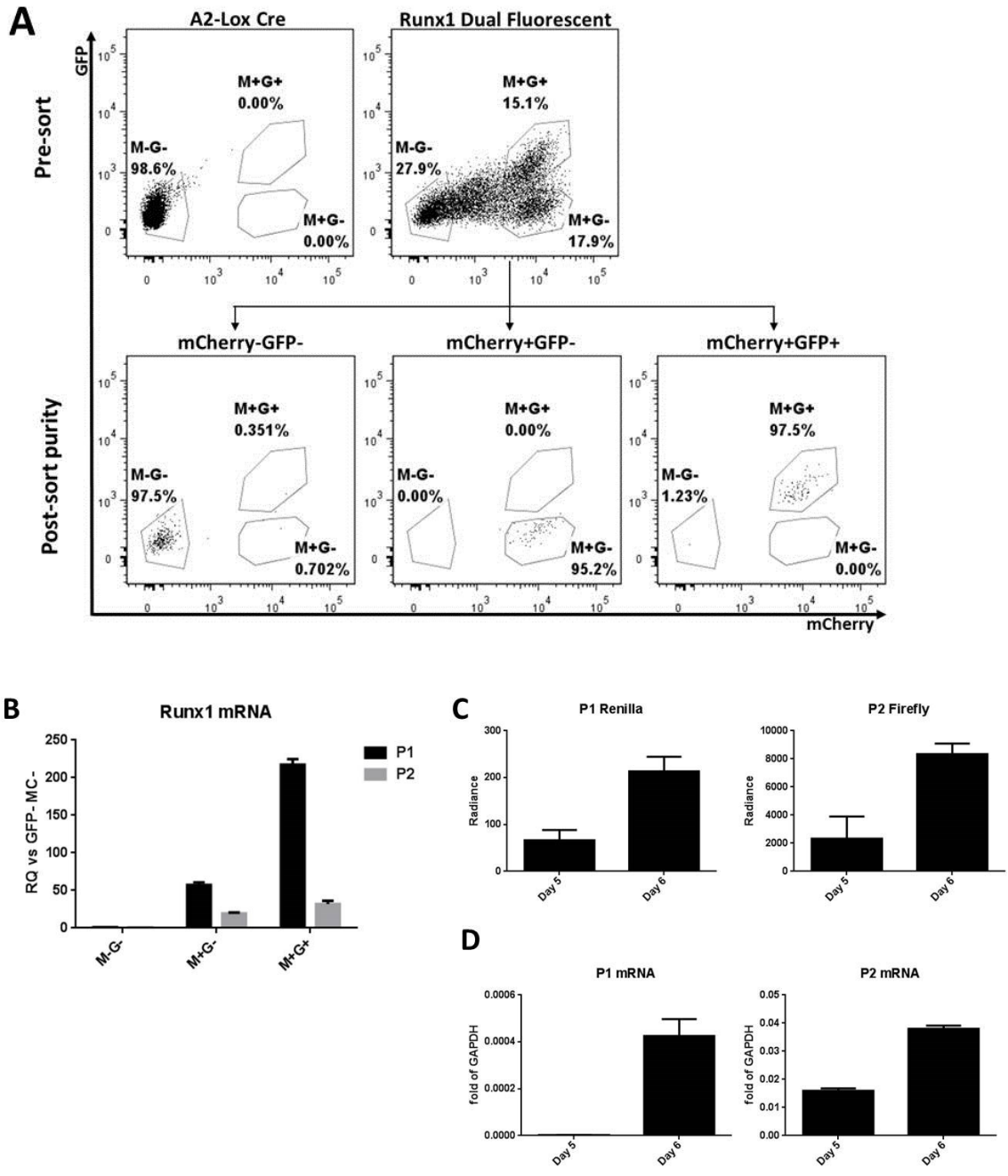
A
A2-Lox Cre
Runx1 Dual Fluorescent
Pre-sort
GFP
M+G+
0.00%
M-G-
98.6%
M+G-
0.00%
M+G+
15.1%
M-G-
27.9%
M+G-
17.9%
mCherry-GFP-
mCherry+GFP-
mCherry+GFP+
Post-sort purity
M+G+
0.351%
M-G-
97.5%
M+G-
0.702%
M+G+
0.00%
M-G-
0.00%
M+G-
95.2%
M+G+
97.5%
M-G-
1.23%
M+G-
0.00%
mCherry
B
Runx1 mRNA
RQ vs GFP- MC-
P1
P2
M-G-
M+G-
M+G+
C
P1 Renilla
P2 Firefly
Radiance
Day 5
Day 6
D
P1 mRNA
P2 mRNA
fold of GAPDH

Figure 4. Relationship of endogenous *Runx1* mRNA isoforms and dual-reporter construct activity.

(A) Fluorescence activated cell sorting (FACS) based purification of mCherry/GFP sub-populations from dual-fluorescent reporter EBs at day 8. (B) RT-qPCR analysis of *Runx1* isoform expression in FACS purified mCherry-GFP- (M-G-), mCherry+GFP- (M+G-), and mCherry+GFP+ (M+G+) subpopulations in day 8 EB. (D) P1-*Renilla* and P2-*Firefly* activity and RT-qPCR analysis of *Runx1* isoform expression in day 5 and 6 dual-bioluminescent EB.

The mCherry+GFP+ population is enriched with definitive hematopoietic potential in day 8 embryoid bodies

The establishment of defined mCherry/GFP subpopulations in day 8 EB (Figure 5 A), suggested that these populations may represent cell types with distinct hematopoietic potential. To investigate this further, we first assessed the surface antigen profile of these subpopulations in day 8 EB. Pan hematopoietic labeling by CD41 in the early embryo is gradually replaced by CD45 beginning at the time of definitive hematopoietic formation in the AGM, and remains the predominant marker of the hematopoietic lineage into the adult [47,156]. This pattern is reflected in EB, where CD45+ cells are not readily detectable until day 7, which lead us to wonder whether the mCherry/GFP subpopulations at day 8 exhibited differential expression of CD41 and CD45. As expected based on our previous results, the mCherry+GFP- and mCherry+GFP+ populations contain higher proportions of CD41+ cells than the mCherry-GFP- population. A subset of CD41+ cells co-express CD45 in both mCherry+GFP- and mCherry+GFP+ populations, however the mCherry+GFP+ fraction contains a dramatically higher proportion of CD41+CD45+ cells (Figure 5 B). Furthermore, it appears that as CD45 expression increases, CD41 expression begins to decrease, suggesting that these cells are transitioning toward a definitive CD41-CD45+ phenotype. To assess the progenitor content of the hematopoietic fractions, we examined the co-expression of cKit in the CD41 and CD45 populations. Similar to our day 6 results, the mCherry+GFP+ population contained the majority of cKit+CD41+ and cKit+CD45+ cells (Figure 5 C), with a greater proportion of cKit+CD41+ cells co-

expressing CD45 in the mCherry+GFP+ fraction (Figure 5 D). It was previously reported that mESC derived HSC derived via the enforced expression of *Cdx4* and *HoxB4* express the HSC specific SLAM family antigen CD150 [157]. Upon examining the expression of CD150 within the mCherry/GFP subpopulations, we found the mCherry+GFP+ population to contain the highest frequency of CD150+ cells, further suggesting that this fraction contains a population enriched with definitive hematopoietic potential (Figure 5 F).

The distinct surface antigen profiles of each subpopulation suggested that there may also exhibit distinct molecular profiles. To examine this possibility, we examined the expression levels of key hematopoietic transcription factors in each subpopulation by RT-qPCR. GATA family members 1-3 play distinct roles during hematopoietic development; *Gata3* expression in non-hematopoietic cells of the AGM promotes HSC formation[158], while both *Gata1* and *Gata2* are cell intrinsic regulators of hematopoietic cell development[64,76,159]. Reflecting this, we find that the predominantly non-hematopoietic mCherry-GFP- population expresses the highest levels of *Gata3*, and while both *Gata1* and *Gata2* mRNA levels are higher in the mCherry+GFP- and mCherry+GFP+ populations, *Gata2* expression is specifically enriched in the mCherry+GFP+ fraction (Figure 5 G). The transcription factor SCL, which is required for hemangioblast formation, is enriched within the mCherry+GFP- and mCherry+GFP+ fractions, as is the transcription factor PU.1, which is critically required for the formation of definitive HSC and is a direct target of Runx1; interestingly, PU.1 expression is highest within the mCherry+GFP+ population (Figure 5 H). Taken together, the surface

antigen profiles and gene expression signatures show that the mCherry/GFP sub-fractions represent phenotypically distinct cell populations. Both the mCherry+GFP- and mCherry+GFP+ populations are enriched with hematopoietic cells; however our data suggest that definitive hematopoietic cells are specifically contained with mCherry+GFP+ population.

Figure 5 A-D

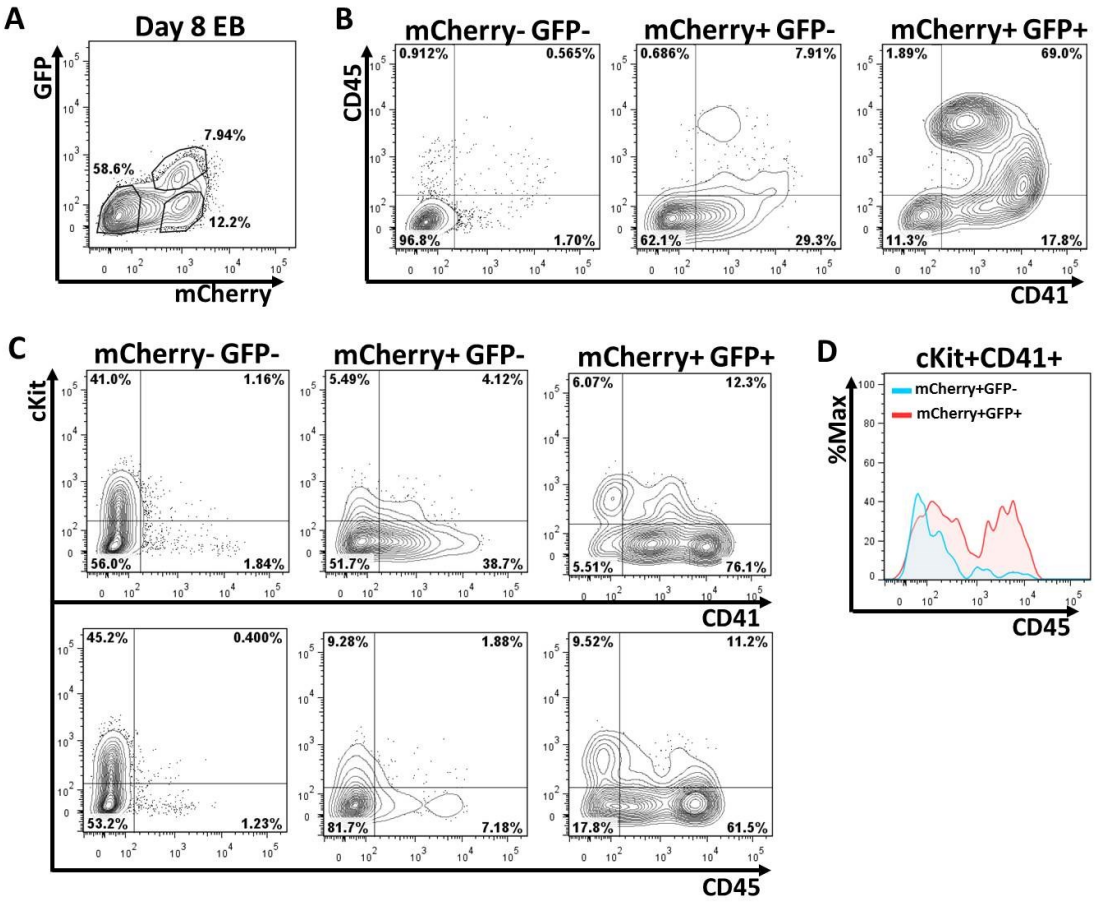
A
Day 8 EB
GFP
mCherry
58.6%
7.94%
12.2%
B
mCherry- GFP-
mCherry+ GFP-
mCherry+ GFP+
CD45
CD41
0.912%
0.565%
96.8%
1.70%
0.686%
7.91%
62.1%
29.3%
1.89%
69.0%
11.3%
17.8%
C
mCherry- GFP-
mCherry+ GFP-
mCherry+ GFP+
cKit
CD41
CD45
41.0%
1.16%
56.0%
1.84%
5.49%
4.12%
51.7%
38.7%
6.07%
12.3%
5.51%
76.1%
45.2%
0.400%
53.2%
1.23%
9.28%
1.88%
81.7%
7.18%
9.52%
11.2%
17.8%
61.5%
D
cKit+CD41+
%Max
mCherry+GFP-
mCherry+GFP+
CD45

Figure 5 E-G

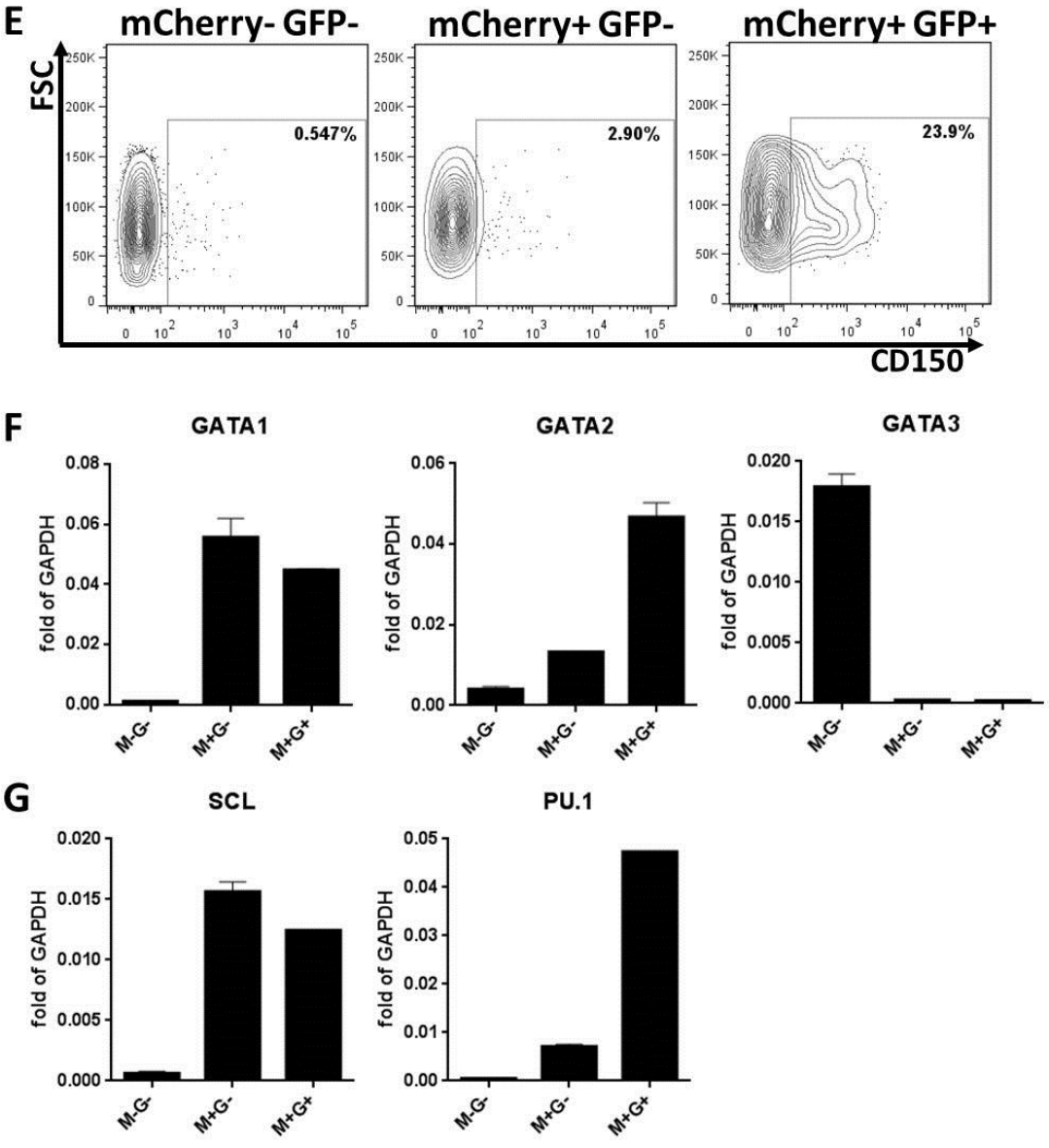
E
mCherry- GFP-
mCherry+ GFP-
mCherry+ GFP+
FSC
CD150
0.547%
2.90%
23.9%
F
GATA1
GATA2
GATA3
fold of GAPDH
M-G-
M+G-
M+G+
G
SCL
PU.1

Figure 5. Phenotypic and molecular analysis of mCherry/GFP subpopulations in day 8 EB.

(A) FACS analysis of mCherry and GFP expression showing the gating strategy used in subsequent analysis. (B) FACS analysis of CD41 and CD45 expression within mCherry/GFP subfractions. (C) FACS analysis of cKit/CD41 and cKit/CD45 expression within mCherry/GFP subfractions. (D) Co-expression of CD45 in the cKit+CD41+ subfraction of the mCherry+GFP- and mCherry+GFP+ populations. (E) FACS analysis of CD150 expression within the mCherry/GFP subfractions. (F) RT-qPCR analysis of *Gata1, Gata2,* and *Gata3* mRNA expression in the mCherry-GFP- (M-G-), mCherry+GFP- (M+G-), and mCherry+GFP+ (M+G+) subfractions. (G) RT-qPCR analysis of *Scl* and *Pu.1* mRNA expression in mCherry-GFP- (M-G-), mCherry+GFP- (M+G-), and mCherry+GFP+ (M+G+) subfractions.

Multi-lineage and definitive erythroid colony forming unit activity resides within the mCherry+GFP+ population

Our phenotypic and molecular analyses suggested that the mCherry+GFP+ population is highly enriched with definitive hematopoietic progenitors. To determine whether this was true at a functional level, we performed methylcellulose based colony forming unit (CFU) assays with the individual mCherry/GFP subpopulations from day 8 EB. Consistent with our phenotypic analysis, virtually all multilineage CFU activity is restricted to the mCherry+GFP+ subfraction (Figure 6 A). While the mCherry+GFP- and mCherry+GFP+ populations contain similar numbers of early forming primitive erythroid CFU (EryP), later-developing definitive erythroid CFU (EryD) are restricted to the mCherry+GFP+ subfraction (Figure 6 B). These data confirm our phenotype based results, and conclusively demonstrate that definitive hematopoietic progenitor activity is restricted to the mCherry+GFP+ subfraction in day 8 EB.

Figure 6

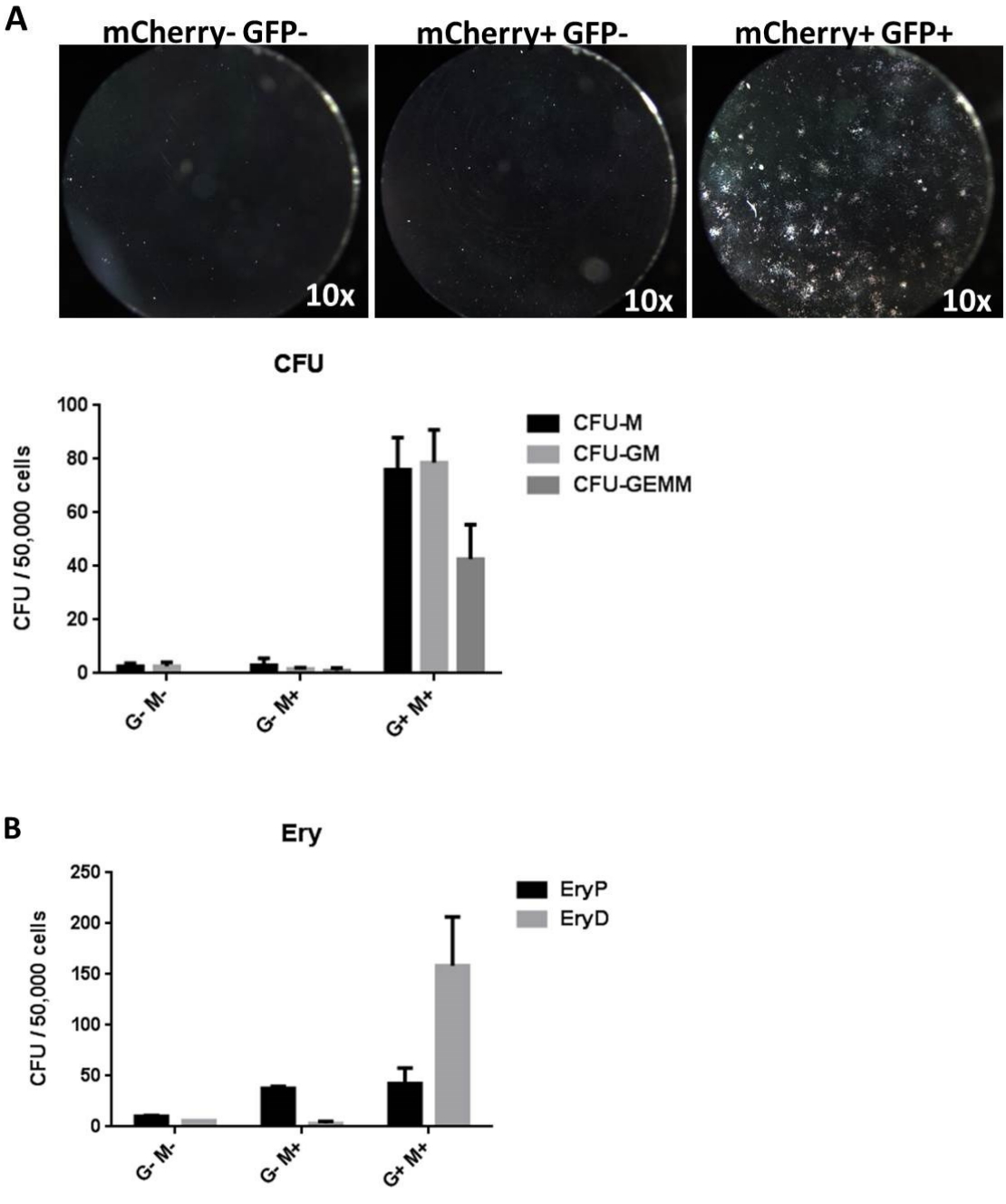
A
mCherry- GFP-
mCherry+ GFP-
mCherry+ GFP+
10x
10x
10x
CFU
CFU / 50,000 cells
100
80
60
40
20
0
CFU-M
CFU-GM
CFU-GEMM
G- M-
G- M+
G+ M+
B
Ery
CFU / 50,000 cells
250
200
150
100
50
0
EryP
EryD
G- M-
G- M+
G+ M+

Figure 6. Colony forming unit activity in day 8 EB mCherry/GFP subfractions.

(A) Qualitative and quantitative analysis of CFU activity in day 8 EB mCherry-GFP- (M-G-), mCherry+GFP- (M+G-), and mCherry+GFP+ (M+G+) subfractions. CFU-M (macrophage), CFU-GM (granulocyte-macrophage), CFU-GEMM (granulocyte-erythrocyte-macrophage-megakaryocyte) (B) Quantitative analysis of erythroid CFU activity in day 8 EB mCherry-GFP- (M-G-), mCherry+GFP- (M+G-), and mCherry+GFP+ (M+G+) subfractions. EryP (primitive erythroid), EryD (definitive erythroid).

Differential effects of hematopoietic stroma and cytokine combinations on the expansion of day 8 EB derived mCherry+GFP+ cells

We next sought to identify preliminary culture conditions that were capable of expanding day 8 EB mCherry+GFP+ derived hematopoietic progenitors. As stromal cells derived from hematopoietic organs have shown utility for this purpose, we tested the capacity of bone marrow derived OP9, and AGM region derived AM20.1B4 and UG26.1B6 stromal lines to expand mCherry+GFP+ progenitors, since these lines have shown the ability to expand and/or support hematopoietic differentiation and expansion from embryonic stem cells[83,151,160]. Since OP9 co-culture coupled with Flt3L, TPO, SCF, and VEGF promotes the efficient expansion of mESC-HSC derived via the overexpression of HOXB4, we used this as our baseline for comparison[87]. Both IL-3 and IL-6 have been shown to promote the formation of embryonic HSC and/or enhance the expansion and maintenance of adult HSC *ex vivo*; therefore we assessed the effect of adding IL-3, or IL-3 and IL-6 to FTSV supplemented stromal co-cultures [93,161,162]. Day 8 EB mCherry+GFP+ were FACS purified and 3.0 x 10^4 viable cells were plated onto sub-confluent stroma and cultured for an additional 6 days (D8+6) before analysis. In general, dual-positivity was retained most effectively by the AGM stromal lines, whereas a fraction of mCherry+GFP- cells was present within the OP9 co-cultures at D8+6. Neither IL-3 or IL-6 had a substantial effect in the AGM lines, however IL-3 appears to promote the retention of mCherry+GFP+ cells on OP9 (Figure 7 A). Bead-enhanced FACS quantification of absolute cell numbers in D8+6 co-cultures found that, in general, the AGM lines are more effective at

expanding mCherry+GFP+ cells than OP9, with the AM20.1B4 line appearing to be most effective (Figure 7 B). The expanding hematopoietic cell populations are morphologically diverse (Supplemental Figure 2 A, B), and predominantly of the myeloid lineage as evidenced by the expression of CD11b (Figure 7 C); particularly in the AGM lines, which unlike OP9, contain a functional M-CSF gene. While this could be interpreted as a higher frequency of differentiation, it is worth noting that definitive HSC in the fetal liver express CD11b[121]. Nonetheless, compared to OP9, the AGM stromal lines maintain the highest percentage of cKit+CD45+ hematopoietic progenitors, and addition of IL-3 and IL-3/IL-6 to the AGM co-cultures does not substantially alter this capacity; however, IL-3 does appear to slightly enhance the retention of cKit+CD45+ cells in the OP9 co-cultures (Figure 7 D). Collectively, these data suggest that the microenvironment present within AGM co-cultures is most conducive to the expansion of both mCherry+GFP+ and cKit+CD45+ cells from day 8 EB. The fact that IL-3 enhances the supportive effects of OP9 but not AGM stroma suggests that OP9 may produce suboptimal levels of endogenous IL-3 compared to the AGM lines, which is consistent with the known production of IL-3 by AGM stroma *in vivo* [161].

Figure 7

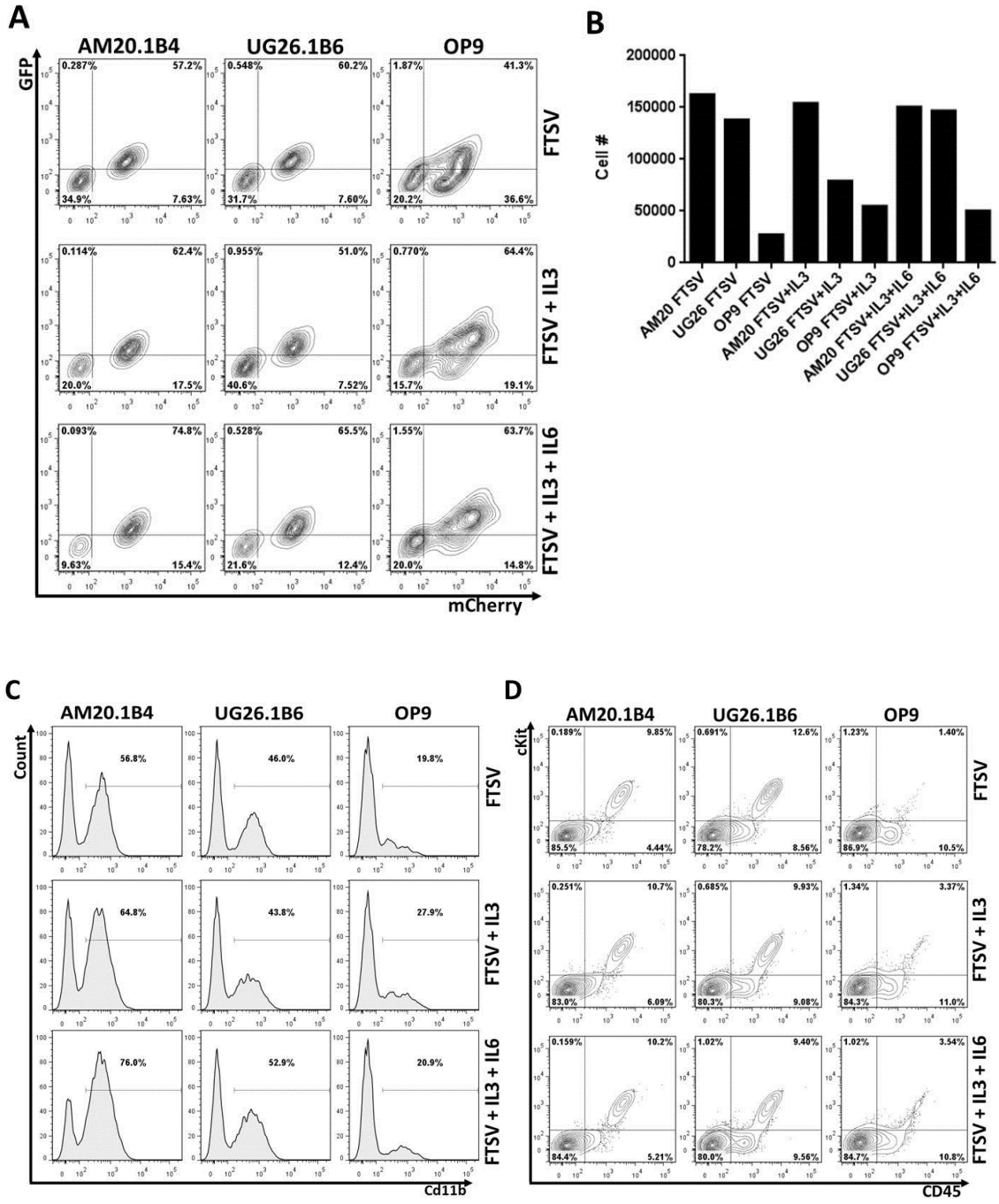
A
AM20.1B4
UG26.1B6
OP9
GFP
mCherry
FTSV
FTSV + IL3
FTSV + IL3 + IL6
0.287%
57.2%
34.9%
7.63%
0.548%
60.2%
31.7%
7.60%
1.87%
41.3%
20.2%
36.6%
0.114%
62.4%
20.0%
17.5%
0.955%
51.0%
40.6%
7.52%
0.770%
64.4%
15.7%
19.1%
0.093%
74.8%
9.63%
15.4%
0.528%
65.5%
21.6%
12.4%
1.55%
63.7%
20.0%
14.8%
B
Cell #
200000
150000
100000
50000
0
AM20 FTSV
UG26 FTSV
OP9 FTSV
AM20 FTSV+IL3
UG26 FTSV+IL3
OP9 FTSV+IL3
AM20 FTSV+IL3+IL6
UG26 FTSV+IL3+IL6
OP9 FTSV+IL3+IL6
C
AM20.1B4
UG26.1B6
OP9
Count
Cd11b
FTSV
FTSV + IL3
FTSV + IL3 + IL6
56.8%
46.0%
19.8%
64.8%
43.8%
27.9%
76.0%
52.9%
20.9%
D
AM20.1B4
UG26.1B6
OP9
cKit
CD45
FTSV
FTSV + IL3
FTSV + IL3 + IL6
0.189%
9.85%
85.5%
4.44%
0.691%
12.6%
78.2%
8.56%
1.23%
1.40%
86.9%
10.5%
0.251%
10.7%
83.0%
6.09%
0.685%
9.93%
80.3%
9.08%
1.34%
3.37%
84.3%
11.0%
0.159%
10.2%
84.4%
5.21%
1.02%
9.40%
80.0%
9.56%
1.02%
3.54%
84.7%
10.8%

Figure 7. Stromal co-culture of mCherry+GFP+ cells from day 8 EB.

(A) FACS analysis of mCherry and GFP expression in D8+6 stromal co-cultures. (B) Total number of mCherry+GFP+ cells in D8+6 stromal co-cultures as determined by bead-enhanced flow cytometry. (C) FACS analysis of CD11b expression in D8+6 stromal co-cultures. (D) FACS analysis of cKit and CD45 expression in D8+6 stromal co-cultures.

Dual-bioluminescent reporter construct allows non-invasive monitoring of *Runx1* expression during *in vitro* differentiation

While the dual-fluorescent reporter mESC line allows the prospective isolation and characterization of promoter specific sub-populations during differentiation, quantitative analysis generally requires culture disruption and modest numbers of cells for analysis, which can be problematic for screening large numbers of small scale cultures. In addition, analysis of promoter expression levels by fluorescent protein intensity is generally less sensitive than that afforded by bioluminescence. We previously demonstrated that our dual-bioluminescent reporter construct accurately reflected *Runx1* promoter switching during EB differentiation (Figure 4 C). To determine whether this reporter could be used to analyze the emergence of P2+ hemogenic endothelium in small scale cultures amenable to high-throughput screening, we plated day 4 EB derived Flk1+ cells in 48-well culture dishes containing basal IMDM, IMDM+FTSV, endothelial supportive EGM2, or EGM2+FTSV, and assessed the activity of P1-*Renilla* and P2-Firelfy after 48hrs in culture. As expected, P1-*Renilla* activity did not reach detectable levels in any condition; however P2-*Firefly* activity was detected in all conditions (Figure 8 A). The highest level of P2-*Firefly* activity was observed with EGM2, suggesting that this media is superior to IMDM in its ability to promote P2+ activity (Figure 8 B). Importantly, this experiment demonstrates that the dual-bioluminescent reporter is suitable for non-invasive analysis of *Runx1* expression within small scale cultures, making it suitable for high-throughput analysis.

Next, we sought to determine whether the dual-bioluminescent reporter was able reflect changes in *Runx1* promoter activity within committed hematopoietic progenitors. The distal isoform of *Runx1* is highly expressed in developing thymocytes, suggesting that signaling pathways promoting the development of T-cells may also regulate the activity of the P1 promoter [106]. Induction of the T-cell lineage from mESC derived hematopoietic progenitors is promoted via co-culture with OP9 engineered to over express the Notch ligand, Delta-like 1[163]. As *Runx1*-Notch interactions have been previously described [164], we wondered whether Notch signaling in OP9-DL1 co-cultures would alter promoter activity in our dual bio-luminescent reporter system. To test this, we first generated definitive hematopoietic progenitors from our dual-bioluminescent mESC via HOXB4 overexpression as previously described[87]. After an initial phase of maturation and expansion on OP9, we passaged the HOXB4 overexpressing hematopoietic progenitors onto either OP9 or OP9-DL1 stroma and assessed the levels of P1-*Renilla* and P2-*Firefly* activity after 5 days (Figure 8 C). Consistent with our previous findings, P1 activity was detected in HOXB4 overexpressing cells on OP9, however co-culture on OP9-DL1 resulted in a significant increase in the level of P1-*Renilla* activity and a decrease in the activity of P2-Firelfy, suggesting that Notch signaling increases *Runx1* P1 expression (Figure 8 D). This effect was also mirrored by mRNA isoform expression, showing that our dual-bioluminescent reporter construct accurately reflects endogenous *Runx1* promoter activity (Figure 8 E). Taken together, these data demonstrate that our dual-bioluminescent reporter system allows the non-

invasive monitoring of *Runx1* promoter activity in committed hematopoietic progenitors; thereby allowing the identification of signaling pathways that modulate their respective activities.

Figure 8

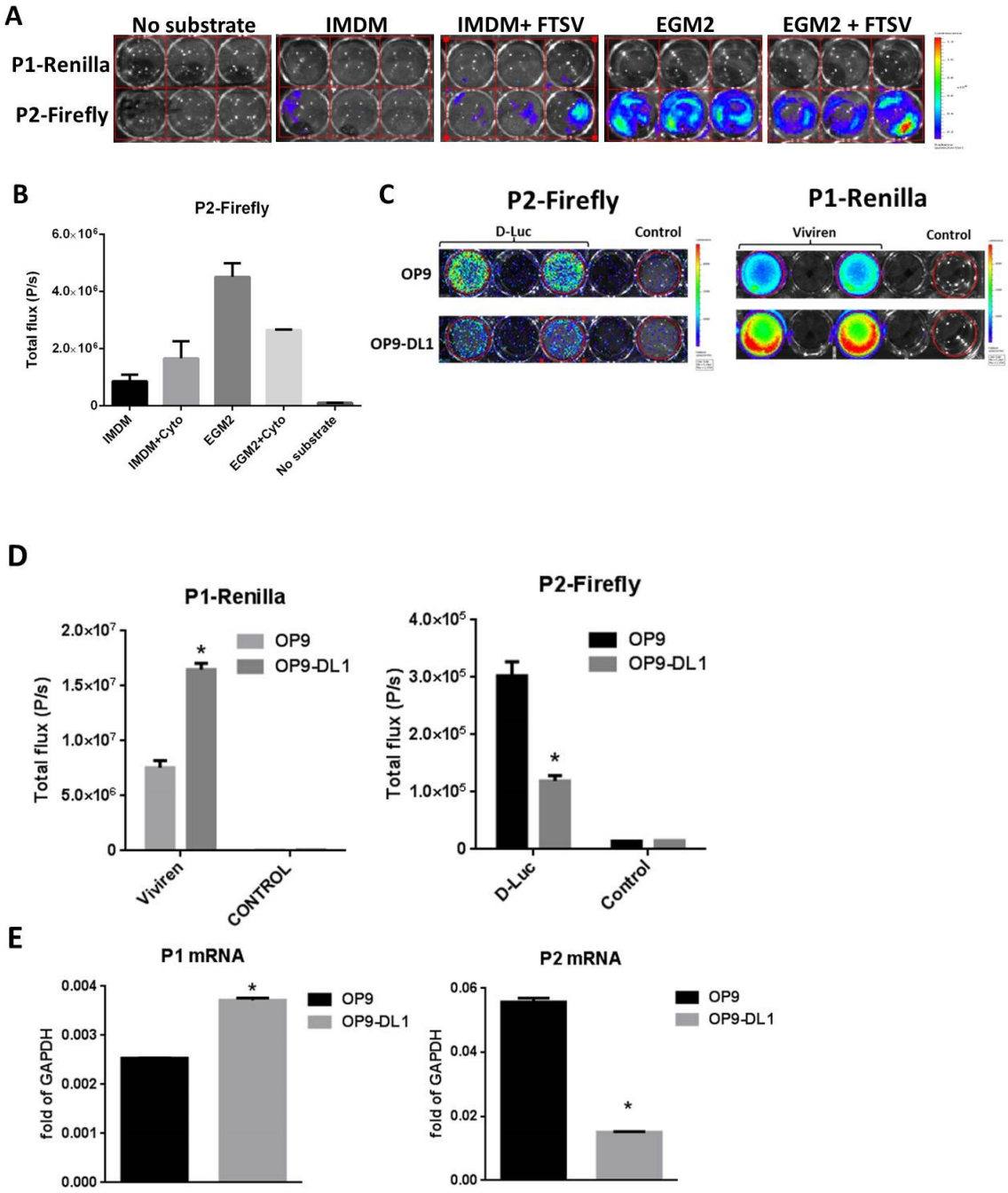
A
No substrate
IMDM
IMDM+ FTSV
EGM2
EGM2 + FTSV
P1-Renilla
P2-Firefly
B
P2-Firefly
Total flux (P/s)
6.0×10^6
4.0×10^6
2.0×10^6
0
IMDM
IMDM+Cyto
EGM2
EGM2+Cyto
No substrate
C
P2-Firefly
D-Luc
Control
P1-Renilla
Viviren
Control
OP9
OP9-DL1
D
P1-Renilla
Total flux (P/s)
2.0×10^7
1.5×10^7
1.0×10^7
5.0×10^6
0
OP9
OP9-DL1
*
Viviren
CONTROL
P2-Firefly
Total flux (P/s)
4.0×10^5
3.0×10^5
2.0×10^5
1.0×10^5
0
OP9
OP9-DL1
*
D-Luc
Control
E
P1 mRNA
fold of GAPDH
0.004
0.003
0.002
0.001
0.000
*
OP9
OP9-DL1
P2 mRNA
fold of GAPDH
0.06
0.04
0.02
0.00
*
OP9
OP9-DL1

Figure 8. Non-invasive monitoring of *Runx1* promoter activity with dual-bioluminescent reporter mESC

(A) Bio-luminescent imaging of P1-*Renilla* and P2-*Firefly* activity in small scale two-dimensional cultures of EB derived Flk1+ mesoderm. (B) Quantification of P2-*Firefly* bio-luminescence activity in different culture media. (C) Bio-luminescent imaging of P1-*Renilla* and P2-*Firefly* activity in HOXB4 overexpressing hematopoietic progenitors cultured on OP9 and OP9-DL1. (D) Quantification of bio-luminescence in HOXB4 overexpressing hematopoietic progenitors cultured on OP9 and OP9-DL1. (E) RT-qPCR analysis of *Runx1* mRNA isoforms in HOXB4 overexpressing hematopoietic progenitors cultured on OP9 and OP9-DL1. Data represent two independent experiments assayed in triplicate. *$p<0.05$.

Discussion

Runx1 is a critical regulator of both embryonic and adult hematopoiesis, and is frequently dis-regulated in hematopoietic malignancy; thus its regulation is an area of intense investigation[108,109,145,148]. *Runx1* transcription initiates from two spatially distant and differentially regulated promoters, and its hematopoietic activity is influenced by the presence of an intronic enhancer (+23) [98-102,106]. Interestingly, proximal (P2) promoter activity gives way to distal (P1) promoter driven expression at the onset of definitive hematopoiesis, suggesting that promoter specific reporters may assist efforts to derive definitive HSC from pluripotent stem cells (PSC). However, both promoters failed to drive hematopoietic specific reporting in transgenic animals and plasmid based reporter assays[99,100]. Reporter constructs targeted to the endogenous promoters accurately reflect their activity[103], but this method is time-consuming and not conducive to combinatorial or mutation based investigation of important regulatory sequences. Knock-in also results in *Runx1* haploinsufficiency, which is known to have biological consequences[148,149]. In the present study, we have demonstrated that targeting of minimal *Runx1* reporter constructs to the transgene permissive[152-154] *Hprt* locus in mESC via ICE recombination allows the unbiased interrogation of regulatory element function during *in vitro* hematopoietic differentiation. In contrast to previous reports, we show that the P1 and P2 promoters are capable of directing hematopoietic specific labeling. This discrepancy could be the result of position and/or copy number effects associated with randomly integrated transgenes and episomal plasmid

constructs, which may generate enough background signal to preclude the reliable detection of low level specificity. As ICE mediated recombination replaces a doxycyclin inducible Cre-recombinase ORF, it is possible that the basal activity of the individual promoter elements is enhanced by the presence of the TRE element, however any effect is likely to be minimal since the activity of this element in the absence of doxycyclin is extremely low, and cannot explain the hematopoietic specific expression. Nonetheless, this issue can be avoided if necessary by simply reversing the orientation of the reporter construct in future experiments. While the hematopoietic specificity of the individual promoter elements differed from previous observations, their specific temporal activities reflected previous observations in that the P2 promoter preferentially labeled CD41-Tie2+ HE, while the P1 promoter was biased toward CD41+Tie2+ HE and fully committed Tie2-CD41+ hematopoietic cells[103]. As expected, the +23 element enhanced the activity of both promoters; however its enhancing capacity appears to be influenced by the regulative capacity of the respective promoter elements in our P1/+23 and P2/+23 constructs, suggesting that the individual elements exert contextual effects on one another. Taken together, these data demonstrate that the *Hprt* locus is permissive to maintaining the activity of exogenous *Runx1* regulatory elements, allowing direct comparison of their individual activities during *in vitro* hematopoietic differentiation of mESC. Replacing homology-based targeting with the ICE system dramatically enhances *Hprt* targeting in mESC [119,165], making it possible to rapidly generate clonal mESC lines harboring single copy reporter constructs. We exploited these

properties to further refine the current understanding of previously defined *Runx1* regulatory elements. Future studies with different regions of each regulatory element, novel elements, or elements containing mutations in suspected transcription factor binding sites will further refine our understanding of *Runx1* regulation.

As our primary interest was to identify novel signatures of definitive hematopoiesis that could be used to optimize *in vitro* differentiation of mESC, we were primarily interested in replicating the definitive specific activity of the P1 promoter. While differences between the activities of the P1 and P2 promoters in our single reporter constructs suggested that they retained some of their inherent specificity in isolation, several observations suggested that neither the P1 or P1/+23 constructs optimally reflected P1 activity. First, our P1 and P1/+23 constructs labeled a considerably higher percentage of cells in day 6 EB than the knock-in results reported by Sroczynska *et al*[103]. Second, the fact that the P1 and P2 promoters differentially impacted the activity of the +23 enhancer suggested that they may also impact the activity of one another; a theory that is supported by the fact that the two promoters share binding sites for hematopoietic transcription factors, including Runx1[100]. Furthermore, the fact that the promoter specific mRNA isoforms exhibit differential methods of translation suggests that protein production from each may differ under specific physiological conditions[105]. Indeed, our dual-reporter constructs show that the inclusion of all three regulatory elements in their appropriate genomic order further specifies P1 and P2 driven reporter activity, and is sufficient to reflect endogenous *Runx1*

promoter switching during *in vitro* differentiation of mESC. The dual-fluorescent reporter allowed us to prospectively isolate and characterize the individual promoter-specific cell populations, which we exploited to demonstrate that definitive hematopoietic progenitor activity is preferentially contained within the P1 expressing mCherry+GFP+ subpopulation in day 8 EB. This mirrors what was observed in the knock-in reporter line[103], suggesting that our constructs not only reflect the expression profile of the individual promoters, but also the functional capacity of the cell populations in which they are active. We then demonstrated that compared to bone marrow derived OP9, AGM region derived AM20.1B4 and UG26.1B6 stromal lines are most effective at maintaining hematopoietic progenitors contained within the mCherry+GFP+ population. This is not particularly surprising considering that the AGM region gives rise to FL and adult HSC; both of which preferentially express the P1 mRNA isoform[113]. Neither IL-3 nor IL-3/IL-6 promoted the supportive capacity of the AGM stroma; however IL-3 did enhance the supportive capacity of OP9, suggesting that this line may produce suboptimal levels of this molecule. The lack of a functional M-CSF gene in OP9 reduces the overproduction of macrophages common in other stromal lines, allowing more effective generation of multiple hematopoietic lineages; thus it is plausible that if supplemented with IL-3 and possibly other factors present in the AGM lines, OP9 may in fact prove a more effective system for the generation of diverse hematopoietic lineages from the mCherry+GFP+ population. Conversely, the emergence of TALEN[166] and CRISPR[167] as highly efficient tools for gene modification should make it feasible to produce M-CSF null AGM lines.

While we focused on the generation of mCherry+GFP+ hematopoietic cells in EB, our reporter constructs should be equally useful in other systems. It would be particularly interesting to compare EB based differentiation to the stroma-only methods reported by others [83,160]. Fully defined differentiation strategies are desirable for future clinical application. Our preliminary experiments in serum-free defined cultures[91] have found that our system functions appropriately in this setting, and is thus a novel tool with which to refine current systems.

Systems amenable to high-throughput screening have allowed the identification of novel modulators of hematopoietic development[12]. In general, highly sensitive readouts that do not require laborious sample processing steps are best suited for high-throughput screens. We have demonstrated that our dual-bioluminescent reporter construct fulfills these criteria. In our small scale analysis, we demonstrated that the commercially available EGM2 media allows efficient generation of *Runx1*-P2+ hematopoietic precursors from Flk1+ mesoderm, making it a suitable baseline for further analysis of cytokines or small molecules that enhance this process. As the bio-luminescent readout does not require cell disruption and is sensitive enough to be readily detected in small scale cultures, our dual-bioluminescent reporter provides a novel platform for future high-throughput screening of hematopoietic specification during *in vitro* differentiation. *Runx1* promoter isoforms play specific roles during lineage commitment in the adult hematopoietic system[107,168,169]. We used our dual-fluorescent reporter line and OP9-DL1 co-culture to demonstrate that Notch signaling promotes P1 activity in mESC derived hematopoietic progenitors

overexpressing HOXB4. This finding is consistent with the observations that developing thymocytes express high levels of P1-Runx1[106], and that the OP9-DL1 system preferentially drives T lineage specification[163]. Taken together, these data demonstrate the dual-bioluminescent reporter is ideally suited for high-throughput screening of conditions that alter *Runx1* promoter activity; whether it is during the initial specification of the hematopoietic lineage, or during differentiation of fully committed hematopoietic progenitors.

Collectively, we have utilized *Hprt* targeting to conduct an unbiased combinatorial analysis of *Runx1* regulatory element function during mESC differentiation. Our dual-reporter mESC lines accurately reflect promoter usage and provide novel tools for the identification of conditions that promote definitive hematopoiesis from PSC. As our constructs are relatively small (~3kb), and contain all elements in *cis*, they can be easily transferred to other cell lines, including pre-existing knock-out mESC lines and disease model iPSC. Since the structure and function of the human *Runx1* locus is highly conserved between mouse and human, it is not unreasonable to suggest that reporters containing the minimal human regulatory elements may also accurately reflect promoter switching.

Supplementary Figure 1

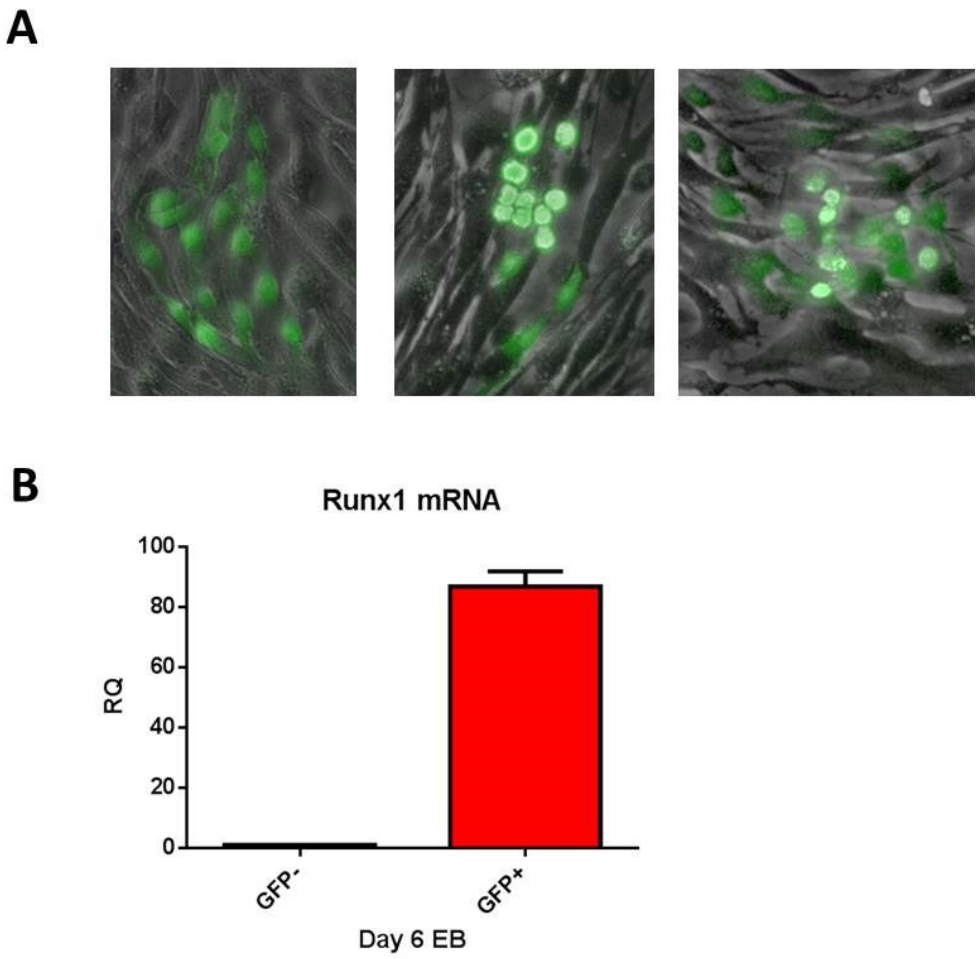

Supplemental Figure 1. P1/+23 reporter activity

(A) GFP expressing cells in OP9 co-cultures from P1/+23 mESC line. (B) RT-qPCR analysis of Runx1 expression in GFP- and GFP+ cells sorted from day 6 P1/+23 EB.

Supplemental Figure 2

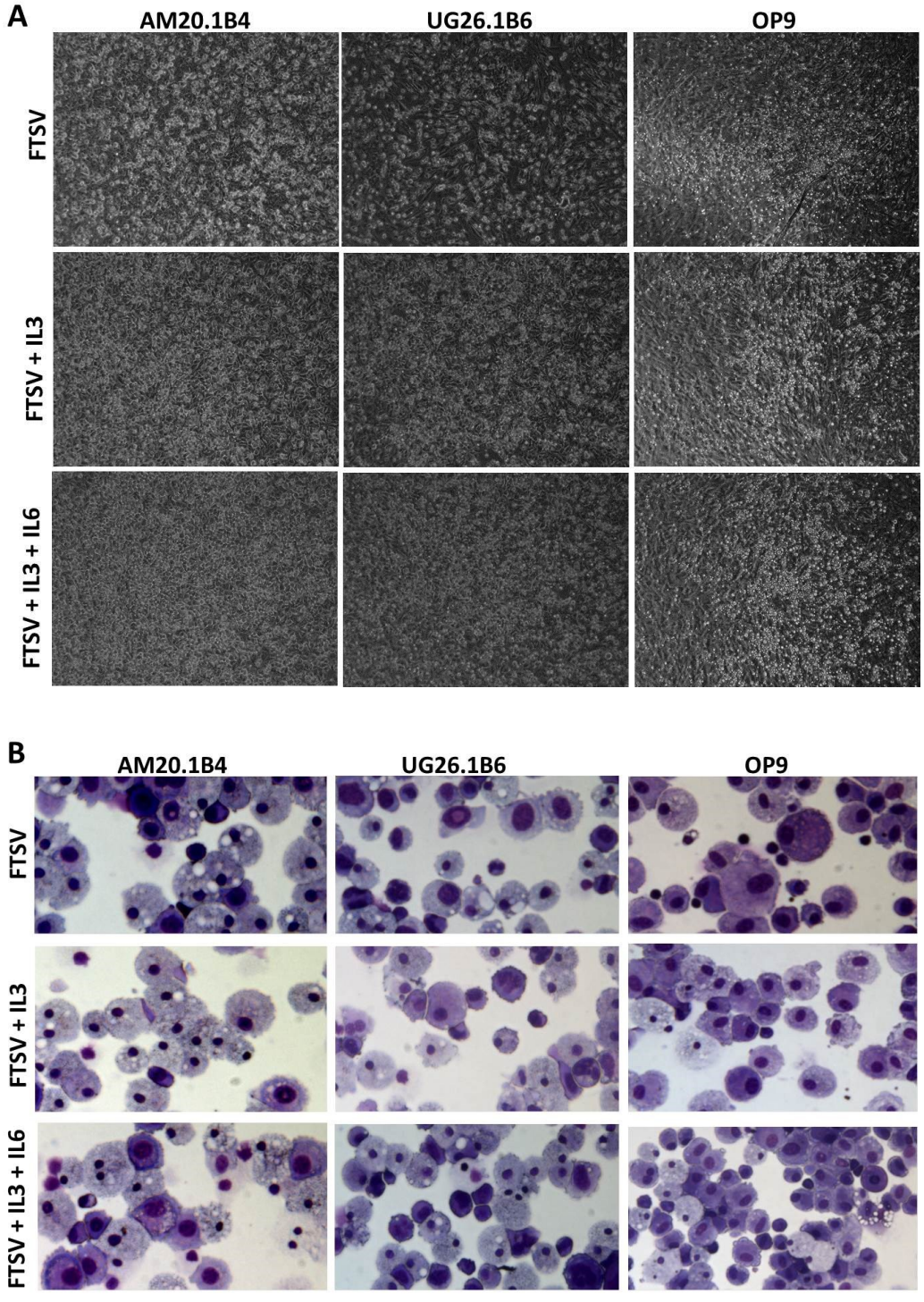

Supplemental Figure 2. Morphology of cells during stromal co-culture

(A). Light microscope images of hematopoietic cells on AGM and OP9 stroma at 100x magnification. (B) Representative Romonowsky stained cytospins from AGM and OP9 stromal co-cultures.

Chapter 4

Concluding Statements and Future Applications

Pluripotent stem cells have the potential to revolutionize the field of regenerative medicine; however in order to achieve this reality, safe and efficient methods for their directed differentiation must be developed. In general, these efforts rely on basic developmental research to provide information that can be applied to guide differentiation and subsequent characterization of terminal cell types. The current work focused primarily on hematopoietic differentiation of mESC, specifically the formation of the definitive wave of hematopoiesis that produces adult HSC. Toward this end, we undertook both discovery (Chapter 2) and application (Chapter 3) based efforts to develop novel signatures of definitive hematopoiesis.

Hematopoietic differentiation of ESC was demonstrated shortly after their discovery[20,77], and the large repertoire of hematopoietic cytokines accumulated over several decades of hematological research fostered the subsequent derivation of many terminal hematopoietic lineages from PSC[14]; however the derivation of HSC capable of long-term multilineage engraftment has not been reported. This is somewhat puzzling considering the accepted models of hematopoietic hierarchy in the adult, where HSC generate all mature hematopoietic lineages. This is likely due to the fact that ESC derived hematopoiesis most closely resembles primitive hematopoiesis of the yolk-sac, which does not appear to produce the precursors of adult HSC[36,38]. At present, functional assays remain the most effective way to distinguish definitive from primitive hematopoiesis; however these assays are inherently retrospective and often laborious, particularly in the case of long-term engraftment assays.

Phenotypic signatures that distinguish primitive and definitive hematopoiesis would make it easier to identify conditions that promote definitive hematopoiesis during *in vitro* differentiation.

It was previously known that *Runx1* expression is specifically required for definitive blood[145], and that its expression switches from a proximal to a distal promoter at the time when definitive hematopoietic cells emerge in the embryo[101-103,112,113], however the mechanisms underlying this promoter switch were unclear. In Chapter 2, we describe a series of experiments exploring epigenetic changes at the *Runx1* locus during hematopoietic development *in vivo,* and during mESC differentiation *in vivo*. As is typical with CpG rich promoter elements, we found that the core, P2 *Runx1* promoter is remarkably unmethylated regardless of lineage or developmental status, a finding that is reflective of its broad expression pattern. Conversely, we found that the hematopoietic specific +23 enhancer element is almost completely methylated in pluripotent mESC and in non-hematopoietic cells, but undergoes a dramatic loss of methylation upon hematopoietic commitment. Of particular interest to the goal of deriving definitive HSC from ESC, the distal P1 *Runx1* promoter element exhibits a loss of methylation that correlates with the transition to definitive HSC *in vivo.* Perhaps not surprisingly then, the P1 promoter is methylated in mESC derived hematopoietic progenitors, and remains methylated even after maturation toward a more definitive, albeit non-engrafting phenotype on adult bone marrow stroma. In order to confirm that our *in vivo* signature would be valid in mESC derived HSC, we exploited the unique capacity of HOXB4 to induce definitive HSC

formation from mESC[87]. Strikingly, we found that HOXB4 overexpression resulted in a loss of P1 methylation similar to that observed *in vivo*, and that this loss of methylation was reflected by a consequent increase in P1 mRNA. While this essentially confirmed that our *in vivo* epigenetic signature could be replicated during *in vitro* differentiation under the appropriate conditions, we took our findings a step further, and identified a direct role for HOXB4 in promoting the epigenetic remodeling of the P1 promoter. DNA methylation patterns are relatively stable after their establishment, and are thought to solidify fate decisions during development [136]. Thus, methylation based signatures like the one described here may be more robust indicators of lineage identity than gene expression, as exemplified by the use of DNA methylation patterns to confirm successful somatic cell reprogramming during iPSC generation. Considering the similarities between human and mouse developmental hematopoiesis, and the conservation of *Runx1* structure and function between the two species, it is likely that this signature will apply to human PSC differentiation. The rapid advancement of next-generation sequencing technology and its application to methylation analysis should make it possible to rapidly assess the methylation profiles of hematopoietic progenitors derived from PSC under different conditions. Bisulfite sequencing is clonal in nature, but standard sequencing techniques are logistically limited to a relatively low number of reads. Next generation sequencing technologies should allow for the analysis of population wide distribution of methylation profiles, providing information on the homogeneity of the population being investigated.

To complement our discovery based approach, we used a previously described system for efficient targeting of DNA constructs the transgene permissive *Hprt* locus in mESC[119,165] to perform an unbiased analysis of the activity of minimal *Runx1* regulatory elements; both alone and in combination. Based on the information from the individual promoter constructs, we were able to develop dual-promoter constructs that accurately reflect *Runx1* promoter switching; which to date had only been accomplished by targeting reporter genes to the endogenous *Runx1* locus. The dual-fluorescent line allowed us to monitor promoter activity during mESC differentiation, and facilitated the isolation of promoter specific subpopulations for further experiments. We demonstrated that the P1 expressing population contains the majority of definitive hematopoietic activity in developing EB, and that the AGM microenvironment was most suited to their subsequent expansion. It will be interesting to use this system to further explore conditions that can produce a higher frequency of these cells during differentiation. As serum free fully defined culture systems are desirable, we have begun to explore the activity of our reporters in these conditions. In preliminary experiments, we have found that the dynamic activity of our reporter lines is maintained in serum-free fully defined culture conditons[91]. Interestingly, around day 10 of EB differentiation in serum free cultures we have observed that a large portion of viable cells detach from the EB and remain viable in suspension. Surprisingly, these cells contain a high proportion of mCherry+GFP+ cells compared to the EB proper, and are enriched with colony forming cells (Figure 1). It will be interesting to further explore this cell population.

Figure 1

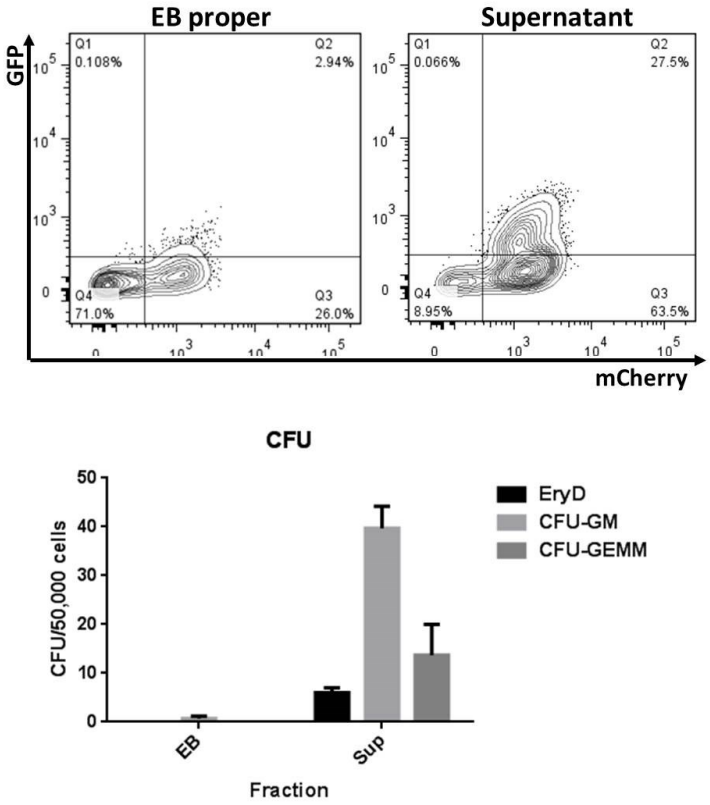

Figure 1. FACS analysis and CFU activity of EB and supernatant cell fractions at day 10.

We also created a dual-bioluminescent reporter construct that effectively reported *Runx1* promoter activity. The high sensitivity of bio-luminescence compared to fluorescence based analysis provides certain advantages, particularly for the analysis of small scale cell cultures that are suited to high throughput analysis. We effectively demonstrated that our reporter construct allows the non-invasive detection of *Runx1* promoter activity in small scale cultures of Flk1+ mesoderm, which allowed us to compare the effectiveness of several culture conditions to promote hematopoietic specification. Furthermore, we showed that this reporter could also be used to assay the effects of certain signaling pathways on promoter activity in committed hematopoietic progenitors. In our example, we demonstrated that Notch signaling promotes that activity of the P1 promoter. Thus this system should be an excellent platform for high-throughput screening of small molecules or cytokine combinations that promote hematopoietic development. The dual-fluorescent reporter could also be useful to examine the behavior and localization of hematopoietic cells post-transplant. Indeed, we performed a pilot experiment in which we transplanted dual-bioluminescent hematopoietic progenitors derived via HOXB4 overexpression and found that bioluminescent activity appears to accurately reflect the engraftment and localization of cells post-transplant (Figure 2 A), though we were only able to detect P2-Firelfy activity in this experiment, probably due to the poor tissue penetration of short-wavelength *Renilla* bioluminescence. To overcome this issue, and the need to deliver two different substrates, we have created constructs that replace *Renilla* and *Firefly* with red and green spectra shifted

luciferase variants that are ideally suited for *in vivo* imaging, can be spectrally separated, and metabolize a common substrate[170]. Furthermore, in an effort to combine the unique capabilities of the dual-fluorescent and dual-bioluminescent reporters, we have generated a construct in which the fluorescent and bioluminescent reporter cDNAs are linked by picornaviral-based 2A sequences[171] (Figure 2 B). These reporters should allow for future studies in which cells can be non-invasively monitored by bioluminescence, FACS purified at desired time-points, and subsequently monitored after transplantation by bioluminescence.

Figure 2

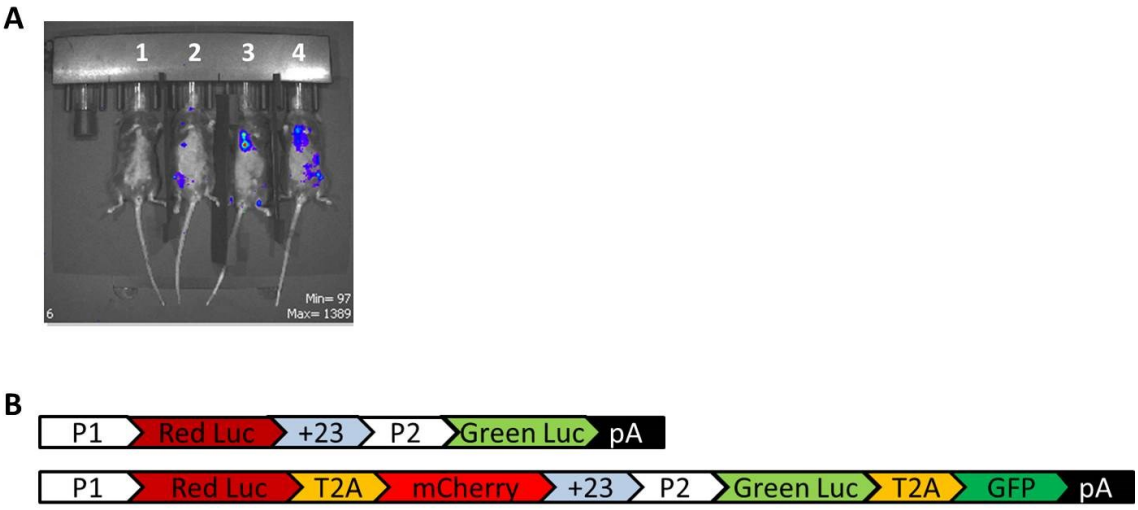

Figure 2. *In vivo* bioluminescence imaging and improved dual-bioluminescent reporter constructs.

(A) Bio-luminescent imaging of P2-*Firefly* activity 1 month post-transplant of HOXB4 overexpressing hematopoietic progenitors derived from dual-bioluminescent reporter mESC. (B) Design of improved dual-bioluminescent and dual-bioluminescent/fluorescent constructs.

In summary, this work has provided new insight into the basic biological processes that regulate the formation of definitive HSC during development, and in doing so has identified a novel molecular signature of definitive hematopoiesis. The reporter constructs and mESC cell lines we have developed will be valuable tools for future efforts to improve their hematopoietic differentiation. In sum, the findings described in this dissertation move us one step closer to the ultimate goal of deriving transplantable HSC from pluripotent stem cells.

Bibliography

1. LORENZ E, UPHOFF D, REID TR, SHELTON E. Modification of irradiation injury in mice and guinea pigs by bone marrow injections. *J Natl Cancer Inst*. 1951;12(1):197-201.
2. Hong R, Cooper MD, Allan MJ, Kay HE, Meuwissen H, Good RA. Immunological restitution in lymphopenic immunological deficiency syndrome. *Lancet*. 1968;1(7541):503-506.
3. Kondo M, Wagers AJ, Manz MG, et al. Biology of hematopoietic stem cells and progenitors: implications for clinical application. *Annu Rev Immunol*. 2003;21:759-806.
4. Krause DS, Theise ND, Collector MI, et al. Multi-organ, multi-lineage engraftment by a single bone marrow-derived stem cell. *Cell*. 2001;105(3):369-377.
5. Spangrude GJ, Heimfeld S, Weissman IL. Purification and characterization of mouse hematopoietic stem cells. *Science*. 1988;241(4861):58-62.
6. Osawa M, Hanada K, Hamada H, Nakauchi H. Long-term lymphohematopoietic reconstitution by a single CD34-low/negative hematopoietic stem cell. *Science*. 1996;273(5272):242-245.
7. MC P, Z. W. Current use and outcome of hematopoietic stem cell transplantation: CIBMTR Summary Slides: CIBMTR; 2012.
8. Hütter G, Nowak D, Mossner M, et al. Long-term control of HIV by CCR5 Delta32/Delta32 stem-cell transplantation. *N Engl J Med*. 2009;360(7):692-698.
9. Wagner JE, Ishida-Yamamoto A, McGrath JA, et al. Bone marrow transplantation for recessive dystrophic epidermolysis bullosa. *N Engl J Med*. 2010;363(7):629-639.
10. Walasek MA, van Os R, de Haan G. Hematopoietic stem cell expansion: challenges and opportunities. *Ann N Y Acad Sci*. 2012;1266:138-150.
11. Grewal SS, Barker JN, Davies SM, Wagner JE. Unrelated donor hematopoietic cell transplantation: marrow or umbilical cord blood? *Blood*. 2003;101(11):4233-4244.
12. North TE, Goessling W, Walkley CR, et al. Prostaglandin E2 regulates vertebrate haematopoietic stem cell homeostasis. *Nature*. 2007;447(7147):1007-1011.
13. Boitano AE, Wang J, Romeo R, et al. Aryl hydrocarbon receptor antagonists promote the expansion of human hematopoietic stem cells. *Science*. 2010;329(5997):1345-1348.
14. Slukvin II. Hematopoietic specification from human pluripotent stem cells: current advances and challenges toward de novo generation of hematopoietic stem cells. *Blood*. 2013.
15. Thomson JA, Itskovitz-Eldor J, Shapiro SS, et al. Embryonic stem cell lines derived from human blastocysts. *Science*. 1998;282(5391):1145-1147.
16. Takahashi K, Tanabe K, Ohnuki M, et al. Induction of pluripotent stem cells from adult human fibroblasts by defined factors. *Cell*. 2007;131(5):861-872.
17. Takahashi K, Yamanaka S. Induction of pluripotent stem cells from mouse embryonic and adult fibroblast cultures by defined factors. *Cell*. 2006;126(4):663-676.
18. Yu J, Vodyanik MA, Smuga-Otto K, et al. Induced pluripotent stem cell lines derived from human somatic cells. *Science*. 2007;318(5858):1917-1920.
19. Park IH, Zhao R, West JA, et al. Reprogramming of human somatic cells to pluripotency with defined factors. *Nature*. 2008;451(7175):141-146.
20. Kaufman DS, Hanson ET, Lewis RL, Auerbach R, Thomson JA. Hematopoietic colony-forming cells derived from human embryonic stem cells. *Proc Natl Acad Sci U S A*. 2001;98(19):10716-10721.
21. Murry CE, Keller G. Differentiation of embryonic stem cells to clinically relevant populations: lessons from embryonic development. *Cell*. 2008;132(4):661-680.

22. Kennedy M, D'Souza SL, Lynch-Kattman M, Schwantz S, Keller G. Development of the hemangioblast defines the onset of hematopoiesis in human ES cell differentiation cultures. *Blood*. 2007;109(7):2679-2687.
23. Sabin F. Studies on the origin of blood vessels and of red blood corpuscles as seen in the living blastoderm of chicks during the second day of incubation. . *Contrib Embryol* 1920;272(9):214.
24. Murray P. The development in vitro of the blood of the early chick embryo. *Proc Royal Soc London*. 1932(11):497-521.
25. Choi K, Kennedy M, Kazarov A, Papadimitriou JC, Keller G. A common precursor for hematopoietic and endothelial cells. *Development*. 1998;125(4):725-732.
26. Fehling HJ, Lacaud G, Kubo A, et al. Tracking mesoderm induction and its specification to the hemangioblast during embryonic stem cell differentiation. *Development*. 2003;130(17):4217-4227.
27. Huber TL, Kouskoff V, Fehling HJ, Palis J, Keller G. Haemangioblast commitment is initiated in the primitive streak of the mouse embryo. *Nature*. 2004;432(7017):625-630.
28. Kennedy M, Firpo M, Choi K, et al. A common precursor for primitive erythropoiesis and definitive haematopoiesis. *Nature*. 1997;386(6624):488-493.
29. Ferkowicz MJ, Yoder MC. Blood island formation: longstanding observations and modern interpretations. *Exp Hematol*. 2005;33(9):1041-1047.
30. Kinder SJ, Tsang TE, Quinlan GA, Hadjantonakis AK, Nagy A, Tam PP. The orderly allocation of mesodermal cells to the extraembryonic structures and the anteroposterior axis during gastrulation of the mouse embryo. *Development*. 1999;126(21):4691-4701.
31. Ueno H, Weissman IL. Clonal analysis of mouse development reveals a polyclonal origin for yolk sac blood islands. *Dev Cell*. 2006;11(4):519-533.
32. Moore MA, Metcalf D. Ontogeny of the haemopoietic system: yolk sac origin of in vivo and in vitro colony forming cells in the developing mouse embryo. *Br J Haematol*. 1970;18(3):279-296.
33. Weismann I, Papaioannou, V. & Gardner, R. . Differentiation of Normal and Neoplastic Hematopoietic Cells. New York: Cold Spring Harbor Laboratory Press; 1978.
34. Dieterlen-Lievre F. On the origin of haemopoietic stem cells in the avian embryo: an experimental approach. *J Embryol Exp Morphol*. 1975;33(3):607-619.
35. Turpen JB, Knudson CM, Hoefen PS. The early ontogeny of hematopoietic cells studied by grafting cytogenetically labeled tissue anlagen: localization of a prospective stem cell compartment. *Dev Biol*. 1981;85(1):99-112.
36. Medvinsky A, Dzierzak E. Definitive hematopoiesis is autonomously initiated by the AGM region. *Cell*. 1996;86(6):897-906.
37. Müller AM, Medvinsky A, Strouboulis J, Grosveld F, Dzierzak E. Development of hematopoietic stem cell activity in the mouse embryo. *Immunity*. 1994;1(4):291-301.
38. de Bruijn MF, Speck NA, Peeters MC, Dzierzak E. Definitive hematopoietic stem cells first develop within the major arterial regions of the mouse embryo. *EMBO J*. 2000;19(11):2465-2474.
39. Kumaravelu P, Hook L, Morrison AM, et al. Quantitative developmental anatomy of definitive haematopoietic stem cells/long-term repopulating units (HSC/RUs): role of the aorta-gonad-mesonephros (AGM) region and the yolk sac in colonisation of the mouse embryonic liver. *Development*. 2002;129(21):4891-4899.
40. Jaffredo T, Bollerot K, Sugiyama D, Gautier R, Drevon C. Tracing the hemangioblast during embryogenesis: developmental relationships between endothelial and hematopoietic cells. *Int J Dev Biol*. 2005;49(2-3):269-277.

41. de Bruijn MF, Ma X, Robin C, Ottersbach K, Sanchez MJ, Dzierzak E. Hematopoietic stem cells localize to the endothelial cell layer in the midgestation mouse aorta. *Immunity*. 2002;16(5):673-683.
42. Zovein AC, Hofmann JJ, Lynch M, et al. Fate tracing reveals the endothelial origin of hematopoietic stem cells. *Cell Stem Cell*. 2008;3(6):625-636.
43. Eilken HM, Nishikawa S, Schroeder T. Continuous single-cell imaging of blood generation from haemogenic endothelium. *Nature*. 2009;457(7231):896-900.
44. Boisset JC, van Cappellen W, Andrieu-Soler C, Galjart N, Dzierzak E, Robin C. In vivo imaging of haematopoietic cells emerging from the mouse aortic endothelium. *Nature*. 2010;464(7285):116-120.
45. Kissa K, Herbomel P. Blood stem cells emerge from aortic endothelium by a novel type of cell transition. *Nature*. 2010;464(7285):112-115.
46. Lancrin C, Sroczynska P, Stephenson C, Allen T, Kouskoff V, Lacaud G. The haemangioblast generates haematopoietic cells through a haemogenic endothelium stage. *Nature*. 2009;457(7231):892-895.
47. Rybtsov S, Sobiesiak M, Taoudi S, et al. Hierarchical organization and early hematopoietic specification of the developing HSC lineage in the AGM region. *J Exp Med*. 2011;208(6):1305-1315.
48. Miura Y, Wilt FH. Tissue interaction and the formation of the first erythroblasts of the chick embryo. *Dev Biol*. 1969;19(2):201-211.
49. Pardanaud L, Dieterlen-Lievre F. Emergence of endothelial and hemopoietic cells in the avian embryo. *Anat Embryol (Berl)*. 1993;187(2):107-114.
50. Wilt FH. Erythropoiesis in the Chick Embryo: the Role of Endoderm. *Science*. 1965;147:1588-1590.
51. Belaoussoff M, Farrington SM, Baron MH. Hematopoietic induction and respecification of A-P identity by visceral endoderm signaling in the mouse embryo. *Development*. 1998;125(24):5009-5018.
52. Pardanaud L, Dieterlen-Lièvre F. Manipulation of the angiopoietic/hemangiopoietic commitment in the avian embryo. *Development*. 1999;126(4):617-627.
53. Gering M, Patient R. Hedgehog signaling is required for adult blood stem cell formation in zebrafish embryos. *Dev Cell*. 2005;8(3):389-400.
54. Byrd N, Becker S, Maye P, et al. Hedgehog is required for murine yolk sac angiogenesis. *Development*. 2002;129(2):361-372.
55. Dyer MA, Farrington SM, Mohn D, Munday JR, Baron MH. Indian hedgehog activates hematopoiesis and vasculogenesis and can respecify prospective neurectodermal cell fate in the mouse embryo. *Development*. 2001;128(10):1717-1730.
56. Kumano K, Chiba S, Kunisato A, et al. Notch1 but not Notch2 is essential for generating hematopoietic stem cells from endothelial cells. *Immunity*. 2003;18(5):699-711.
57. Cheng X, Huber TL, Chen VC, Gadue P, Keller GM. Numb mediates the interaction between Wnt and Notch to modulate primitive erythropoietic specification from the hemangioblast. *Development*. 2008;135(20):3447-3458.
58. Winnier G, Blessing M, Labosky PA, Hogan BL. Bone morphogenetic protein-4 is required for mesoderm formation and patterning in the mouse. *Genes Dev*. 1995;9(17):2105-2116.
59. Lindsley RC, Gill JG, Kyba M, Murphy TL, Murphy KM. Canonical Wnt signaling is required for development of embryonic stem cell-derived mesoderm. *Development*. 2006;133(19):3787-3796.
60. Nottingham WT, Jarratt A, Burgess M, et al. Runx1-mediated hematopoietic stem-cell emergence is controlled by a Gata/Ets/SCL-regulated enhancer. *Blood*. 2007;110(13):4188-4197.

61. Landry JR, Kinston S, Knezevic K, et al. Runx genes are direct targets of Scl/Tal1 in the yolk sac and fetal liver. *Blood*. 2008;111(6):3005-3014.
62. Lengerke C, Schmitt S, Bowman TV, et al. BMP and Wnt specify hematopoietic fate by activation of the Cdx-Hox pathway. *Cell Stem Cell*. 2008;2(1):72-82.
63. Paik EJ, Mahony S, White RM, et al. A Cdx4-Sall4 Regulatory Module Controls the Transition from Mesoderm Formation to Embryonic Hematopoiesis. *Stem Cell Reports*. 2013;1(5):425-436.
64. Fujiwara Y, Chang AN, Williams AM, Orkin SH. Functional overlap of GATA-1 and GATA-2 in primitive hematopoietic development. *Blood*. 2004;103(2):583-585.
65. Porcher C, Swat W, Rockwell K, Fujiwara Y, Alt FW, Orkin SH. The T cell leukemia oncoprotein SCL/tal-1 is essential for development of all hematopoietic lineages. *Cell*. 1996;86(1):47-57.
66. Bollerot K, Pouget C, Jaffredo T. The embryonic origins of hematopoietic stem cells: a tale of hemangioblast and hemogenic endothelium. *Apmis*. 2005;113(11-12):790-803.
67. Warren AJ, Colledge WH, Carlton MB, Evans MJ, Smith AJ, Rabbitts TH. The oncogenic cysteine-rich LIM domain protein rbtn2 is essential for erythroid development. *Cell*. 1994;78(1):45-57.
68. Yamada Y, Pannell R, Forster A, Rabbitts TH. The oncogenic LIM-only transcription factor Lmo2 regulates angiogenesis but not vasculogenesis in mice. *Proc Natl Acad Sci U S A*. 2000;97(1):320-324.
69. Spyropoulos DD, Pharr PN, Lavenburg KR, et al. Hemorrhage, impaired hematopoiesis, and lethality in mouse embryos carrying a targeted disruption of the Fli1 transcription factor. *Mol Cell Biol*. 2000;20(15):5643-5652.
70. Yokomizo T, Hasegawa K, Ishitobi H, et al. Runx1 is involved in primitive erythropoiesis in the mouse. *Blood*. 2008;111(8):4075-4080.
71. Chen MJ, Yokomizo T, Zeigler BM, Dzierzak E, Speck NA. Runx1 is required for the endothelial to haematopoietic cell transition but not thereafter. *Nature*. 2009;457(7231):887-891.
72. Shivdasani RA, Mayer EL, Orkin SH. Absence of blood formation in mice lacking the T-cell leukaemia oncoprotein tal-1/SCL. *Nature*. 1995;373(6513):432-434.
73. Lancrin C, Sroczynska P, Stephenson C, Allen T, Kouskoff V, Lacaud G. The haemangioblast generates haematopoietic cells through a haemogenic endothelium stage. *Nature*. 2009;457(7231):892-895.
74. Iacovino M, Chong D, Szatmari I, et al. HoxA3 is an apical regulator of haemogenic endothelium. *Nat Cell Biol*. 2011;13(1):72-78.
75. Clarke RL, Yzaguirre AD, Yashiro-Ohtani Y, et al. The expression of Sox17 identifies and regulates haemogenic endothelium. *Nat Cell Biol*. 2013;15(5):502-510.
76. Pimanda JE, Ottersbach K, Knezevic K, et al. Gata2, Fli1, and Scl form a recursively wired gene-regulatory circuit during early hematopoietic development. *Proc Natl Acad Sci U S A*. 2007;104(45):17692-17697.
77. Doetschman TC, Eistetter H, Katz M, Schmidt W, Kemler R. The in vitro development of blastocyst-derived embryonic stem cell lines: formation of visceral yolk sac, blood islands and myocardium. *J Embryol Exp Morphol*. 1985;87:27-45.
78. Kyba M, Daley GQ. Hematopoiesis from embryonic stem cells: lessons from and for ontogeny. *Exp Hematol*. 2003;31(11):994-1006.
79. Lindenbaum MH, Grosveld F. An in vitro globin gene switching model based on differentiated embryonic stem cells. *Genes Dev*. 1990;4(12A):2075-2085.

80. Burkert U, von Rüden T, Wagner EF. Early fetal hematopoietic development from in vitro differentiated embryonic stem cells. *New Biol*. 1991;3(7):698-708.
81. Potocnik AJ, Kohler H, Eichmann K. Hemato-lymphoid in vivo reconstitution potential of subpopulations derived from in vitro differentiated embryonic stem cells. *Proc Natl Acad Sci U S A*. 1997;94(19):10295-10300.
82. Müller AM, Dzierzak EA. ES cells have only a limited lymphopoietic potential after adoptive transfer into mouse recipients. *Development*. 1993;118(4):1343-1351.
83. Nakano T, Kodama H, Honjo T. Generation of lymphohematopoietic cells from embryonic stem cells in culture. *Science*. 1994;265(5175):1098-1101.
84. Yoder MC, Hiatt K, Mukherjee P. In vivo repopulating hematopoietic stem cells are present in the murine yolk sac at day 9.0 postcoitus. *Proc Natl Acad Sci U S A*. 1997;94(13):6776-6780.
85. Perlingeiro RC, Kyba M, Daley GQ. Clonal analysis of differentiating embryonic stem cells reveals a hematopoietic progenitor with primitive erythroid and adult lymphoid-myeloid potential. *Development*. 2001;128(22):4597-4604.
86. Ran D, Shia WJ, Lo MC, et al. RUNX1a enhances hematopoietic lineage commitment from human embryonic stem cells and inducible pluripotent stem cells. *Blood*. 2013;121(15):2882-2890.
87. Kyba M, Perlingeiro RC, Daley GQ. HoxB4 confers definitive lymphoid-myeloid engraftment potential on embryonic stem cell and yolk sac hematopoietic progenitors. *Cell*. 2002;109(1):29-37.
88. Rideout WM, Hochedlinger K, Kyba M, Daley GQ, Jaenisch R. Correction of a genetic defect by nuclear transplantation and combined cell and gene therapy. *Cell*. 2002;109(1):17-27.
89. Hanna J, Wernig M, Markoulaki S, et al. Treatment of sickle cell anemia mouse model with iPS cells generated from autologous skin. *Science*. 2007;318(5858):1920-1923.
90. Pelton TA, Sharma S, Schulz TC, Rathjen J, Rathjen PD. Transient pluripotent cell populations during primitive ectoderm formation: correlation of in vivo and in vitro pluripotent cell development. *J Cell Sci*. 2002;115(Pt 2):329-339.
91. Pearson S, Sroczynska P, Lacaud G, Kouskoff V. The stepwise specification of embryonic stem cells to hematopoietic fate is driven by sequential exposure to Bmp4, activin A, bFGF and VEGF. *Development*. 2008;135(8):1525-1535.
92. Irion S, Clarke RL, Luche H, et al. Temporal specification of blood progenitors from mouse embryonic stem cells and induced pluripotent stem cells. *Development*. 2010;137(17):2829-2839.
93. Fan R, Bonde S, Gao P, et al. Dynamic HoxB4-regulatory network during embryonic stem cell differentiation to hematopoietic cells. *Blood*. 2012;119(19):e139-147.
94. Look AT. Oncogenic transcription factors in the human acute leukemias. *Science*. 1997;278(5340):1059-1064.
95. Wang Q, Stacy T, Binder M, Marin-Padilla M, Sharpe AH, Speck NA. Disruption of the Cbfa2 gene causes necrosis and hemorrhaging in the central nervous system and blocks definitive hematopoiesis. *Proc Natl Acad Sci U S A*. 1996;93(8):3444-3449.
96. Chen MJ, Yokomizo T, Zeigler BM, Dzierzak E, Speck NA. Runx1 is required for the endothelial to haematopoietic cell transition but not thereafter. *Nature*. 2009;457(7231):887-891.
97. Lichtinger M, Ingram R, Hannah R, et al. RUNX1 reshapes the epigenetic landscape at the onset of haematopoiesis. *EMBO J*. 2012;31(22):4318-4333.
98. Nottingham WT, Jarratt A, Burgess M, et al. Runx1-mediated hematopoietic stem-cell emergence is controlled by a Gata/Ets/SCL-regulated enhancer. *Blood*. 2007;110(13):4188-4197.

99. Bee T, Ashley EL, Bickley SR, et al. The mouse Runx1 +23 hematopoietic stem cell enhancer confers hematopoietic specificity to both Runx1 promoters. *Blood*. 2009;113(21):5121-5124.
100. Ghozi MC, Bernstein Y, Negreanu V, Levanon D, Groner Y. Expression of the human acute myeloid leukemia gene AML1 is regulated by two promoter regions. *Proc Natl Acad Sci U S A*. 1996;93(5):1935-1940.
101. Bee T, Liddiard K, Swiers G, et al. Alternative Runx1 promoter usage in mouse developmental hematopoiesis. *Blood Cells Mol Dis*. 2009;43(1):35-42.
102. Bee T, Swiers G, Muroi S, et al. Nonredundant roles for Runx1 alternative promoters reflect their activity at discrete stages of developmental hematopoiesis. *Blood*. 2010;115(15):3042-3050.
103. Sroczynska P, Lancrin C, Kouskoff V, Lacaud G. The differential activities of Runx1 promoters define milestones during embryonic hematopoiesis. *Blood*. 2009;114(26):5279-5289.
104. Levanon D, Brenner O, Negreanu V, et al. Spatial and temporal expression pattern of Runx3 (Aml2) and Runx1 (Aml1) indicates non-redundant functions during mouse embryogenesis. *Mech Dev*. 2001;109(2):413-417.
105. Pozner A, Goldenberg D, Negreanu V, et al. Transcription-coupled translation control of AML1/RUNX1 is mediated by cap- and internal ribosome entry site-dependent mechanisms. *Mol Cell Biol*. 2000;20(7):2297-2307.
106. Telfer JC, Rothenberg EV. Expression and function of a stem cell promoter for the murine CBFalpha2 gene: distinct roles and regulation in natural killer and T cell development. *Dev Biol*. 2001;229(2):363-382.
107. Wong WF, Nakazato M, Watanabe T, et al. Over-expression of Runx1 transcription factor impairs the development of thymocytes from the double-negative to double-positive stages. *Immunology*. 2010;130(2):243-253.
108. Okuda T, van Deursen J, Hiebert SW, Grosveld G, Downing JR. AML1, the target of multiple chromosomal translocations in human leukemia, is essential for normal fetal liver hematopoiesis. *Cell*. 1996;84(2):321-330.
109. Cai Z, de Bruijn M, Ma X, et al. Haploinsufficiency of AML1 affects the temporal and spatial generation of hematopoietic stem cells in the mouse embryo. *Immunity*. 2000;13(4):423-431.
110. Lacaud G, Gore L, Kennedy M, et al. Runx1 is essential for hematopoietic commitment at the hemangioblast stage of development in vitro. *Blood*. 2002;100(2):458-466.
111. Speck NA, Gilliland DG. Core-binding factors in haematopoiesis and leukaemia. *Nat Rev Cancer*. 2002;2(7):502-513.
112. Pozner A, Lotem J, Xiao C, et al. Developmentally regulated promoter-switch transcriptionally controls Runx1 function during embryonic hematopoiesis. *BMC Dev Biol*. 2007;7:84.
113. Challen GA, Goodell MA. Runx1 isoforms show differential expression patterns during hematopoietic development but have similar functional effects in adult hematopoietic stem cells. *Exp Hematol*. 2010;38(5):403-416.
114. Challen GA, Sun D, Jeong M, et al. Dnmt3a is essential for hematopoietic stem cell differentiation. *Nat Genet*. 2012;44(1):23-31.
115. Trowbridge JJ, Snow JW, Kim J, Orkin SH. DNA methyltransferase 1 is essential for and uniquely regulates hematopoietic stem and progenitor cells. *Cell Stem Cell*. 2009;5(4):442-449.
116. Jaenisch R. DNA methylation and imprinting: why bother? *Trends Genet*. 1997;13(8):323-329.

117. Song F, Smith JF, Kimura MT, et al. Association of tissue-specific differentially methylated regions (TDMs) with differential gene expression. *Proc Natl Acad Sci U S A*. 2005;102(9):3336-3341.
118. Maunakea AK, Nagarajan RP, Bilenky M, et al. Conserved role of intragenic DNA methylation in regulating alternative promoters. *Nature*. 2010;466(7303):253-257.
119. Iacovino M, Hernandez C, Xu Z, Bajwa G, Prather M, Kyba M. A conserved role for Hox paralog group 4 in regulation of hematopoietic progenitors. *Stem Cells Dev*. 2009;18(5):783-792.
120. Morgan K, Kharas M, Dzierzak E, Gilliland DG. Isolation of early hematopoietic stem cells from murine yolk sac and AGM. *J Vis Exp*. 2008(16).
121. Morrison SJ, Hemmati HD, Wandycz AM, Weissman IL. The purification and characterization of fetal liver hematopoietic stem cells. *Proc Natl Acad Sci U S A*. 1995;92(22):10302-10306.
122. Boyer LA, Lee TI, Cole MF, et al. Core transcriptional regulatory circuitry in human embryonic stem cells. *Cell*. 2005;122(6):947-956.
123. Weber M, Davies JJ, Wittig D, et al. Chromosome-wide and promoter-specific analyses identify sites of differential DNA methylation in normal and transformed human cells. *Nat Genet*. 2005;37(8):853-862.
124. Weber M, Hellmann I, Stadler MB, et al. Distribution, silencing potential and evolutionary impact of promoter DNA methylation in the human genome. *Nat Genet*. 2007;39(4):457-466.
125. Zambidis ET, Peault B, Park TS, Bunz F, Civin CI. Hematopoietic differentiation of human embryonic stem cells progresses through sequential hematoendothelial, primitive, and definitive stages resembling human yolk sac development. *Blood*. 2005;106(3):860-870.
126. Consortium EP. A user's guide to the encyclopedia of DNA elements (ENCODE). *PLoS Biol*. 2011;9(4):e1001046.
127. Ferkowicz MJ, Starr M, Xie X, et al. CD41 expression defines the onset of primitive and definitive hematopoiesis in the murine embryo. *Development*. 2003;130(18):4393-4403.
128. Hoivik EA, Bjanesoy TE, Mai O, et al. DNA methylation of intronic enhancers directs tissue-specific expression of steroidogenic factor 1/adrenal 4 binding protein (SF-1/Ad4BP). *Endocrinology*. 2011;152(5):2100-2112.
129. Bernstein BE, Mikkelsen TS, Xie X, et al. A bivalent chromatin structure marks key developmental genes in embryonic stem cells. *Cell*. 2006;125(2):315-326.
130. Nishida H, Suzuki T, Kondo S, Miura H, Fujimura Y, Hayashizaki Y. Histone H3 acetylated at lysine 9 in promoter is associated with low nucleosome density in the vicinity of transcription start site in human cell. *Chromosome Res*. 2006;14(2):203-211.
131. Okano M, Bell DW, Haber DA, Li E. DNA methyltransferases Dnmt3a and Dnmt3b are essential for de novo methylation and mammalian development. *Cell*. 1999;99(3):247-257.
132. Okano M, Xie S, Li E. Cloning and characterization of a family of novel mammalian DNA (cytosine-5) methyltransferases. *Nat Genet*. 1998;19(3):219-220.
133. Lei H, Oh SP, Okano M, et al. De novo DNA cytosine methyltransferase activities in mouse embryonic stem cells. *Development*. 1996;122(10):3195-3205.
134. Levanon D, Glusman G, Bangsow T, et al. Architecture and anatomy of the genomic locus encoding the human leukemia-associated transcription factor RUNX1/AML1. *Gene*. 2001;262(1-2):23-33.
135. Levanon D, Groner Y. Structure and regulated expression of mammalian RUNX genes. *Oncogene*. 2004;23(24):4211-4219.
136. Song F, Mahmood S, Ghosh S, et al. Tissue specific differentially methylated regions (TDMR): Changes in DNA methylation during development. *Genomics*. 2009;93(2):130-139.

137. Fujita Y, Nishimura M, Taniwaki M, Abe T, Okuda T. Identification of an alternatively spliced form of the mouse AML1/RUNX1 gene transcript AML1c and its expression in early hematopoietic development. *Biochem Biophys Res Commun*. 2001;281(5):1248-1255.
138. Lorincz MC, Dickerson DR, Schmitt M, Groudine M. Intragenic DNA methylation alters chromatin structure and elongation efficiency in mammalian cells. *Nat Struct Mol Biol*. 2004;11(11):1068-1075.
139. Szabo E, Rampalli S, Risueño RM, et al. Direct conversion of human fibroblasts to multilineage blood progenitors. *Nature*. 2010;468(7323):521-526.
140. Deng J, Shoemaker R, Xie B, et al. Targeted bisulfite sequencing reveals changes in DNA methylation associated with nuclear reprogramming. *Nat Biotechnol*. 2009;27(4):353-360.
141. Meissner A, Mikkelsen TS, Gu H, et al. Genome-scale DNA methylation maps of pluripotent and differentiated cells. *Nature*. 2008;454(7205):766-770.
142. Thillainadesan G, Chitilian JM, Isovic M, et al. TGF-β-dependent active demethylation and expression of the p15ink4b tumor suppressor are impaired by the ZNF217/CoREST complex. *Mol Cell*. 2012;46(5):636-649.
143. Bruniquel D, Schwartz RH. Selective, stable demethylation of the interleukin-2 gene enhances transcription by an active process. *Nat Immunol*. 2003;4(3):235-240.
144. Nagae G, Isagawa T, Shiraki N, et al. Tissue-specific demethylation in CpG-poor promoters during cellular differentiation. *Hum Mol Genet*. 2011;20(14):2710-2721.
145. North T, Gu TL, Stacy T, et al. Cbfa2 is required for the formation of intra-aortic hematopoietic clusters. *Development*. 1999;126(11):2563-2575.
146. Telfer JC, Rothenberg EV. Expression and Function of a Stem Cell Promoter for the Murine CBFα2 Gene: Distinct Roles and Regulation in Natural Killer and T Cell Development. *Developmental Biology*. 2001;229(2):363-382.
147. Pimanda JE, Donaldson IJ, de Bruijn MF, et al. The SCL transcriptional network and BMP signaling pathway interact to regulate RUNX1 activity. *Proc Natl Acad Sci U S A*. 2007;104(3):840-845.
148. Sun W, Downing JR. Haploinsufficiency of AML1 results in a decrease in the number of LTR-HSCs while simultaneously inducing an increase in more mature progenitors. *Blood*. 2004;104(12):3565-3572.
149. Lacaud G, Kouskoff V, Trumble A, Schwantz S, Keller G. Haploinsufficiency of Runx1 results in the acceleration of mesodermal development and hemangioblast specification upon in vitro differentiation of ES cells. *Blood*. 2004;103(3):886-889.
150. Gibson DG, Young L, Chuang RY, Venter JC, Hutchison CA, Smith HO. Enzymatic assembly of DNA molecules up to several hundred kilobases. *Nat Methods*. 2009;6(5):343-345.
151. Oostendorp RA, Medvinsky AJ, Kusadasi N, et al. Embryonal subregion-derived stromal cell lines from novel temperature-sensitive SV40 T antigen transgenic mice support hematopoiesis. *J Cell Sci*. 2002;115(Pt 10):2099-2108.
152. Wilkinson AC, Goode DK, Cheng YH, et al. Single site-specific integration targeting coupled with embryonic stem cell differentiation provides a high-throughput alternative to in vivo enhancer analyses. *Biol Open*. 2013;2(11):1229-1238.
153. Evans V, Hatzopoulos A, Aird WC, Rayburn HB, Rosenberg RD, Kuivenhoven JA. Targeting the Hprt locus in mice reveals differential regulation of Tie2 gene expression in the endothelium. *Physiol Genomics*. 2000;2(2):67-75.
154. Minami T, Donovan DJ, Tsai JC, Rosenberg RD, Aird WC. Differential regulation of the von Willebrand factor and Flt-1 promoters in the endothelium of hypoxanthine phosphoribosyltransferase-targeted mice. *Blood*. 2002;100(12):4019-4025.

155. Dang SM, Kyba M, Perlingeiro R, Daley GQ, Zandstra PW. Efficiency of embryoid body formation and hematopoietic development from embryonic stem cells in different culture systems. *Biotechnol Bioeng*. 2002;78(4):442-453.
156. North TE, de Bruijn MF, Stacy T, et al. Runx1 expression marks long-term repopulating hematopoietic stem cells in the midgestation mouse embryo. *Immunity*. 2002;16(5):661-672.
157. McKinney-Freeman SL, Naveiras O, Yates F, et al. Surface antigen phenotypes of hematopoietic stem cells from embryos and murine embryonic stem cells. *Blood*. 2009;114(2):268-278.
158. Fitch SR, Kimber GM, Wilson NK, et al. Signaling from the sympathetic nervous system regulates hematopoietic stem cell emergence during embryogenesis. *Cell Stem Cell*. 2012;11(4):554-566.
159. Yokomizo T, Takahashi S, Mochizuki N, et al. Characterization of GATA-1(+) hemangioblastic cells in the mouse embryo. *EMBO J*. 2007;26(1):184-196.
160. Ledran MH, Krassowska A, Armstrong L, et al. Efficient hematopoietic differentiation of human embryonic stem cells on stromal cells derived from hematopoietic niches. *Cell Stem Cell*. 2008;3(1):85-98.
161. Robin C, Ottersbach K, Durand C, et al. An unexpected role for IL-3 in the embryonic development of hematopoietic stem cells. *Dev Cell*. 2006;11(2):171-180.
162. Dahl L, Richter K, Hägglund AC, Carlsson L. Lhx2 expression promotes self-renewal of a distinct multipotential hematopoietic progenitor cell in embryonic stem cell-derived embryoid bodies. *PLoS One*. 2008;3(4):e2025.
163. Schmitt TM, de Pooter RF, Gronski MA, Cho SK, Ohashi PS, Zúñiga-Pflücker JC. Induction of T cell development and establishment of T cell competence from embryonic stem cells differentiated in vitro. *Nat Immunol*. 2004;5(4):410-417.
164. Burns CE, Traver D, Mayhall E, Shepard JL, Zon LI. Hematopoietic stem cell fate is established by the Notch-Runx pathway. *Genes Dev*. 2005;19(19):2331-2342.
165. Iacovino M, Bosnakovski D, Fey H, et al. Inducible cassette exchange: a rapid and efficient system enabling conditional gene expression in embryonic stem and primary cells. *Stem Cells*. 2011;29(10):1580-1588.
166. Christian M, Cermak T, Doyle EL, et al. Targeting DNA double-strand breaks with TAL effector nucleases. *Genetics*. 2010;186(2):757-761.
167. Mali P, Yang L, Esvelt KM, et al. RNA-guided human genome engineering via Cas9. *Science*. 2013;339(6121):823-826.
168. Wong WF, Looi CY, Kon S, et al. T-cell receptor signaling induces proximal Runx1 transactivation via a calcineurin-NFAT pathway. *Eur J Immunol*. 2013.
169. Mukai K, BenBarak MJ, Tachibana M, et al. Critical role of P1-Runx1 in mouse basophil development. *Blood*. 2012;120(1):76-85.
170. Maguire CA, van der Mijn JC, Degeling MH, Morse D, Tannous BA. Codon-optimized Luciola italica luciferase variants for mammalian gene expression in culture and in vivo. *Mol Imaging*. 2012;11(1):13-21.
171. Osborn MJ, Panoskaltsis-Mortari A, McElmurry RT, et al. A picornaviral 2A-like sequence-based tricistronic vector allowing for high-level therapeutic gene expression coupled to a dual-reporter system. *Mol Ther*. 2005;12(3):569-574.